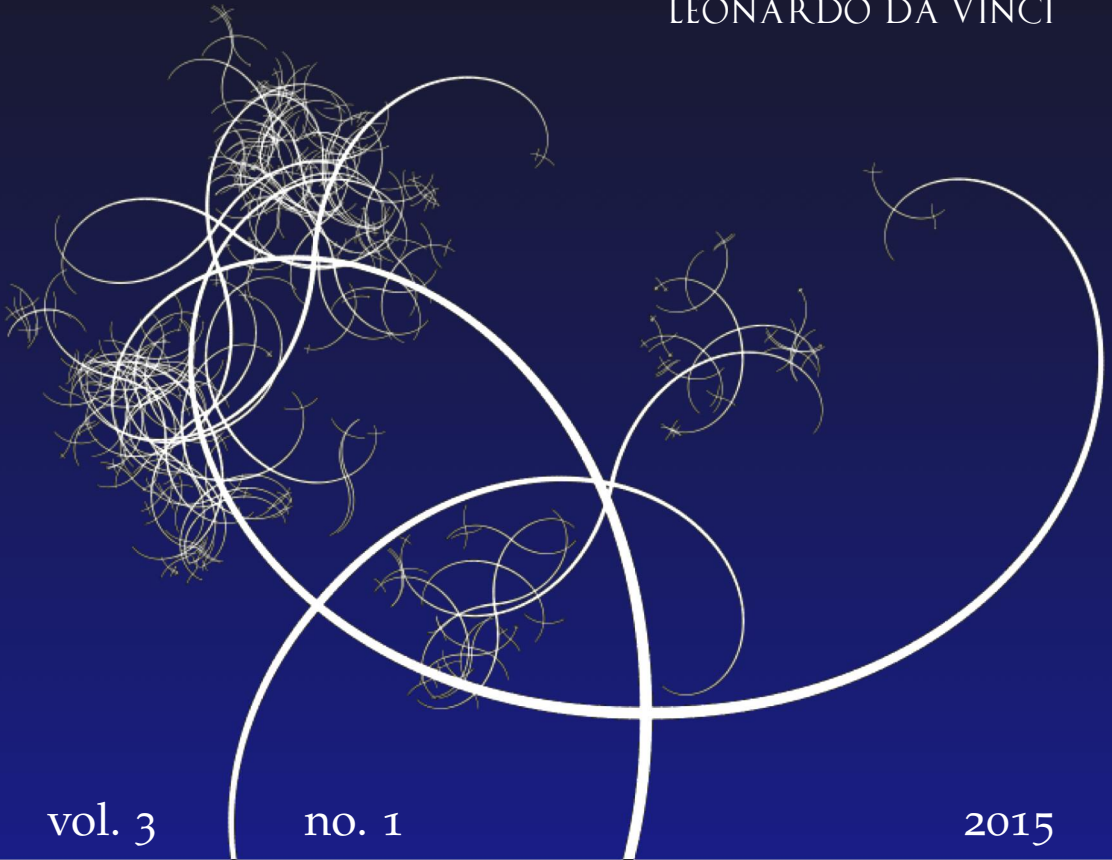


NISSUNA UMANA INVESTIGAZIONE SI PUO DIMANDARE
VERA SCIENZA S'ESSA NON PASSA PER LE
MATEMATICHE DIMOSTRAZIONI
LEONARDO DA VINCI



vol. 3

no. 1

2015

MATHEMATICS AND MECHANICS
of
Complex Systems



MATHEMATICS AND MECHANICS OF COMPLEX SYSTEMS

msp.org/memocs

EDITORIAL BOARD

ANTONIO CARCATERRA	Università di Roma “La Sapienza”, Italia
ERIC A. CARLEN	Rutgers University, USA
FRANCESCO DELL’ISOLA	(CO-CHAIR) Università di Roma “La Sapienza”, Italia
RAFFAELE ESPOSITO	(TREASURER) Università dell’Aquila, Italia
ALBERT FANNJIANG	University of California at Davis, USA
GILLES A. FRANCFORT	(CO-CHAIR) Université Paris-Nord, France
PIERANGELO MARCATI	Università dell’Aquila, Italy
JEAN-JACQUES MARIGO	École Polytechnique, France
PETER A. MARKOWICH	DAMTP Cambridge, UK, and University of Vienna, Austria
MARTIN OSTOJA-STARZEWSKI	(CHAIR MANAGING EDITOR) Univ. of Illinois at Urbana-Champaign, USA
PIERRE SEPPECHER	Université du Sud Toulon-Var, France
DAVID J. STEIGMANN	University of California at Berkeley, USA
PAUL STEINMANN	Universität Erlangen-Nürnberg, Germany
PIERRE M. SUQUET	LMA CNRS Marseille, France

MANAGING EDITORS

MICOL AMAR	Università di Roma “La Sapienza”, Italia
CORRADO LATTANZIO	Università dell’Aquila, Italy
ANGELA MADEO	Université de Lyon–INSA (Institut National des Sciences Appliquées), France
MARTIN OSTOJA-STARZEWSKI	(CHAIR MANAGING EDITOR) Univ. of Illinois at Urbana-Champaign, USA

ADVISORY BOARD

ADNAN AKAY	Carnegie Mellon University, USA, and Bilkent University, Turkey
HOLM ALTENBACH	Otto-von-Guericke-Universität Magdeburg, Germany
MICOL AMAR	Università di Roma “La Sapienza”, Italia
HARM ASKES	University of Sheffield, UK
TEODOR ATANACKOVIĆ	University of Novi Sad, Serbia
VICTOR BERDICHEVSKY	Wayne State University, USA
GUY BOUCHITTÉ	Université du Sud Toulon-Var, France
ANDREA BRAIDES	Università di Roma Tor Vergata, Italia
ROBERTO CAMASSA	University of North Carolina at Chapel Hill, USA
MAURO CARFORE	Università di Pavia, Italia
ERIC DARVE	Stanford University, USA
FELIX DARVE	Institut Polytechnique de Grenoble, France
ANNA DE MASI	Università dell’Aquila, Italia
GIANPIETRO DEL PIERO	Università di Ferrara and International Research Center MEMOCS, Italia
EMMANUELE DI BENEDETTO	Vanderbilt University, USA
BERNOLD FIEDLER	Freie Universität Berlin, Germany
IRENE M. GAMBA	University of Texas at Austin, USA
SERGEY GAVRILYUK	Université Aix-Marseille, France
TIMOTHY J. HEALEY	Cornell University, USA
DOMINIQUE JEULIN	École des Mines, France
ROGER E. KHAYAT	University of Western Ontario, Canada
CORRADO LATTANZIO	Università dell’Aquila, Italy
ROBERT P. LIPTON	Louisiana State University, USA
ANGELO LUONGO	Università dell’Aquila, Italia
ANGELA MADEO	Université de Lyon–INSA (Institut National des Sciences Appliquées), France
JUAN J. MANFREDI	University of Pittsburgh, USA
CARLO MARCHIORO	Università di Roma “La Sapienza”, Italia
GÉRARD A. MAUGIN	Université Paris VI, France
ROBERTO NATALINI	Istituto per le Applicazioni del Calcolo “M. Picone”, Italy
PATRIZIO NEFF	Universität Duisburg-Essen, Germany
ANDREY PIATNITSKI	Narvik University College, Norway, Russia
ERRICO PRESUTTI	Università di Roma Tor Vergata, Italy
MARIO PULVIRENTI	Università di Roma “La Sapienza”, Italia
LUCIO RUSSO	Università di Roma “Tor Vergata”, Italia
MIGUEL A. F. SANJUAN	Universidad Rey Juan Carlos, Madrid, Spain
PATRICK SELVADURAI	McGill University, Canada
ALEXANDER P. SEYRANIAN	Moscow State Lomonosov University, Russia
MIROSLAV ŠILHAVÝ	Academy of Sciences of the Czech Republic
GUIDO SWEERS	Universität zu Köln, Germany
ANTOINETTE TORDESILLAS	University of Melbourne, Australia
LEV TRUSKINOVSKY	École Polytechnique, France
JUAN J. L. VELÁZQUEZ	Bonn University, Germany
VINCENZO VESPRI	Università di Firenze, Italia
ANGELO VULPIANI	Università di Roma La Sapienza, Italia

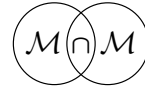
MEMOCS (ISSN 2325-3444 electronic, 2326-7186 printed) is a journal of the International Research Center for the Mathematics and Mechanics of Complex Systems at the Università dell’Aquila, Italy.

Cover image: “Tangle” by © John Horigan; produced using the *Context Free* program (contextfreeart.org).

PUBLISHED BY

 **mathematical sciences publishers**
nonprofit scientific publishing
<http://msp.org/>

© 2015 Mathematical Sciences Publishers



EFFECTS OF DAMPING ON THE STABILITY OF THE COMPRESSED NICOLAI BEAM

ANGELO LUONGO, MANUEL FERRETTI AND ALEXANDER P. SEYRANIAN

The Nicolai problem concerning the stability of a quasisymmetric cantilever beam embedded in a three-dimensional space, under a compressive dead load and a follower torque, is addressed. The effect of external and internal damping on stability is investigated. The partial differential equations of motion, accounting for the pretwist contribution, are recast in weak form via the Galerkin method, and a linear algebraic problem, governing the stability of the rectilinear configuration of the beam, is derived. Perturbation methods are used to analytically compute the eigenvalues, starting with an unperturbed, undamped, symmetric, untwisted beam, axially loaded, in both the subcritical and critical regimes. Accordingly, an asymmetry parameter, the torque, the damping, and the load increment are taken as perturbation parameters. Maclaurin series are used for semisimple eigenvalues occurring in subcritical states, and Puiseux series for the quadruple-zero eigenvalue existing at the Euler point. Based on the eigenvalue behavior described by the asymptotic expansions, the stability domains are constructed in the two or three-dimensional space of the bifurcation parameters. It is found that dynamic bifurcations occur in the subcritical regime, and dynamic or static bifurcations in the critical regime. It is shown that stability is governed mostly by the bifurcation of the lowest eigenvalue. In all cases the Nicolai paradox is recovered, and the beneficial effects of asymmetry and damping are highlighted.

1. Introduction

The fascinating mechanical problem first formulated by Nicolai [1928] and now bearing his name consists in determining the critical value of a follower (tangential) torque acting at the free end of a uniform elastic cantilever beam embedded in a three-dimensional space, with equal moments of inertia in the two planes. The Nicolai paradox consists in the fact that the bifurcation value of the torque is zero, in the sense that *a vanishingly small torque is able to cause (dynamic) instability*

Communicated by Antonio Carcaterra.

MSC2010: 74H10, 74H55, 74H60.

Keywords: stability of beams, nonconservative system, Nicolai paradox, perturbation methods, semisimple eigenvalues, quadruple-zero eigenvalue.

of the beam. Nicolai found this (apparently) surprising result by using a simplified two-degree of freedom model with lumped mass; he also found that damping is stabilizing. Subsequently he analyzed the effects of small asymmetries in the two inertia moments, and found they have a beneficial effect on stability [Nicolai 1929].

The paradox has recently been explained in [Seyranian and Mailybaev 2011], where it has been shown to be due to the bifurcation of a double semisimple eigenvalue, which leads to a stability domain with a conic singularity at the origin of parameter space, where the ideal symmetric system is located. Therefore, an infinitesimal perturbation of this state can lead the system out of the cone, causing instability. In the same paper the authors, by referring to a general discrete system, briefly investigated damping effects, arriving at a justification of the findings of Nicolai. In their paper, however, although they accounted for the presence of an axial load, they assumed it as below the Euler critical value.

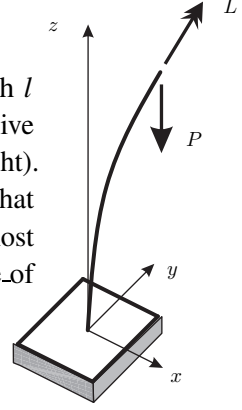
In [Seyranian et al. 2014], the continuous model was enriched by accounting for the pretwist generated by the torque in the reference configuration. This effect, which had been neglected in previous papers, was, however, found to not affect the stability domain. The authors, by using analytical and numerical methods, also studied the neighborhood of the Euler point, although they did not address the (complex) mechanism of bifurcation. Moreover, they did not account for damping.

In this paper we reconsider the problem of Nicolai using a continuous model of a beam with pretwisting and introducing damping forces. We mainly focus on the influence of damping on the stability domains of the system. Thus, the problem of Nicolai is studied in greater depth, with multiple aims, namely: to thoroughly analyze the effects on stability of external and internal damping acting on the beam; to study the regimes of subcritical and critical axial loads and their influence on the critical value of the torque; to investigate the role of eigenvalues higher than the first in affecting stability; and to explain, by analytical methods, the mechanism of the bifurcation of the quadruple-zero eigenvalue which occurs at the Euler critical load. All these aspects are believed to be new; the latter, moreover, could have value that transcends the issue at hand.

The paper is organized as follows. In Section 2 the equations of motion are recalled, a Galerkin reduction is carried out, and a linear eigenvalue problem is drawn. In Section 3 the stability problem for subcritically loaded beams is addressed by performing a perturbation of semisimple eigenvalues. In Section 4 the stability problem for nearly critically loaded beams is tackled. Here it is shown that a Puiseux series expansion must be used to analyze bifurcation of the quadruple nonsemisimple eigenvalue. Differences in the algorithms for undamped and damped systems are also extensively commented upon for this occurrence. In all cases two or three-dimensional stability domains are constructed and the type of bifurcation (static or dynamic) occurring at the different branches of the boundaries is commented upon.

2. Problem formulation

Continuous model. We consider a cantilever beam, of length l and mass per unit length m , loaded at the free end by a compressive axial dead load P and a follower torque L (see figure on the right). The system is assumed to be “nearly symmetric”, in the sense that its geometric characteristics in the two principal planes are almost equal. The goal of this analysis is to evaluate the critical value of the torque at which the beam loses stability, by accounting for asymmetries, axial load, and damping.



The equations of motion for the elastic beam, modeled according to the Euler–Bernoulli hypotheses, were derived in [Bolotin 1963]; in [Seyranian et al. 2014] the effect of the pretwist induced by the torque was included in the analysis. In this paper we consider a further improved model by accounting for internal and external dampings. The relevant equations of motion (see Appendix C for derivation) are

$$\begin{aligned} m\ddot{u} + EI_y u^{IV} + L \left(1 - 2 \frac{E}{G} \frac{I_x + I_y}{J} \right) v''' + P u'' - 2P \frac{L}{GJ} v' + \xi \dot{u} + \eta I_y \dot{u}^{IV} &= 0, \\ m\ddot{v} + EI_x v^{IV} - L \left(1 - 2 \frac{E}{G} \frac{I_x + I_y}{J} \right) u''' + P v'' + 2P \frac{L}{GJ} u' + \xi \dot{v} + \eta I_x \dot{v}^{IV} &= 0, \end{aligned} \quad (1)$$

with the boundary conditions

$$\begin{aligned} u(0) = u'(0) = 0, \quad EI_y u''(l) + \eta I_y \dot{u}''(l) - 2L \frac{EI_y}{GJ} v'(l) &= 0, \\ v(0) = v'(0) = 0, \quad EI_x v''(l) + \eta I_x \dot{v}''(l) + 2L \frac{EI_x}{GJ} u'(l) &= 0, \\ -EI_y u'''(l) - \eta I_y \dot{u}'''(l) - P \left(u'(l) - \frac{L}{GJ} v(l) \right) &= 0, \\ -EI_x v'''(l) - \eta I_x \dot{v}'''(l) - P \left(v'(l) + \frac{L}{GJ} u(l) \right) &= 0. \end{aligned} \quad (2)$$

Here $u(z, t)$ and $v(z, t)$ are the transverse displacements of the centroid at the abscissa z and time t , along the principal x and y axes, respectively; E is the Young modulus of the material; I_x and I_y are the principal inertia moments of the cross-section and J is its torsional inertia moment; ξ and η are the external damping and viscosity coefficients, respectively; a dash denotes differentiation with respect to z ; and a dot denotes differentiation with respect to t . When the damping coefficients are set to zero, the equations studied in [Seyranian et al. 2014] are recovered. These equations govern the small oscillations of the pretwisted beam around the rectilinear configuration.

The following nondimensional quantities are introduced:

$$\begin{aligned}
\tilde{z} &:= \frac{z}{l}, & \tilde{u} &:= \frac{u}{l}, & \tilde{v} &:= \frac{v}{l}, & \beta &:= 2 \frac{E}{G} \frac{I_x + I_y}{J}, & \gamma &:= 2 \frac{E}{G} \frac{I_0}{J}, \\
\tilde{L} &:= \frac{Ll}{EI_0}, & \tilde{P} &:= \frac{Pl^2}{EI_0}, & \tilde{I}_y &:= \frac{I_y}{I_0}, & \tilde{I}_x &:= \frac{I_x}{I_0}, & \tilde{m} &:= \frac{m}{m_0}, \\
\tilde{t} &:= t \sqrt{\frac{EI_0}{m_0 l^4}}, & \tilde{\xi} &:= \xi \sqrt{\frac{l^4}{m_0 EI_0}}, & \tilde{\eta} &:= \eta \sqrt{\frac{I_0}{m_0 l^4 E}},
\end{aligned} \tag{3}$$

where I_0 and m_0 are an inertia moment and mass per unit length, respectively, taken as characteristics of a “close” ideal symmetric system, from which the actual system can be generated via a small perturbation (see Appendix A). With definitions (3), the equations of motion transform into

$$\begin{aligned}
m\ddot{u} + I_y u^{IV} + L(1 - \beta)v''' + Pu'' - PL\gamma v' + \xi\dot{u} + \eta I_y \dot{u}^{IV} &= 0, \\
m\ddot{v} + I_x v^{IV} - L(1 - \beta)u''' + Pv'' + PL\gamma u' + \xi\dot{v} + \eta I_x \dot{v}^{IV} &= 0,
\end{aligned} \tag{4}$$

and the boundary conditions into

$$\begin{aligned}
u(0) = u'(0) = 0, & \quad I_y u''(1) + \eta I_y \dot{u}''(1) - \gamma L I_y v'(1) = 0, \\
v(0) = v'(0) = 0, & \quad I_x v''(1) + \eta I_x \dot{v}''(1) + \gamma L I_x u'(1) = 0, \\
-I_y u'''(1) - \eta I_y \dot{u}'''(1) - P(u'(1) - \frac{1}{2}L\gamma v(1)) &= 0, \\
-I_x v'''(1) - \eta I_x \dot{v}'''(1) - P(v'(1) + \frac{1}{2}L\gamma u(1)) &= 0,
\end{aligned} \tag{5}$$

where the tilde has been suppressed for notational convenience.

Discrete model. A weak form of the problem (4), (5) is derived according to the weighted residuals (or extended Galerkin [Leipholz 1974; Zienkiewicz et al. 2005]) method. The unknown displacement fields are expressed as linear combinations of $2N$ unknown time-dependent amplitudes, $\mathbf{x} := (x_i(t))^T$ and $\mathbf{y} := (y_i(t))^T$, and N known space-dependent trial functions $\boldsymbol{\phi} := (\phi_i(z))^T$, namely

$$\begin{aligned}
u(z, t) &= \boldsymbol{\phi}^T \mathbf{x}, \\
v(z, t) &= \boldsymbol{\phi}^T \mathbf{y},
\end{aligned} \tag{6}$$

where $\phi_i(0) = \phi_i'(0) = 0$ satisfy the geometrical boundary conditions; however, they are not required to satisfy the mechanical boundary conditions [Leipholz 1974; Zienkiewicz et al. 2005].

By substituting (6) into the field equations (4) and boundary conditions (5), residuals in the domain and at the free end $z = 1$ are found, which are required to be orthogonal to the trial function itself:

$$\begin{aligned}
& \sum_{i=1}^N \left\{ \int_0^1 \phi_j [m\phi_i \ddot{x}_i + I_y \phi_i^{IV} x_i + L(1-\beta)\phi_i''' y_i + P\phi_i'' x_i - PL\gamma\phi_i' y_i \right. \\
& \quad + \xi\phi_i \dot{x}_i + \eta I_y \phi_i^{IV} \dot{x}_i] dz + \phi_j' [I_y \phi_i'' x_i + \eta I_y \phi_i'' \dot{x}_i - \gamma L I_y \phi_i' y_i]_{z=1} \\
& \quad \left. + \phi_j \left[-I_y \phi_i''' x_i - \eta I_y \phi_i''' \dot{x}_i - P\phi_i' x_i + \frac{PL\gamma}{2} \phi_i y_i \right]_{z=1} \right\} = 0, \\
& \sum_{i=1}^N \left\{ \int_0^1 \phi_j [m\phi_i \ddot{y}_i + I_x \phi_i^{IV} y_i - L(1-\beta)\phi_i''' x_i + P\phi_i'' y_i + PL\gamma\phi_i' x_i \right. \\
& \quad + \xi\phi_i \dot{y}_i + \eta I_x \phi_i^{IV} \dot{y}_i] dz + \phi_j' [I_x \phi_i'' y_i + \eta I_x \phi_i'' \dot{y}_i + \gamma L I_x \phi_i' x_i]_{z=1} \\
& \quad \left. + \phi_j \left[-I_x \phi_i''' y_i - \eta I_x \phi_i''' \dot{y}_i - P\phi_i' y_i - \frac{PL\gamma}{2} \phi_i x_i \right]_{z=1} \right\} = 0,
\end{aligned} \tag{7}$$

where $j = 1, 2, \dots, N$. After integration by parts and accounting for the geometric boundary conditions, all terms at the boundaries disappear. From these, a set of $2N$ ordinary differential equations is derived:

$$\mathbf{M}\ddot{\mathbf{q}} + \mathbf{C}\dot{\mathbf{q}} + (\mathbf{K} + \mathbf{H})\mathbf{q} = \mathbf{0}, \tag{8}$$

where $\mathbf{q} := (\mathbf{x}, \mathbf{y})^T$ is a $2N$ column vector of the unknown amplitudes, and \mathbf{M} is the mass, \mathbf{C} the damping, \mathbf{K} the stiffness, and \mathbf{H} the circulatory matrices, all of dimension $2N \times 2N$, defined by

$$\begin{aligned}
\mathbf{C} &:= \begin{bmatrix} \xi \mathbf{m} + \eta I_y \mathbf{k}_E & \mathbf{0} \\ \mathbf{0} & \xi \mathbf{m} + \eta I_x \mathbf{k}_E \end{bmatrix}, & \mathbf{M} &:= m \begin{bmatrix} \mathbf{m} & \mathbf{0} \\ \mathbf{0} & \mathbf{m} \end{bmatrix}, \\
\mathbf{K} &:= \begin{bmatrix} I_y \mathbf{k}_E + P \mathbf{k}_G & \mathbf{0} \\ \mathbf{0} & I_x \mathbf{k}_E + P \mathbf{k}_G \end{bmatrix}, & \mathbf{H}_u &:= \begin{bmatrix} \mathbf{0} & \mathbf{h}_1 \\ -\mathbf{h}_1 & \mathbf{0} \end{bmatrix}, \\
\mathbf{H}_t &:= \begin{bmatrix} \mathbf{0} & -\beta \mathbf{h}_1 - P\gamma \mathbf{h}_2 - \gamma I_y \mathbf{h}_3 \\ \beta \mathbf{h}_1 + P\gamma \mathbf{h}_2 + \gamma I_x \mathbf{h}_3 & \mathbf{0} \end{bmatrix}, & \mathbf{H} &:= L(\mathbf{H}_u + \mathbf{H}_t).
\end{aligned} \tag{9}$$

In these equations, the following $N \times N$ submatrices appear, which depend on the trial functions only:

$$\begin{aligned}
\mathbf{m} &= \int_0^1 \boldsymbol{\phi} \boldsymbol{\phi}^T dz, & \mathbf{k}_E &= \int_0^1 \boldsymbol{\phi}'' \boldsymbol{\phi}''^T dz, \\
\mathbf{k}_G &= - \int_0^1 \boldsymbol{\phi}' \boldsymbol{\phi}'^T dz, & \mathbf{h}_1 &= \int_0^1 \boldsymbol{\phi} \boldsymbol{\phi}'''^T dz, \\
\mathbf{h}_2 &= \int_0^1 \boldsymbol{\phi} \boldsymbol{\phi}'^T dz - \frac{1}{2} \boldsymbol{\phi} \boldsymbol{\phi}^T \Big|_{z=1}, & \mathbf{h}_3 &= \boldsymbol{\phi}' \boldsymbol{\phi}'^T \Big|_{z=1},
\end{aligned} \tag{10}$$

where the indices E and G refer to the elastic and geometric parts of the stiffness matrix and the indices u and t refer to the untwisted and twisted beams, that is, to the torsionally rigid or torsionally elastic beams. Notice that the coupling between the \mathbf{x} and \mathbf{y} variables is exclusively due to the torque.

In the numerical simulations to be performed ahead, we will take as trial functions the (mutually orthogonal) eigenfunctions of the free undamped oscillations of the unstressed planar cantilever (see Appendix B). Due to their orthogonality properties and normalization, it follows that $\mathbf{m} = \mathbf{I}$ and $\mathbf{k}_E = \text{diag}(\omega_i^2)$, where ω_i are the (nondimensional) natural frequencies; in contrast, \mathbf{k}_G and \mathbf{h}_i , $i = 1, \dots, 3$, are full matrices. Moreover, while \mathbf{M} , \mathbf{C} , and \mathbf{K} are symmetric matrices, \mathbf{H} is not symmetric nor antisymmetric. Finally, the damping submatrices are linear combinations of the mass and elastic stiffness submatrices, as in the Rayleigh model of damping.

The algebraic eigenvalue problem. Substitution of $\mathbf{q}(t) = \mathbf{w}e^{\lambda t}$ in (8) and premultiplication by \mathbf{M}^{-1} leads to the algebraic eigenvalue problem

$$(\mathbf{A} + \lambda \mathbf{D} + \lambda^2 \mathbf{I})\mathbf{w} = \mathbf{0}, \quad (11)$$

in which $\mathbf{A} := \mathbf{M}^{-1}(\mathbf{K} + \mathbf{H})$ and $\mathbf{D} := \mathbf{M}^{-1}\mathbf{C}$. The trivial equilibrium is (asymptotically) stable if $\text{Re } \lambda < 0$ for all λ , and is unstable if $\text{Re } \lambda > 0$ for at least one λ .

When the system is undamped (that is, $\mathbf{D} = \mathbf{0}$), the eigenvalue problem is more conveniently recast in the standard form:

$$(\mathbf{A} - \mu \mathbf{I})\mathbf{w} = \mathbf{0}, \quad (12)$$

where $\mu := -\lambda^2$. The trivial equilibrium is stable if all μ are real and positive (that is, λ is purely imaginary), and it is unstable if at least one μ is negative or complex (entailing that one root λ has a positive real part).

3. Stability analysis for subcritically compressed beams

The perturbed eigenvalue problem. We address the stability problem for the case in which the (nondimensional) axial load P is lower than the (nondimensional) Eulerian critical load $P_E := \pi^2/4$. We assume that the cross-section is nearly symmetric, affected by a small asymmetry parameter α ; both the internal, η , and external, ξ , damping coefficients are small; and the follower torque, L , is also small. Accordingly, we introduce the following parameter rescaling:

$$(\alpha, L, \xi, \eta) \rightarrow \varepsilon(\alpha, L, \xi, \eta), \quad (13)$$

where $0 < \varepsilon \ll 1$ is a perturbation parameter (artificially introduced, and to be reabsorbed at the end of the procedure). The (nondimensional) geometric characteristics and the mass per unit length (with a proper choice of I_0 and m_0 appearing in (3)), after series expansion, read (see Appendix A for an example)

$$\begin{pmatrix} I_x \\ I_y \\ m \end{pmatrix} = \begin{pmatrix} 1 \\ 1 \\ 1 \end{pmatrix} + \varepsilon \alpha \begin{pmatrix} I_{x_1} \\ I_{y_1} \\ m_1 \end{pmatrix} + O(\varepsilon^2); \quad (14)$$

moreover, $\beta = \beta_0 + O(\varepsilon)$ and $\gamma = \gamma_0 + O(\varepsilon)$, with $\beta_0 = 2\gamma_0$. Consequently, the matrices in (11) can also be expressed in series form as

$$\mathbf{A} = \mathbf{A}_0 + \varepsilon \mathbf{A}_1 + O(\varepsilon^2), \quad \mathbf{D} = \varepsilon \mathbf{D}_1 + O(\varepsilon^2), \quad (15)$$

where

$$\begin{aligned} \mathbf{A}_0 &= \begin{bmatrix} \mathbf{k}_E + P\mathbf{k}_G & \mathbf{0} \\ \mathbf{0} & \mathbf{k}_E + P\mathbf{k}_G \end{bmatrix}, \\ \mathbf{A}_1 &= \mathbf{A}_{1_u} + \mathbf{A}_{1_t}, \\ \mathbf{A}_{1_u} &= \begin{bmatrix} \alpha(I_{y1} - m_1)\mathbf{k}_E - \alpha m_1 P\mathbf{k}_G & L\mathbf{h}_1 \\ -L\mathbf{h}_1 & \alpha(I_{x1} - m_1)\mathbf{k}_E - \alpha m_1 P\mathbf{k}_G \end{bmatrix} \\ \mathbf{A}_{1_t} &= \begin{bmatrix} \mathbf{0} & -L(\beta_0\mathbf{h}_1 + P\gamma_0\mathbf{h}_2 + \gamma_0\mathbf{h}_3) \\ L(\beta_0\mathbf{h}_1 + P\gamma_0\mathbf{h}_2 + \gamma_0\mathbf{h}_3) & \mathbf{0} \end{bmatrix}, \\ \mathbf{D}_1 &= \begin{bmatrix} \xi\mathbf{m} + \eta\mathbf{k}_E & \mathbf{0} \\ \mathbf{0} & \xi\mathbf{m} + \eta\mathbf{k}_E \end{bmatrix}. \end{aligned} \quad (16)$$

The eigenvalue problem (11), therefore, appears as a perturbation of the problem relevant to the symmetric, undamped, subcritically prestressed beam, with no torque, namely:

$$[\mathbf{A}_0 + \lambda^2 \mathbf{I} + \varepsilon(\mathbf{A}_1 + \lambda \mathbf{D}_1) + \dots] \mathbf{w} = \mathbf{0}, \quad (17)$$

where \mathbf{A}_1 accounts for (first-order) asymmetry and torque, while \mathbf{D}_1 accounts for damping.

Perturbation analysis.

The damped case. The eigenvalue problem (17) is solved by a perturbation method. Due to the symmetry of the unperturbed mechanical system, the eigenvalue λ_0 is a semisimple eigenvalue for the matrix \mathbf{A}_0 , that is, two independent eigenvectors are associated with any eigenvalue, each representing a mode of oscillation in the (x, z) -plane or the (y, z) -plane. Such an eigenvalue and its associated eigenvectors admit Maclaurin series expansion [Seyranian and Mailybaev 2003]:

$$\lambda = \lambda_0 + \varepsilon\lambda_1 + \dots, \quad \mathbf{w} = \mathbf{w}_0 + \varepsilon\mathbf{w}_1 + \dots \quad (18)$$

By introducing (18) in the eigenvalue problem (17) and separately equating to zero terms with the same powers of ε , the following perturbation equations are obtained:

$$\begin{aligned} \varepsilon^0: (\mathbf{A}_0 + \lambda_0^2 \mathbf{I}) \mathbf{w}_0 &= \mathbf{0}, \\ \varepsilon^1: (\mathbf{A}_0 + \lambda_0^2 \mathbf{I}) \mathbf{w}_1 &= -(\mathbf{A}_1 + \lambda_0 \mathbf{D}_1 + 2\lambda_0 \lambda_1 \mathbf{I}) \mathbf{w}_0. \end{aligned} \quad (19)$$

Since A_0 is symmetric and positive definite, its eigenvalues λ_0 are pairs of complex conjugate purely imaginary numbers, that is, $\pm i\omega_k$, $k = 1, 2, \dots, N$. The associated eigenvectors are real, and right and left eigenvectors coincide. We take $\lambda_0 = +i\omega_k$, and denote by \mathbf{u}_1 and \mathbf{u}_2 the associated eigenvectors, which are mutually orthogonal and normalized, that is, $\mathbf{u}_i^T \mathbf{u}_j = \delta_{ij}$. Hence, the ε^0 -order perturbation equation admits the general solution

$$\mathbf{w}_0 = \mathbf{U}\mathbf{a}, \quad (20)$$

where $\mathbf{U} = (\mathbf{u}_1, \mathbf{u}_2)$ is a $2N \times 2$ modal matrix and $\mathbf{a} = (a_1, a_2)^T$ is a column vector listing two unknown amplitudes. Note that, at this order, any linear combination of \mathbf{u}_1 and \mathbf{u}_2 is an eigenvector, the indeterminacy being resolved only at the next order.

With (20), the ε -order equation reads

$$(\mathbf{A}_0 + \lambda_0^2 \mathbf{I})\mathbf{w}_1 = -(\mathbf{A}_1 + \lambda_0 \mathbf{D}_1 + 2\lambda_0 \lambda_1 \mathbf{I})\mathbf{U}\mathbf{a}. \quad (21)$$

This is a nonhomogeneous problem in which the linear operator $\mathbf{A}_0 + \lambda_0^2 \mathbf{I}$ is singular. In order to solve it, the right-hand member must be orthogonal to the kernel of the adjoint operator (the compatibility condition). Since this space is spanned by the rows of \mathbf{U}^T , the compatibility reads

$$(\hat{\mathbf{A}}_1 + \lambda_0 \hat{\mathbf{D}}_1 + 2\lambda_0 \lambda_1 \mathbf{I})\mathbf{a} = \mathbf{0}, \quad (22)$$

where

$$\hat{\mathbf{A}}_1 := \mathbf{U}^T \mathbf{A}_1 \mathbf{U} \quad \text{and} \quad \hat{\mathbf{D}}_1 := \mathbf{U}^T \mathbf{D}_1 \mathbf{U} \quad (23)$$

are 2×2 matrices representing the restrictions of \mathbf{A}_1 and \mathbf{D}_1 to the plane spanned by the columns of \mathbf{U} ; moreover, $\mathbf{U}^T \mathbf{U} = \mathbf{I}$ has been used, which follows from the orthonormalization properties of the eigenvectors. A remarkable result is that the matrix $\hat{\mathbf{A}}_1$ does not depend on the pretwist, since the restriction of the matrix \mathbf{A}_1 to the plane of the eigenvectors is zero (see Appendix D for details). Therefore, to first order, stability is unaffected by the pretwist.

Equation (22) is an eigenvalue problem in the λ_1 unknown. The relevant characteristic equation is

$$\lambda_1^2 + I_1 \lambda_1 + I_2 = 0, \quad (24)$$

where

$$I_1 := \frac{1}{2\lambda_0} \text{tr}(\hat{\mathbf{A}}_1 + \lambda_0 \hat{\mathbf{D}}_1) \quad \text{and} \quad I_2 := \frac{1}{4\lambda_0^2} \det(\hat{\mathbf{A}}_1 + \lambda_0 \hat{\mathbf{D}}_1) \quad (25)$$

are linear and quadratic invariants, respectively, which are complex numbers. From (24) two (generally distinct) roots, $\lambda_1^\pm := (-I_1 \pm \sqrt{I_1^2 - 4I_2})/2$, are drawn, which cause the splitting (or bifurcation) of the double semisimple eigenvalue $i\omega_k$ into

$$\lambda^\pm = i\omega_k + \varepsilon \lambda_1^\pm. \quad (26)$$

Each eigenvalue λ_1^\pm is associated with a (distinct) eigenvector \mathbf{a}^\pm ; therefore $\mathbf{w}^\pm = U\mathbf{a}^\pm + O(\varepsilon)$, so that the indeterminacy of the eigenvectors is resolved at this order.

The undamped case. To tackle the undamped system one would most easily start from the standard form (12) of the eigenvalue problem. However, the same results can be derived from the general damped case, by letting $\hat{\mathbf{D}}_1 = \mathbf{0}$ in (22). Since $\mu := -\lambda^2$, or, in series form, $\mu_0 + \varepsilon\mu_1 + \dots = -(\lambda_0^2 + 2\varepsilon\lambda_0\lambda_1 + \dots)$, we have $\mu_0 = -\lambda_0^2$ and $\mu_1 := -2\lambda_0\lambda_1$. Therefore, (22) becomes

$$(\hat{\mathbf{A}}_1 - \mu_1 \mathbf{I})\mathbf{a} = \mathbf{0}, \quad (27)$$

which has the advantage of having real coefficients. The relevant characteristic equation,

$$\mu_1^2 - (\text{tr } \hat{\mathbf{A}}_1)\mu_1 + \det \hat{\mathbf{A}}_1 = 0, \quad (28)$$

provides the roots $\mu_1^\pm := (\text{tr } \hat{\mathbf{A}}_1 \pm \sqrt{\text{tr}^2 \hat{\mathbf{A}}_1 - 4 \det \hat{\mathbf{A}}_1})/2$; hence

$$\mu^\pm = \omega_k^2 + \varepsilon\mu_1^\pm. \quad (29)$$

Stability domains. We look for the stability domains of the trivial equilibrium in the plane of the bifurcation parameters α and L , for fixed axial load P and damping ξ and η , taken as auxiliary parameters. We separately address the undamped and damped cases.

Undamped system. As we said earlier, the equilibrium is stable when $\mu > 0$; since, in (29), $\varepsilon\mu_1^\pm$ is a small correction of ω_k^2 , this happens when μ_1^\pm is real, irrespective of its sign, that is, when the discriminant of the second-degree (28) is positive. Since

$$\text{tr}^2 \hat{\mathbf{A}}_1 - 4 \det \hat{\mathbf{A}}_1 = \alpha^2 c_\alpha^2 - L^2 c_L^2, \quad (30)$$

where c_α and c_L are numerical coefficients, the stability condition reads

$$L^2 \leq \left(\frac{c_\alpha}{c_L} \right)^2 \alpha^2. \quad (31)$$

This equation expresses the Nicolai paradox: when the asymmetry parameter α is zero (an ideal system), then an evanescent torque makes the equilibrium unstable; when, instead, a small asymmetry exists ($\alpha \neq 0$), a small threshold L_c exists, proportional to α , which has to be reached by L to make the system unstable. Note that the stable domain depends on the order number k of the eigenvalue $\lambda_0 = i\omega_k$ which bifurcates. Therefore, we have to analyze *all* the eigenvalues in order to determine which of them prevails in triggering instability.

Figure 1 reports the numerical results for the elliptical cross-section. Figure 1a shows the stable domain (the shaded zone) relevant to the lower eigenvalue ($k = 1$), when the axial load is zero, by comparing asymptotic (thick lines) and numerical

(thin lines) results, the latter deriving from the exact solution of the algebraic eigenvalue problem. The domain is found to be independent of the number N of trial functions used, since, due to the fact the elastic stiffness matrix is diagonal, the eigenvectors \mathbf{u}_1 and \mathbf{u}_2 are canonical vectors. The angular coefficient of the boundary lines is equal, in its absolute value, to 3.26. In the figure, a sketch on the complex plane of the four λ -eigenvalues involved (that is, the double $\pm i\omega_1$ eigenvalues) and their “velocities” is also given. It is seen that in the stable zone the eigenvalues are purely imaginary and distinct; on the boundary of the region they coalesce in pairs on the imaginary axis; and out of the stable zone, they separate in two pairs of stable and unstable eigenvalues. Therefore, in crossing the boundaries, a *dynamic bifurcation* takes place. The boundaries are a codimension-1 geometrical locus on which the degeneracy of the eigenvalues, existing in the symmetrical unloaded system, persists. The origin of the parameter plane is therefore a codimension-2 bifurcation point.

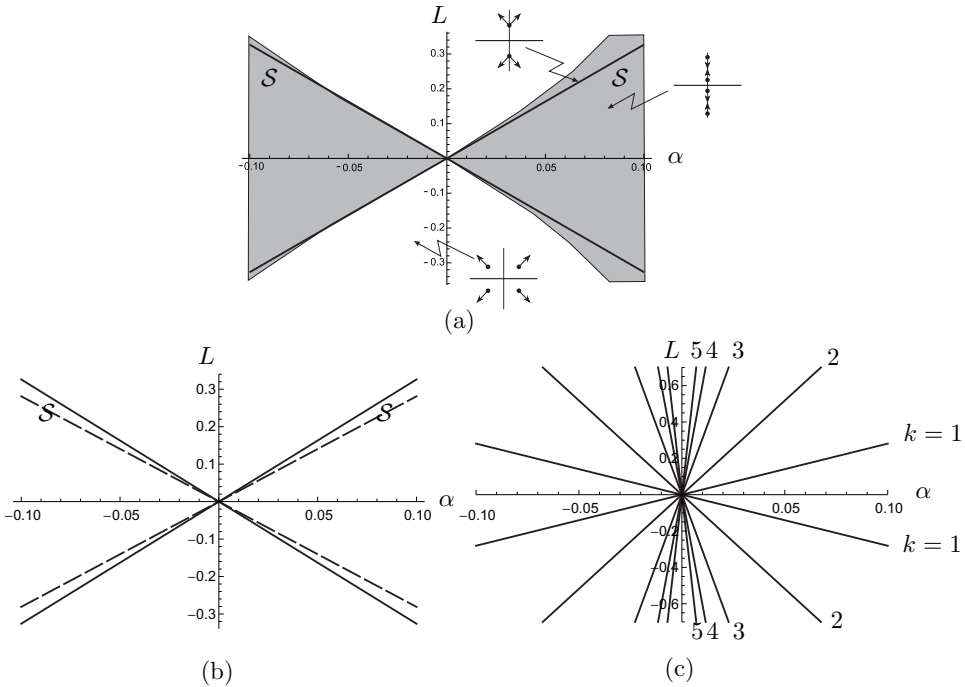


Figure 1. Stability domain \mathcal{S} in the (α, L) -plane for the undamped system subcritically loaded: (a) $k = 1, P = 0$ (thick line: asymptotic results; thin line: numerical results); (b) $k = 1, P = 0$ (solid line) and $P = P_E/2$ (dashed line), with $N = 5$ trial functions; (c) higher eigenvalue domains ($k = 1, \dots, 5, N = 5$) when $P = P_E/2$.

Figure 1b compares the domains relevant to the lower eigenvalue when P is 0 and $P_E/2$, showing a moderate reduction produced by the axial load (the angular coefficient reduces from 3.26 to 2.81). When $P \neq 0$, the domain depends on the discretization adopted. It was found that when $N = 5$ (that is, when the system is reduced to ten degrees of freedom) a numerical convergence is reached; this number of trial functions will be therefore adopted ahead. Finally, Figure 1c compares the stability domains relevant to the higher eigenvalues ($k = 1, \dots, 5$). It is found that the domains of higher modes include the domains of the lower modes (that is, when the lowest eigenvalue bifurcates, the higher ones are still on the imaginary axis, so that just the first mode is significant for stability).

Damped system. When the system is damped, its eigenvalues are given by (26), and the analysis, with major difficulties, must be carried out on complex quantities. The trivial equilibrium is asymptotically stable when $\text{Re } \lambda^\pm < 0$, that is, when $\text{Re } \lambda_1^\pm < 0$. In order for (24) to admit roots with real parts less than zero, the following conditions must be satisfied (the Bilharz theorem; see [Seyranian and Mailybaev 2003, p. 15]):

$$\text{Re } I_1 > 0, \quad (\text{Im } I_2)^2 - \text{Re } I_1 \text{Im } I_1 \text{Im } I_2 - (\text{Re } I_1)^2 \text{Re } I_2 < 0. \quad (32)$$

Condition (32)₁ is always satisfied when the damping coefficients are positive; (32)₂ instead gives the following (asymptotic) stability condition:

$$L^2 < \left(\frac{c_\alpha}{c_L} \right)^2 \alpha^2 + \left(\frac{c_\xi}{c_L} \xi + \frac{c_\eta}{c_L} \eta \right)^2, \quad (33)$$

where the c 's are numerical coefficients. It turns out that damping, both external and internal, as well as asymmetries, has a stabilizing effect on the equilibrium. If $\xi = \eta = 0$, then the result relevant to the undamped system is recovered. The numerical values of the c -coefficients are reported in Table 1 for the elliptical section and selected values of the compressive dead load P , when $N = 5$.

Figure 2 shows the stability domain for a damped system, as compared with Figure 1 for the corresponding undamped system. As already noted in [Seyranian and Mailybaev 2011], it appears (see Figure 2a) that damping destroys the Nicolai paradox, since a nonzero torque is needed to trigger instability at $\alpha = 0$. The figure also illustrates the mechanism of bifurcation. Inside the stability domain

	c_α/c_L	c_ξ/c_L	c_η/c_L
$P = 0$	3.26	0.93	11.47
$P = \frac{1}{2}P_E$	2.81	0.57	7.12

Table 1. Numerical coefficients in (33) when $k = 1$.

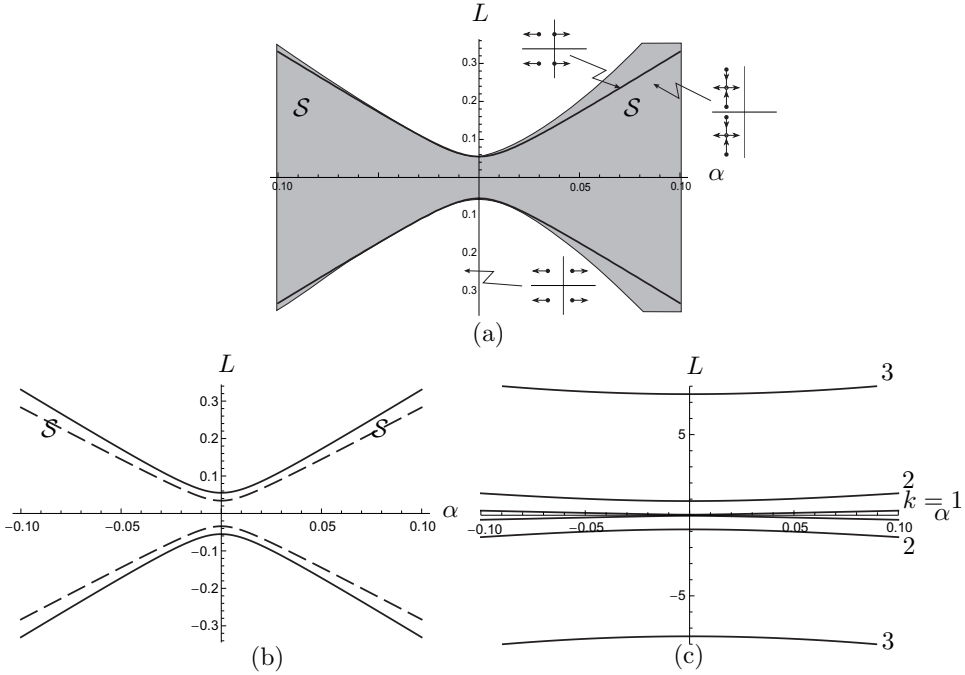


Figure 2. Stability domain \mathcal{S} in the (α, L) -plane for the damped system ($\xi = 0.01$, $\eta = 0.004$): (a) $k = 1$, $P = 0$ (thick line: asymptotic results; thin line: numerical results); (b) $k = 1$, $P = 0$ (solid line) and $P = P_E/2$ (dashed line), with $N = 5$ trial functions; (c) higher eigenvalue domains ($k = 1, \dots, 3$, $N = 5$) when $P = P_E/2$.

the eigenvalues are complex in the left half-plane. By approaching the boundary moving parallel to the L -axis, the eigenvalues approach each other by keeping their real parts constant; then, after the collision, they move in opposite directions by varying their real parts, up to crossing the imaginary axis. As for the undamped system, the effect of the axial load is weak (see Figure 2b), and the higher modes are ineffective in determining stability. However, under very particular choices of the parameters, stability can be governed by the second mode, which is consistent with results found in [Seyranian and Mailybaev 2011].

4. Stability analysis for critically compressed beams

We address now the stability problem of the beam when the axial load is close to the Eulerian critical load. Accordingly, since the codimension of the problem is higher, we introduce a third bifurcation parameter $\delta P := P - P_E$, and look for a stability domain in the three-dimensional $(\alpha, L, \delta P)$ parameter space.

Perturbation analysis for semisimple eigenvalues. Guided by the results obtained for the subcritically loaded beam, we introduce the rescaling

$$(\alpha, L, \delta P, \xi, \eta) \rightarrow \varepsilon(\alpha, L, \delta P, \xi, \eta), \quad (34)$$

in which all the quantities are ordered at the same level. Accordingly, the matrices \mathbf{A} and \mathbf{D} admit series expansions as in (15), but with new meanings for the coefficients:

$$\begin{aligned} \mathbf{A}_0 &= \begin{bmatrix} \mathbf{k}_E + P_E \mathbf{k}_G & \mathbf{0} \\ \mathbf{0} & \mathbf{k}_E + P_E \mathbf{k}_G \end{bmatrix}, \\ \mathbf{A}_1 &= \mathbf{A}_{1_u} + \mathbf{A}_{1_t}, \\ \mathbf{A}_{1_u} &= \begin{bmatrix} \alpha(I_{y1} - m_1) \mathbf{k}_E + (\delta P - \alpha m_1 P_E) \mathbf{k}_G & L \mathbf{h}_1 \\ -L \mathbf{h}_1 & \alpha(I_{x1} - m_1) \mathbf{k}_E + (\delta P - \alpha m_1 P_E) \mathbf{k}_G \end{bmatrix}, \\ \mathbf{A}_{1_t} &= \begin{bmatrix} \mathbf{0} & -L(\beta_0 \mathbf{h}_1 + P_E \gamma_0 \mathbf{h}_2 + \gamma_0 \mathbf{h}_3) \\ L(\beta_0 \mathbf{h}_1 + P_E \gamma_0 \mathbf{h}_2 + \gamma_0 \mathbf{h}_3) & \mathbf{0} \end{bmatrix}, \\ \mathbf{D}_1 &= \begin{bmatrix} \xi \mathbf{m} + \eta \mathbf{k}_E & \mathbf{0} \\ \mathbf{0} & \xi \mathbf{m} + \eta \mathbf{k}_E \end{bmatrix}. \end{aligned} \quad (35)$$

Here \mathbf{A}_0 is evaluated at the Eulerian bifurcation point, \mathbf{A}_1 accounts for the (first-order) asymmetry, torque, pretwist, and axial load increment, and \mathbf{D}_1 describes the damping. The eigenvalue problem formally appears as in (17), with matrices updated. By assuming the series expansions (18) for the eigenvalues and eigenvectors, the perturbation (19) is still obtained. The generating problem (19)₁, however, now admits a multiplicity-four zero eigenvalue, in addition to nonzero, purely imaginary, double eigenvalues; therefore $\lambda_0 = 0, \pm i\omega_2, \dots, \pm i\omega_N$. Here the zero eigenvalue can be thought of as produced by the coalescence of two vanishingly small double eigenvalues $\omega_1 = \pm i\varepsilon$, when $\varepsilon \rightarrow 0$. Since only two eigenvectors are associated with the zero eigenvalue, this latter is nonsemisimple (or defective), while the nonzero eigenvalues are semisimple. Therefore:

- (1) When we take $\lambda_0 = i\omega_k$, with $k = 2, \dots, N$, we recover the results of the previous section, that is, (26) for the damped case and (29) for the undamped case.
- (2) When we take $\lambda_0 = 0$, the ε -order perturbation equation (19)₂ becomes

$$(\mathbf{A}_0 + \lambda_0^2 \mathbf{I}) \mathbf{w}_1 = -\mathbf{A}_1 \mathbf{w}_0, \quad (36)$$

that is, *it does not contain the first-order eigenvalue sensitivity* λ_1 . As a consequence, since $\mathbf{A}_1 \mathbf{w}_0$ is generally out of the range of the operator, the

compatibility condition cannot be satisfied and the equation cannot be solved! This means that the series expansion (18) lacks the ability to describe the splitting mechanism of the nonsemisimple eigenvalue, similarly to what happens for coalescent eigenvalues of more general nonconservative systems [Luongo et al. 2000; Seyranian and Mailybaev 2003].

This drawback does not manifest itself when the system is undamped, and the standard form (12) of the eigenvalue problem is used. As a matter of fact, the relevant perturbation equations read

$$\begin{aligned}\varepsilon^0: (A_0 - \mu_0 I)\mathbf{w}_0 &= \mathbf{0}, \\ \varepsilon^1: (A_0 - \mu_0 I)\mathbf{w}_1 &= -(A_1 - \mu_1 I)\mathbf{w}_0.\end{aligned}\tag{37}$$

Now, compatibility for the ε -order equation can be written either for $\mu_0 \neq 0$ or $\mu_0 = 0$. The reason for this different behavior lies in the fact that $\mu_0 = 0$ is a semisimple (not defective!) root for the characteristic equation $\det(A_0) = 0$. Moreover, since $\mu = \mu_0 + \varepsilon\mu_1 + \dots = -\lambda^2$, when $\mu_0 = 0$ then $\lambda = O(\varepsilon^{1/2})$ so that a Puiseux series of the type $\lambda = \varepsilon^{1/2}\lambda_{1/2} + \dots$ must be used, instead of a Maclaurin series. Note that, in (37), μ_1 assumes a different meaning, according to the value of λ_0 ; it is $\mu_1 := -2\lambda_0\lambda_1$ when $\lambda_0 \neq 0$, but it is $\mu_1 := -\lambda_{1/2}^2$ when $\lambda_0 = 0$!

Summarizing: in the undamped case, (29) describes the eigenvalue sensitivities, both for zero and nonzero eigenvalues; in the damped case, (26) describes the sensitivities of the nonzero eigenvalues only. To complete the analysis, we have therefore still to analyze perturbations of the quadruple zero in the damped case.

Perturbation analysis for nonsemisimple zero-eigenvalues. We tackle the problem of finding the sensitivities of the nonsemisimple quadruple zero eigenvalue by using a Puiseux series of order $\varepsilon^{1/2}$, that is,

$$\lambda = \varepsilon^{1/2}\lambda_{1/2} + \varepsilon\lambda_1 + \dots, \quad \mathbf{w} = \mathbf{w}_0 + \varepsilon^{1/2}\mathbf{w}_{1/2} + \varepsilon\mathbf{w}_1 + \dots.\tag{38}$$

This problem is similar to the perturbation of a Jordan block of order 2, admitting just one eigenvector [Luongo 1993; Seyranian and Mailybaev 2003].

To ensure that the damping and bifurcation parameters appear at the same level in the perturbation scheme, we use a different ordering for them, namely

$$(\alpha, L, \delta P) \rightarrow \varepsilon(\alpha, L, \delta P), \quad (\xi, \eta) \rightarrow \varepsilon^{1/2}(\xi, \eta).\tag{39}$$

Accordingly,

$$\begin{aligned}\mathbf{A} &= \mathbf{A}_0 + \varepsilon\mathbf{A}_1 + O(\varepsilon^2), \\ \mathbf{D} &= \varepsilon^{1/2}\mathbf{D}_{1/2} + O(\varepsilon^{3/2}),\end{aligned}\tag{40}$$

where A_0 and A_1 are defined in $(35)_1$ and $(35)_2$, and $D_{1/2}$ coincides with D_1 in $(35)_5$.

The following perturbation equations are found:

$$\begin{aligned}\varepsilon^0: \quad A_0 \mathbf{w}_0 &= \mathbf{0}, \\ \varepsilon^{1/2}: \quad A_0 \mathbf{w}_{1/2} &= \mathbf{0}, \\ \varepsilon^1: \quad A_0 \mathbf{w}_1 &= -(A_1 + \lambda_{1/2}^2 \mathbf{I} + \lambda_{1/2} D_{1/2}) \mathbf{w}_0.\end{aligned}\tag{41}$$

The solution to the ε^0 -equation is still expressed by $\mathbf{w}_0 = U\mathbf{a}$, in which $U = (\mathbf{u}_1, \mathbf{u}_2)$ collects the *real* eigenvectors associated with the zero-eigenvalue. Then, the $\varepsilon^{1/2}$ -order equation admits a similar solution $\mathbf{w}_{1/2} = U\mathbf{b}$, with \mathbf{b} as arbitrary constants, which, however, are inessential to our (truncated) analysis. Finally, the ε^1 -order equation calls for the following compatibility condition to be satisfied:

$$(\hat{A}_1 + \lambda_{1/2} \hat{D}_{1/2} + \lambda_{1/2}^2 \mathbf{I})\mathbf{a} = \mathbf{0},\tag{42}$$

where

$$\hat{A}_1 := U^T A_1 U, \quad \hat{D}_{1/2} := U^T D_{1/2} U.\tag{43}$$

Like in the subcritical analysis the matrix \hat{A}_1 does not depend on the pretwist, which therefore does not influence the stability, even close to the Eulerian load. Equation (42) is an eigenvalue problem in nonstandard form, whose characteristic equation reads

$$\lambda_{1/2}^4 + J_1 \lambda_{1/2}^3 + J_2 \lambda_{1/2}^2 + J_3 \lambda_{1/2} + J_4 = 0,\tag{44}$$

the invariants of which are real and assume the following expressions:

$$\begin{aligned}J_1 &:= \text{tr } \hat{D}_{1/2}, & J_2 &:= \text{tr } \hat{A}_1 + \det \hat{D}_{1/2}, \\ J_3 &:= \det(\hat{A}_1 + \hat{D}_{1/2}) - \det \hat{A}_1 - \det \hat{D}_{1/2}, & J_4 &:= \det \hat{A}_1.\end{aligned}\tag{45}$$

The fourth-degree equation (44) generally admits four roots $\lambda_{1/2}^{(i)}$, $i = 1, \dots, 4$. They describe the bifurcation of the quadruple zero-eigenvalue in four distinct roots $\lambda^{(i)} = \varepsilon^{1/2} \lambda_{1/2}^{(i)} + O(\varepsilon)$. To each of them, a distinct eigenvector $\mathbf{a}^{(i)}$ is associated, so that four distinct eigenvectors $\mathbf{w}^{(i)} = U\mathbf{a}^{(i)} + O(\varepsilon^{1/2})$ are found.

When damping vanishes ($\hat{D}_{1/2} = \mathbf{0}$), then $J_1 = J_3 = 0$, and (44) reduces to

$$\lambda_{1/2}^4 + (\text{tr } \hat{A}_1) \lambda_{1/2}^2 + \det \hat{A}_1 = 0,\tag{46}$$

which is identical to (28), once $\mu_1 = -\lambda_{1/2}^2$ is accounted for, as discussed before. Therefore, the present algorithm, tailored to damped systems, also works for undamped systems.

Stability domains. In evaluating the stability domains, we have to distinguish bifurcations of the lower zero-eigenvalue, governed by (28) or (44) (holding in the undamped and damped cases, respectively), and bifurcations of the higher nonzero eigenvalues, governed by (28) or (24). We will focus our attention on the zero-eigenvalue, and then check the behavior of higher eigenvalues.

Undamped system. Stability requires that μ be real and positive. Since $\mu = \mu_0 + \varepsilon\mu_1^\pm + \dots$, when $\mu_0 = 0$, μ_1^\pm itself must be real and positive (unlike the $P < P_E$ case, in which it only was required to be real). This occurrence is satisfied when

$$\text{tr}^2 \hat{A}_1 - 4 \det \hat{A}_1 > 0, \quad \text{tr} \hat{A}_1 > 0, \quad \det \hat{A}_1 > 0. \quad (47)$$

When these inequalities are written out in terms of bifurcation parameters, they assume the form

$$\begin{aligned} c_\alpha \alpha^2 + c_L L^2 &> 0, \\ b_\alpha \alpha + b_\delta \delta P &> 0, \\ d_L L^2 + d_\alpha \alpha^2 + d_{\alpha\delta} \alpha \delta P + d_\delta \delta P^2 &> 0, \end{aligned} \quad (48)$$

where the b , c , and d are numerical coefficients. For the elliptical cross-section, with $N = 5$, these assume the values shown in Table 2. When the inequalities are replaced by equalities, we obtain the equations of, in order: a pair of planes parallel to the δP -axis (and containing the origin), a plane parallel to the L -axis (ditto); and a cone (with vertex at the origin). The four surfaces bound the three-dimensional domain shown in Figure 3 from different views, where contour plots $P = \text{const.}$ are drawn to facilitate the reading of the image. The equilibrium is stable in the volume subtended by the portion of conical surface represented in the picture. This figure also contains a sketch of the four nearly zero λ -eigenvalues involved in the bifurcation, represented on an $\alpha = \text{const.}$ plane. On the vertical planes two complex conjugate eigenvalues cross the imaginary axes, so that a *dynamic bifurcation occurs*; on the cone surface, a zero eigenvalue crosses the axis, so that a *static bifurcation* takes place; at the two straight lines, intersections of the vertical planes and the cone, the four eigenvalues are coincident at the origin, so that the lines select a codimension-2 family of degenerate systems around which static and dynamic bifurcations are expected to exist. The origin of parameter space is therefore a codimension-3 bifurcation point. The figure also illustrates the mechanisms of bifurcations along three different paths. Along path I (L increasing),

c_α	c_L	b_α	b_δ	d_L	d_α	$d_{\alpha\delta}$	d_δ
6.24	-1	4.94	-1	0.053	1	-0.54	0.055

Table 2. Numerical coefficients in (48).

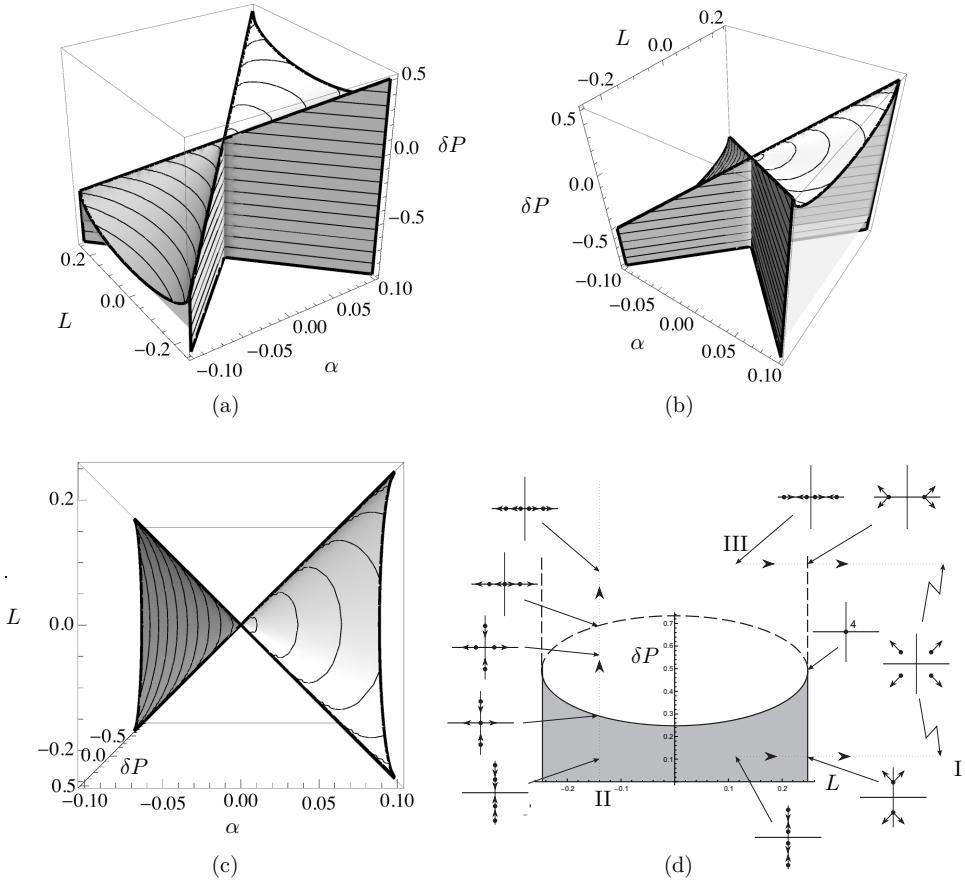


Figure 3. Stability domain in $(\alpha, L, \delta P)$ -space for the undamped system critically loaded: (a)–(c) different views, and (d) sketches of the four nearly zero eigenvalues on the $\alpha = 0.1$ plane.

the eigenvalue behavior is identical to that previously illustrated for the subcritical regime. Along path II (δP increasing), when the conical surface is crossed, two zero eigenvalues occur, splitting in opposite real eigenvalues, while the remaining two eigenvalues are purely imaginary; a successive static bifurcation occurs at the upper branch. Path III illustrates how the velocities of the quadruple zero eigenvalue depend on the region entered by the variation of the parameters.

As a general comment on the effect of the axial load on stability, we observe that, when $\alpha > 0$ (that is, when the beam is stiffened by asymmetries), overcritical states $P > P_E$ can be visited, except for $L = 0$, for which the static bifurcation always occurs at $P = P_E$ in the plane of minimum stiffness. When $\alpha < 0$ (that is, when the beam is weakened by asymmetries) instead, the static bifurcation occurs at a subcritical value $P > P_E$. As a main result, *the axial load is ineffective*

on the critical torque, which only depends on the asymmetry α , thus confirming the weak dependence we found in the subcritical field (recall Figure 1b). The reverse, however, is not true! Indeed, for a given α , a moderately small torque has a beneficial effect on the stability, since it increases the maximum axial load bearable by the beam.

When higher eigenvalues were studied, it was found that the relevant stability domains include that relevant to the first zero-eigenvalue. Therefore stability is only governed by this latter.

Damped system. The damped system is asymptotically stable when its eigenvalues have negative real parts. Since the zero eigenvalue bifurcates into four eigenvalues $\lambda = \varepsilon^{1/2}\lambda_{1/2}^{(i)} + \dots$, we have to require that all of them move to the left part of the complex plane. This is ensured by the conditions stated by the Routh–Hurwitz criterion, when applied to the real-coefficient fourth-degree equation (44), namely

$$\begin{aligned} J_i &> 0, \quad i = 1, \dots, 4, \\ J_1 J_2 - J_3 &> 0, \quad J_1 J_2 J_3 - J_3^2 - J_1^2 J_4 > 0. \end{aligned} \quad (49)$$

Since the damping coefficients are positive, only three out of six conditions are meaningful, and they turn out to be of the following form:

$$\begin{aligned} c_\alpha \alpha + c_\delta \delta P &> 0, \\ b_L L^2 + b_\alpha \alpha^2 + b_{\alpha\delta} \alpha \delta P + b_\delta \delta P^2 &> 0, \\ d_L L^2 + d_\alpha \alpha (d_\xi \xi + d_\eta \eta)^2 + d_{\alpha\alpha} \alpha^2 + d_\delta \delta P (d_\xi \xi + d_\eta \eta)^2 &> 0, \end{aligned} \quad (50)$$

where the b , c , and d 's are numerical coefficients. Their values are reported in Table 3 for an elliptical cross-section and $N = 5$. The relevant stability domain is shown in Figure 4 from different views. By comparing these with Figure 3, it is seen that damping has a smoothing effect close to the vertical axis, as already noticed in the subcritical regime (see Figure 2); moreover, the cone is unaffected by damping. Figure 4 also shows the eigenvalues at the boundaries of the domain, and the different mechanisms of bifurcation. Dynamic and static bifurcations still occur at the lateral surface of the domain and at the cone, respectively, as for the undamped case; however, the coalescence on the imaginary axis, peculiar to circulatory systems, is now destroyed. Similarly, the two intersection lines for the origin are loci of double (no longer quadruple) zero eigenvalues. Analysis of higher eigenvalues confirms that they are not relevant in determining stability.

c_α	c_δ	b_L	b_α	$b_{\alpha\delta}$	b_δ	d_L	d_α	$d_{\alpha\alpha}$	d_δ	d_ξ	d_η
4.94	-1	0.053	1	-0.54	0.055	-1	0.93	6.24	-0.19	1	13.42

Table 3. Numerical coefficients in (50).

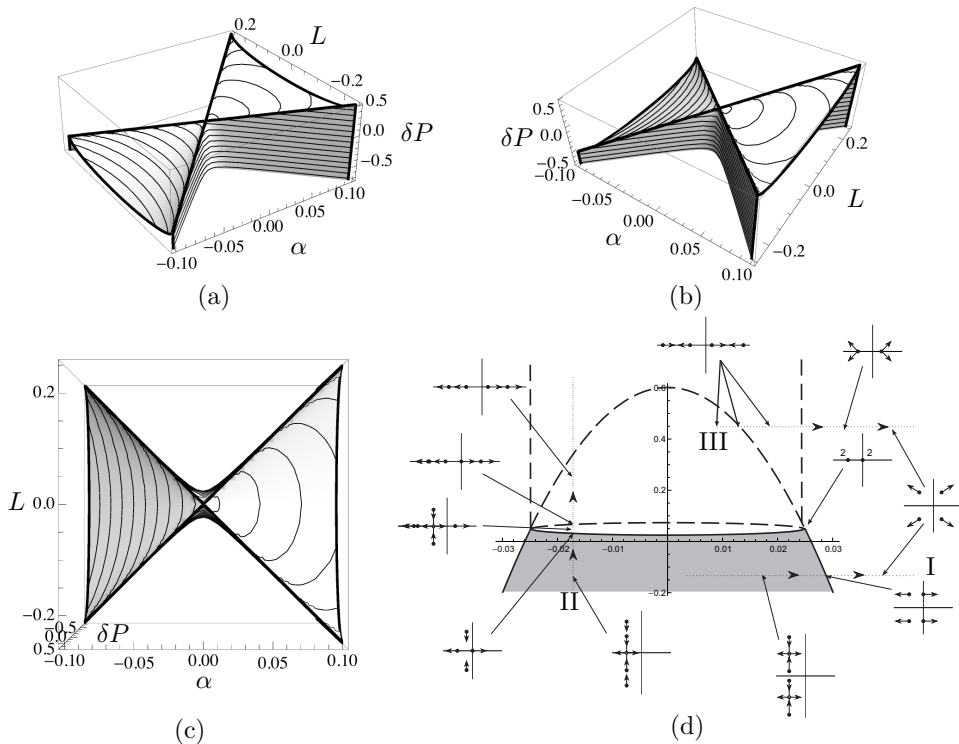


Figure 4. Stability domain in $(\alpha, L, \delta P)$ -space for a damped system critically loaded ($\xi = 0.01$, $\eta = 0.005$): (a)–(c) different views, and (d) sketches of the four nearly zero eigenvalues on the $\alpha = 0.01$ plane.

Comparison between asymptotic and numerical results for the algebraic eigenvalue problem is performed in Figure 5 for some $L = \text{const.}$ cross-sections of the three-dimensional solid domains in Figures 3 and 4. Excellent agreement is found in the regions considered.

5. Conclusions

The Nicolai problem of the stability of a quasisymmetric cantilever beam in three dimensions, loaded by a compressive dead load and a follower torque, has been considered. Attention has been focused on the effects of damping, of both external and internal types, and on the axial load, both lower than or close to the Eulerian critical value. The problem has first been formulated in a strong form, by accounting for the pretwist produced by the torque when the beam is rectilinear, and then recast in a weak form via the Galerkin method, by using the planar eigenmodes of the stress-free beam as trial functions.

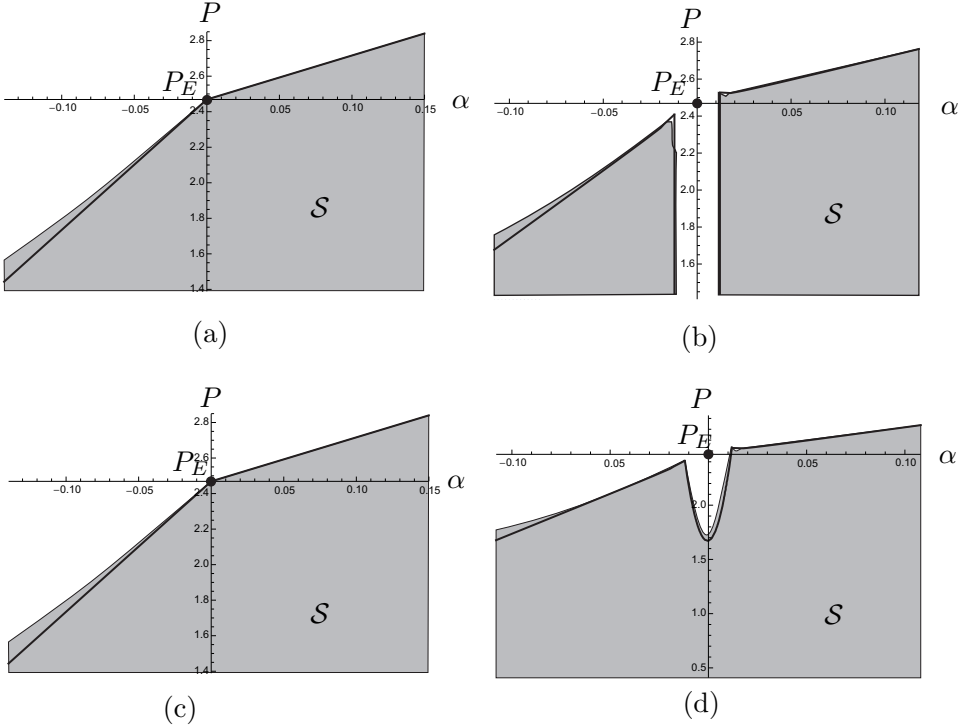


Figure 5. Comparison between asymptotic (thick lines) and numerical (thin lines) stability regions for a critically loaded system: (a) undamped system, $L = 0$; (b) undamped system, $L = 0.03$; (c) damped system ($\xi = 0.01$, $\eta = 0.005$), $L = 0$; (d) damped system ($\xi = 0.01$, $\eta = 0.005$), $L = 0.03$.

The eigenvalue problem, governing the motion around the rectilinear configuration, has been derived, both in nonstandard form (for damped systems) and in standard form (for undamped systems). Perturbation methods have been used to solve it, and are able to analytically describe the dependence of the eigenvalues on the bifurcation parameters. An ideally undamped symmetric system, consisting of a beam with equal geometrical characteristics in the two principal planes of inertia, axially loaded but free of torque, has been considered as the generator system for the perturbation process. The unperturbed eigenvalues, due to the symmetry, are double semisimple purely imaginary eigenvalues associated with two independent eigenvectors, each describing an oscillation mode in a different inertial plane. An exception, however occurs at the Eulerian load, where two semisimple eigenvalues coalesce at zero, thus giving rise to a quadruple non-semisimple root, at which only two eigenvectors are associated (the buckling modes in the two planes).

Accordingly, while semisimple eigenvalues can be tackled by standard perturbation methods, entailing the use of Taylor series, the nonsemisimple zero eigenvalue calls for the use of Puiseux series. In undamped systems, however, the overdegeneracy of the quadruple eigenvalue does not entail any drawbacks, if the eigenvalue problem is stated in standard form, since here it still appears as semisimple.

Stability domains have been built up both for subcritically loaded beams, in the two-dimensional (asymmetry and torque) parameter plane, and for critically loaded beams in the three-dimensional (asymmetry-torque-load) parameter space. The following main results have been drawn.

The stability domains are governed mostly by bifurcations of the lowest eigenvalue of the ideal system, purely imaginary or zero. Therefore, although higher eigenvalues can bifurcate into unstable eigenvalues, this happens in regions of parameters which are already unstable, due to bifurcation of the lowest eigenvalue. However, special systems have been detected in a narrow region of the damping parameters plane in which the second mode is leading.

In the subcritical range, the stability domain of the undamped system is a portion of the plane bounded by two straight lines passing through the origin and including the asymmetry axis. Therefore, if the system is symmetric, an evanescent torque causes instability (the Nicolai paradox); however, finite small asymmetries entail a finite (but small) threshold of the torque, which increases with the asymmetry. The straight lines are loci of systems admitting a double semisimple eigenvalue. When they are crossed from the inside, a dynamic bifurcation takes place. When damping is added, the lines change in smooth curves external to the origin, so that a finite critical torque exists even for symmetric systems, that is, damping has a stabilizing effect, which destroys the paradox of Nicolai. The effect of the axial load on the torque is weak.

In the critical range, the stability domain is a portion of the space which is bounded by three planes and a conical surface. Both static and dynamic bifurcations can occur through these surfaces. Axial loads have no effect on the critical torque, which only depends on the asymmetry magnitude. In contrast, a small torque has a beneficial effect on the static instability triggered by the axial force. When damping is introduced, the sharp edges of the stability domain are smoothed, and a stabilizing effect on the dynamic instability is produced.

In a remarkable result, the stability of the Nicolai beam has been found not to depend on the pretwist, to a first-order approximation, neither in the subcritical nor in the critical range.

Asymptotic analysis gives results in excellent agreement with numerical solutions of the algebraic eigenvalue problem relevant to the discretized beam.

Appendix A: Geometrical characteristics of perturbed cross-sections

Let us consider a cross-section having identical elastogeometrical characteristics with respect to the principal axes x and y . When one of the two major dimensions is perturbed by a small nondimensional parameter $\|\alpha\| \ll 1$, its characteristics modify into

$$\begin{aligned} A &= A_0 + \alpha A_1, & I_x &= I_0 + \alpha I_{x_1}, \\ I_y &= I_0 + \alpha I_{y_1} + O(\alpha^2), & J &= J_0 + \alpha J_1 + O(\alpha^2). \end{aligned} \quad (\text{A.1})$$

Since the mass per unit length is proportional to the area, it is

$$m = m_0 + \alpha m_1, \quad (\text{A.2})$$

where $m_0 = m_1 = A_0 \varrho$, ϱ being the density. The magnitudes m_0 and I_0 have been used in (3) to define nondimensional quantities. Two examples are given here.

Elliptical cross-section. A slightly eccentric ellipse is considered, with half-axes $a = R(1 + \alpha)$ and $b = R$, along x and y , respectively. When $\alpha = 0$, the cross-section becomes circular with radius R . The (dimensional) geometric characteristics read as in (A.1), where

$$\begin{aligned} A_0 &:= \pi R^2, & I_0 &:= \frac{\pi R^4}{4}, & J_0 &:= \frac{\pi R^4}{2}, \\ A_1 &:= \pi R^2, & I_{x_1} &:= \frac{\pi R^4}{4}, & I_{y_1} &:= \frac{3\pi R^4}{4}, & J_1 &:= \pi R^4. \end{aligned} \quad (\text{A.3})$$

Consequently, the nondimensional geometrical characteristics and mass per unit length reads

$$\begin{aligned} \tilde{I}_x &= 1 + \alpha, & \tilde{I}_y &= 1 + 3\alpha + O(\alpha^2), \\ \beta &= \beta_0 + O(\alpha^2), & \gamma &= \gamma_0(1 - 2\alpha) + O(\alpha^2), & \tilde{m} &= 1 + \alpha, \end{aligned} \quad (\text{A.4})$$

where $\beta_0 := 2E/G$ and $\gamma_0 := E/G$.

Rectangular cross-section. We consider a rectangle of sides $a = h(1 + \alpha)$ and $b = h$, along x and y , respectively. When $\alpha = 0$, the cross-section becomes a square, of side h . The (dimensional) geometric characteristics are given by (A.1), where

$$\begin{aligned} A_0 &:= h^2, & I_0 &:= \frac{h^4}{12}, & J_0 &:= 0.141h^4, \\ A_1 &:= h^2, & I_{x_1} &:= \frac{h^4}{12}, & I_{y_1} &:= \frac{h^4}{4}, & J_1 &:= 0.141h^4, \end{aligned} \quad (\text{A.5})$$

and the corresponding nondimensional quantities become

$$\begin{aligned}\tilde{I}_x &= 1 + \alpha, & \tilde{I}_y &= 1 + 3\alpha + O(\alpha^2), \\ \beta &= \beta_0 + O(\alpha), & \gamma &= \gamma_0 + O(\alpha), & \tilde{m} &= 1 + \alpha,\end{aligned}\tag{A.6}$$

where $\beta_0 := 2.364E/G$ and $\gamma_0 := 1.182E/G$.

Appendix B: Trial functions used in the Galerkin projection

The trial functions used in (6) are taken as the modes of the free oscillations of a planar unstressed cantilever. The relevant boundary value problem is

$$\phi^{IV} - \omega^2\phi = 0, \quad \phi(0) = \phi'(0) = \phi''(1) = \phi'''(1) = 0,\tag{B.1}$$

where ω is a nondimensional natural frequency. The solution reads

$$\phi(z) = c \left\{ \sin(\gamma z) - \sinh(\gamma z) - \frac{[\sin(\gamma) + \sinh(\gamma)][\cos(\gamma z) - \cosh(\gamma z)]}{\cos(\gamma) + \cosh(\gamma)} \right\},\tag{B.2}$$

where $\gamma := \sqrt{\omega}$ is a root of the characteristic equation

$$\cos(\gamma) \cosh(\gamma) + 1 = 0.\tag{B.3}$$

Moreover c is an arbitrary constant, to be determined via the normalization condition

$$\int_0^1 \phi^2(z) dz = 1.\tag{B.4}$$

Table 4 reports the values of γ and c for the first five modes. The eigenfunctions satisfy the orthogonality conditions:

$$\int_0^1 \phi_i \phi_j dz = \delta_{ij}, \quad \int_0^1 \phi_i'' \phi_j'' dz = \delta_{ij} \omega_i^2,\tag{B.5}$$

where δ_{ij} is the Kronecker symbol.

	1	2	3	4	5
γ	1.8751	4.6941	7.8548	10.9955	14.1372
c	0.734098	1.018460	0.999220	1.000040	0.999996

Table 4. Values of γ and c in (B.2) for the first five modes.

Appendix C: Equations of motion

The motion of the beam, taking into account inertial effects, is governed by the following equations, derived in [Bolotin 1963]:

$$\begin{aligned}
 T'_x - \tilde{\kappa}_z T_y - \kappa_y P + f_x &= 0, \\
 T'_y + \tilde{\kappa}_z T_x + \kappa_x P + f_y &= 0, \\
 M'_x - \tilde{\kappa}_z M_y + \kappa_y L - T_y &= 0, \\
 M'_y + \tilde{\kappa}_z M_x - \kappa_x L + T_x &= 0,
 \end{aligned} \tag{C.1}$$

where T_x and T_y are the shear forces, M_x and M_y are the bending moments, $f_x = -m\ddot{u}$ and $f_y = -m\ddot{v}$ are the inertial forces, κ_x and κ_y are the curvatures of the beam in the two principal inertial planes, and $\tilde{\kappa}_z = L/(GJ)$ is the pretwisting angle. All other symbols and notations appearing in the previous and subsequent equations are the same as those specified in Section 1.

The kinematic relations are [Bolotin 1963]

$$\varphi = -v' - \tilde{\kappa}_z u, \quad \psi = u' - \tilde{\kappa}_z v, \quad \kappa_x = \varphi' - \tilde{\kappa}_z \psi, \quad \kappa_y = \psi' + \tilde{\kappa}_z \varphi, \tag{C.2}$$

where φ and ψ are the rotations. From these, the curvatures are expressed in terms of displacements:

$$\begin{aligned}
 \kappa_x &= -v'' - 2\tilde{\kappa}_z u' + \tilde{\kappa}_z^2 v, \\
 \kappa_y &= u'' - 2\tilde{\kappa}_z v' - \tilde{\kappa}_z^2 u.
 \end{aligned} \tag{C.3}$$

To account for internal damping, the longitudinal unit strain is written as $\varepsilon = \kappa_x y - \kappa_y x$. By using the Kelvin–Voigt constitutive law, that is, $\sigma = E\varepsilon + \eta\dot{\varepsilon}$, where σ is the normal stress, ε the longitudinal unit strain, and η the viscosity coefficient, and integrating over the area A of the cross-section, we find

$$\begin{aligned}
 M_x &= \int_A \sigma y \, dA = EI_x \kappa_x + \eta I_x \dot{\kappa}_x, \\
 M_y &= - \int_A \sigma x \, dA = EI_y \kappa_y + \eta I_y \dot{\kappa}_y.
 \end{aligned} \tag{C.4}$$

Then, differentiating the last two equations of (C.1) with respect to the space variable and using (C.4) and (C.1) (solved with respect to T'_x , T'_y , T_x , and T_y), we obtain

$$\begin{aligned}
 EI_x \kappa_x'' + (L - 2\tilde{\kappa}_z EI_y) \kappa_y' + (P - \tilde{\kappa}_z^2 EI_x + \tilde{\kappa}_z L) \kappa_x \\
 + \eta EI_x \dot{\kappa}_x'' - 2\tilde{\kappa}_z \eta I_y \dot{\kappa}_y' - \tilde{\kappa}_z^2 \eta I_x \dot{\kappa}_x + f_y &= 0, \\
 EI_y \kappa_y'' - (L - 2\tilde{\kappa}_z EI_x) \kappa_x' + (P - \tilde{\kappa}_z^2 EI_y + \tilde{\kappa}_z L) \kappa_y \\
 + \eta EI_x \dot{\kappa}_y'' + 2\tilde{\kappa}_z \eta I_x \dot{\kappa}_x' - \tilde{\kappa}_z^2 \eta I_y \dot{\kappa}_y - f_x &= 0.
 \end{aligned} \tag{C.5}$$

These equations are further simplified by assuming (see [Seyranian et al. 2014]) that the displacements, curvatures, pretwisting $\tilde{\kappa}_z$, torque, and viscosity coefficient are small quantities of the first order, while third- and higher-order terms are neglected. By adding an external damping ξ , which accounts for the interaction of the beam with the surrounding air, the field equations (1) follow.

The boundary conditions at the clamped end of the beam require that the displacements u and v and rotations φ and ψ vanish (by (2)₂). The boundary conditions at the free end require that the bending moments vanish:

$$M_x = 0, \quad M_y = 0, \quad (\text{C.6})$$

and that the shear forces equate the projection of the gravitational force onto the principal inertial axes in the current configuration:

$$T_x = P\psi, \quad T_y = -P\varphi. \quad (\text{C.7})$$

By using (C.4) and (C.3) in (C.6) and linearizing, (2)₂ are obtained; then, by using (C.1)₃, (C.1)₄, (C.3), (C.4), and (C.6) and linearizing, (2)₃ follow.

Appendix D: Independence of stability of the pretwist

We prove that, to the first asymptotic order, the stability of the Nicolai beam does not depend on the pretwist. To this end, it will be sufficient to prove that the contribution of the pretwist to the matrix \hat{A}_1 that appears in (23) and (43) vanishes.

Remembering that $A_1 = A_{1_u} + A_{1_t}$, (see (16)₂ and (35)₂), we obtain

$$\hat{A}_1 = U^T A_{1_u} U + U^T A_{1_t} U.$$

Since, moreover,

$$U = \begin{bmatrix} \mathbf{w} & \mathbf{0} \\ \mathbf{0} & \mathbf{w} \end{bmatrix},$$

the contribution of the pretwist to \hat{A}_1 is

$$\begin{aligned} & U^T A_{1_t} U \\ &= L \begin{bmatrix} \mathbf{0} & \mathbf{w}^T ((\beta_0 \mathbf{h}_1 + P_E \gamma_0 \mathbf{h}_2 + \gamma_0 \mathbf{h}_3)) \mathbf{w} \\ -\mathbf{w}^T ((\beta_0 \mathbf{h}_1 + P_E \gamma_0 \mathbf{h}_2 + \gamma_0 \mathbf{h}_3)) \mathbf{w} & \mathbf{0} \end{bmatrix}. \quad (\text{D.1}) \end{aligned}$$

By using definition (10)₅ for the \mathbf{h}_2 matrix, integrating by parts, and using the geometric boundary conditions, it is easy to check that $h_{2_{ij}} = -h_{2_{ji}}$, that is, that \mathbf{h}_2 is antisymmetric. Analogously, by considering the matrix $\beta_0 \mathbf{h}_1 + \gamma_0 \mathbf{h}_3$, with \mathbf{h}_1 and \mathbf{h}_3 given by (10)₄ and (10)₆, accounting for $\beta_0 = 2\gamma_0$, integrating by parts and using the mechanical boundary conditions satisfied by the trial functions adopted, it follows that $2h_{1_{ij}} + h_{3_{ij}} = -2h_{1_{ji}} - h_{3_{ji}}$, that is, $\beta_0 \mathbf{h}_1 + \gamma_0 \mathbf{h}_3$ is antisymmetric. Therefore, the off-diagonal blocks in (D.1), and therefore the matrix itself, vanish.

Acknowledgments

This work was supported by a grant from the Italian Ministry of Education, Universities and Research, under the PRIN10-11 program, project N. 2010MBJK5B. Seyranian expresses his gratitude for the scientific visit to University of L'Aquila in June and July of 2012, supported by Regional Funds PO FSE Abruzzo 2007–2013.

References

- [Bolotin 1963] V. V. Bolotin, *Nonconservative problems of the theory of elastic stability*, Pergamon, New York, 1963.
- [Leipholz 1974] H. H. E. Leipholz, “On the convergence of Ritz and Galerkin’s method in the case of certain nonconservative systems and using admissible coordinate functions”, *Acta Mech.* **19**:1-2 (1974), 57–76.
- [Luongo 1993] A. Luongo, “Eigensolutions sensitivity for nonsymmetric matrices with repeated eigenvalues”, *AIAA J.* **31**:7 (1993), 1321–1328.
- [Luongo et al. 2000] A. Luongo, A. Paolone, and A. Di Egidio, “Sensitivities and linear stability analysis around a double-zero eigenvalue”, *AIAA J.* **38**:4 (2000), 702–710.
- [Nicolai 1928] E. L. Nicolai, “Об устойчивости прямолинейной формы равновесия сжатого и скрученного стержня (On the stability of the rectilinear equilibrium shape of a rod under compression and torsion)”, *Izvestiia Leningradskogo Politehnicheskogo Instituta Imeni M. I. Kalinina* **31** (1928), 201–231. Reprinted as pp. 356–387 in his Труды по механике (*Mechanical works*), Gostekhizdat, Moscow, 1955.
- [Nicolai 1929] E. L. Nicolai, “К вопросу об устойчивости скрученного стержня (On the stability problem for a rod under torsion)”, *Vestnik Mekhaniki i Prikladnoi Matematiki* **1** (1929), 41–58. Reprinted as pp. 388–406 in his Труды по механике (*Mechanical works*), Gostekhizdat, Moscow, 1955.
- [Seyranian and Mailybaev 2003] A. P. Seyranian and A. A. Mailybaev, *Multiparameter stability theory with mechanical applications*, Series on Stability, Vibration and Control of Systems, Series A **13**, World Scientific, River Edge, NJ, 2003.
- [Seyranian and Mailybaev 2011] A. P. Seyranian and A. A. Mailybaev, “Paradox of Nicolai and related effects”, *Z. Angew. Math. Phys.* **62**:3 (2011), 539–548.
- [Seyranian et al. 2014] A. P. Seyranian, A. Di Egidio, A. Contento, and A. Luongo, “Solution to the problem of Nicolai”, *J. Sound Vib.* **333**:7 (2014), 1932–1944.
- [Zienkiewicz et al. 2005] O. C. Zienkiewicz, R. L. Taylor, and J. Z. Zhu, *The finite element method: its basis and fundamentals*, 6th ed., Butterworth-Heinemann, Oxford, 2005.

Received 7 Mar 2013. Revised 13 Nov 2013. Accepted 31 Dec 2013.

ANGELO LUONGO: angelo.luongo@univaq.it

Dipartimento di Ingegneria Civile, Edile-Architettura e Ambientale, Università degli studi dell’Aquila, Via Giovanni Gronchi 18, Zona industriale di Pile, 67100 L’Aquila, Italy

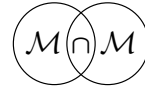
MANUEL FERRETTI: manuel.ferretti@univaq.it

Dipartimento di Ingegneria Civile, Edile-Architettura e Ambientale, Università degli studi dell’Aquila, Via Giovanni Gronchi 18, Zona industriale di Pile, 67100 L’Aquila, Italy

ALEXANDER P. SEYRANIAN: aseyranian@mail.ru

Institute of Mechanics, Moscow State Lomonosov University, Michurinsky pr. 1, Moscow, 119192, Russia





RESPONSES OF FIRST-ORDER DYNAMICAL SYSTEMS TO MATÉRN, CAUCHY, AND DAGUM EXCITATIONS

LIHUA SHEN, MARTIN OSTOJA-STARZEWSKI AND EMILIO PORCU

The responses of dynamical systems under random forcings is a well-understood area of research. The main tool in this area, as it has evolved over a century, falls under the heading of stochastic differential equations. Most works in the literature are related to random forcings with a known parametric spectral density. This paper considers a new framework: the Cauchy and Dagum covariance functions indexing the random forcings do not have a closed form for the associated spectral density, while allowing decoupling of the fractal dimension and Hurst effect. On the basis of a first-order stochastic differential equation, we calculate the transient second-order characteristics of the response under these two covariances and make comparisons to responses under white, Ornstein–Uhlenbeck, and Matérn noises.

1. Introduction

A vast amount of research in mathematics, physics, and mechanics has, since the time of Einstein, Langevin, and Smoluchowski, been motivated by the responses of dynamical systems under random forcings. The main tool used in this area, as it has evolved over a century of investigations, falls under the heading of stochastic differential equations. While it seems that linear stochastic dynamical systems (that is, those governed by linear differential equations) form a very well-established body of knowledge, the subject of such systems driven by wide-sense stationary (WSS) random noises with no Fourier transforms has not been explored. The point is that, when dealing with a WSS process, all studies tacitly assume a spectral density exists. However, this is not that case with WSS processes — and, generally, WSS random fields in \mathbb{R}^3 — with either Cauchy [Gneiting and Schlather 2004] or Dagum [Porcu et al. 2007] covariance functions. An additional intriguing fact about the Cauchy and Dagum functions is that they can model fractal as well as Hurst effects. Roughly speaking, the former is a roughness measure of a profile

Communicated by Antonio Carcaterra.

MSC2010: primary 34F05, 60H10; secondary 28A80, 62H10.

Keywords: random dynamical system, stochastic ordinary differential equation, fractal, Hurst effect.

(that is, a realization on the real line) or surface of \mathbb{R}^n , whilst the latter reflects possible long-memory dependence in a time series or a random field.

The celebrated works [Matheron 1965; Stein 1999; Christakos 2000] (along with the references therein) illustrate how several properties of random fields enjoying Cauchy or Dagum covariance can be studied through their correlation functions. In particular, the local and global behavior is sketched in the next sections.

While fractals are quite well known as “those enchanting, self-similar things” [CFA], the Hurst effect, being less well known, warrants a few words here. The effect is modeled by an exponent H , which, in the context of a time series, is a measure of long-term memory. While $0 < H < 0.5$ indicates a time series with negative autocorrelation (for example, a decrease between values will likely be followed by an increase), $0.5 < H < 1$ indicates a time series with positive autocorrelation (an increase between values followed by another increase). The case $H = 0.5$ indicates a true random walk, where there is no preference for a decrease or increase following any particular value.

We consider the transient response of a linear, time-invariant system obeying the equation

$$\begin{aligned} cX' + kX &= c(\beta + \gamma t)U(t)F(t), \\ X(0) &= 0, \end{aligned} \tag{1}$$

to a wide-sense stationary random excitation $F(t)$ having either a white noise, Ornstein–Uhlenbeck (OU), Matérn, Cauchy, or Dagum covariance function. In (1) c, k, β , and γ are deterministic constants, while $U(t)$ is the Heaviside function:

$$U(t) := \begin{cases} 1 & \text{if } t \geq 0, \\ 0 & \text{if } t < 0. \end{cases} \tag{2}$$

Letting $a = k/c$ and $Y(t) = (\beta + \gamma t)U(t)F(t)$ we have

$$X' + aX = Y(t). \tag{3}$$

It is easy to see that the specific solution $X(t)$ of the above ordinary differential equation can be expressed as

$$X(t) = \int_0^t h_a(t - \tau)Y(\tau) d\tau, \tag{4}$$

where $h_a(t) = e^{-at}U(t)$, $a > 0$, is the elementary solution of this ordinary differential equation. We assume that $\mathbb{E}[F(t)] = 0$, which in turn implies $\mathbb{E}[X(t)] = 0$. For simplicity, we shall make use of the special case $\beta = 1$, $\gamma = 0$ in most parts of the paper, without loss of generality.

Our objective in this study is to determine the second-order characteristics of $X(t)$ (and make relative comparisons), assuming that $F(t)$ is a Gaussian random process with either a white noise, OU, Matérn [Matérn 1986], generalized Cauchy

[Gneiting and Schlather 2004], or Dagum [Porcu et al. 2007] covariance function. The intriguing thing about generalized Cauchy and Dagum covariances is that they are natural decouplers of fractal dimension and Hurst effects, in the sense that the associated Gaussian random process is not self-similar. This, in turn, has considerable advantages from the statistical viewpoint, since the parameters indexing fractal dimension and the Hurst effect can be estimated separately. For many facts on these classes of covariance functions and their properties in terms of fractal dimension and the Hurst effect, the reader is referred to the survey in [Porcu and Stein 2012].

Of course, white noise and Matérn have no Hurst effects (and white noise is not even a fractal). We include them in our study because the former is the most well-known random noise, while the latter is proposed as superior for multiscale modeling.

The plan of the paper is as follows: In Section 2 we review the basic facts on the covariance functions of Cauchy and Dagum types, including their fractal dimensions and Hurst effects. In Sections 3 and 4, respectively, we compute the variance and correlation structure of responses $X(\cdot)$ for five different random forcings $F(\cdot)$.

2. Background

2.1. Covariance functions, fractal dimension, and the Hurst effect. This section is largely expository and reports the basic facts needed for a better understanding of the subsequent sections. As stated through Section 1, the process $F(\cdot)$ in (1) is a zero-mean second-order stationary Gaussian random process defined on the real line, so that its distribution is completely specified by its associated covariance function $C(\cdot, \cdot) : \mathbb{R} \times \mathbb{R} \rightarrow \mathbb{R}$, defined as

$$C(t_1, t_2) := \text{Cov}(F(t_1), F(t_2)), \quad t_1, t_2 \in \mathbb{R}.$$

As a consequence of the assumption of second-order stationarity, there exists a mapping $C_F : \mathbb{R}_+ \cup \{0\} \rightarrow \mathbb{R}$ such that

$$C(t_1, t_2) = C_F(|t_1 - t_2|).$$

Such a framework allows us to identify some important properties of the random processes we want to study.

The local properties of a time series or a surface of \mathbb{R}^n are related to the fractal dimension, D , which is a roughness measure with range $[n, n + 1)$. Higher values indicate rougher surfaces. Long memory in a time series or spatial data is associated with power law correlations, and is often referred to as the Hurst effect.

Long-memory dependence is characterized by the H parameter [Mateu et al. 2007]. Let us see how these properties relate to those of the associated correlation function.

As far as the local behavior is concerned, in the weakly stationary (read: second-order stationary) case, if, for some $\alpha \in (0, 1)$,

$$\lim_{r \rightarrow 0} (C_F(0) - C_F(r))r^{-\alpha} = K, \quad 0 < K < \infty, \quad r > 0, \quad (5)$$

then, with probability one, the random process $F(\cdot)$ satisfies

$$D = \dim(\text{Gr } F) = \min\left(\frac{1}{\alpha/2}, 1 - \alpha/2\right),$$

where, as before, C_F denotes the covariance function of F . Here, $\text{Gr } F$ denotes $\text{graph}(F) = \{(t, F(t)), t \in [-1, 1]\} \subset \mathbb{R}^2$. Thus, the estimate of α determines that of the fractal dimension D . Equation (5) refers to the issue of scaling laws, which describe the way in which rather elementary measurements vary with the size of the measurement unit, and we refer to [Hall and Wood 1993] for a detailed analysis of the relation between the fractal index α and the fractal dimension D , as well as to the work in [Adler 1981] on Gaussian index- β random fields, with $\beta = \alpha/2$ in this case.

On the other hand, if, for some $\beta \in (0, 1)$,

$$\lim_{r \rightarrow \infty} C_F(r)r^{-1+\beta} = 1, \quad (6)$$

then the process is said to have long memory, with Hurst coefficient $H = \beta/2$. For $H \in (1/2, 1)$ or $H \in (0, 1/2)$ the correlation is said to be, respectively, persistent or antipersistent. In the spectral domain, under the conditions stated in the tauberian and abelian theorems, the interpretation of parameters α and β is given in the opposite fashion, so that the same properties can be studied with respect to the Fourier transform of the covariance function, called the spectral density. Basically, the parameter α is associated with the velocity of decay of the spectral density, while the parameter β is associated with the local behavior of the spectral density in the neighborhood of zero frequencies.

2.2. Parametric classes for the process $F(\cdot)$. Throughout the paper we shall examine how the response $X(\cdot)$ is affected by random excitation and in what ways it is sensitive to specific classes of covariance functions that allow (or don't allow) it to index fractal dimensions and the Hurst effect. We shall make use of the following functions:

- (i) *White noise.* In this case F is a Gaussian white noise, and its covariance is written as

$$C_{\text{WN}}(r) := \delta(r), \quad r \geq 0, \quad (7)$$

with δ denoting the Dirac delta function.

- (ii) *Ornstein–Uhlenbeck*. In this case F is an Ornstein–Uhlenbeck process (denoted $F = \text{OU}$), and its covariance function is of the negative exponential type. It is written as follows:

$$C_{\text{OU}}(r; \nu) := \frac{\nu}{2} e^{-\nu r}, \quad r \geq 0, \quad (8)$$

where ν is a positive scaling parameter and where we parametrized C_{OU} in such a way that

$$\lim_{\nu \rightarrow \infty} C_{\text{OU}}(\cdot; \nu) = C_{\text{WN}}(\cdot).$$

- (iii) *Matérn* [1986]. A Gaussian process F has a Matérn covariance if

$$C_{\mathcal{M}}(r; \nu) := r^\nu \mathcal{K}_\nu(r), \quad r \geq 0, \quad (9)$$

where ν is a parameter that determines the smoothness at the origin of $C_{\mathcal{M}}$, and thus the mean square differentiability of F . Here \mathcal{K}_ν is a modified Bessel function of order ν . Special cases of interest are

- $C_{\mathcal{M}}(r; 1/2) = e^{-r}$,
- $C_{\mathcal{M}}(r; 3/2) = (1 + r)C_{\mathcal{M}}(r; 1/2)$, and
- $C_{\mathcal{M}}(r; 5/2) = (1 + r + 3r^2/2)C_{\mathcal{M}}(r; 1/2)$.

- (iv) *Generalized Cauchy* [Gneiting and Schlather 2004]. In this case,

$$C_{\mathcal{C}}(r; \theta, \eta) := (1 + r^\theta)^{-\eta/\theta}, \quad (10)$$

where $\eta > 0$ and $0 < \theta \leq 2$ are necessary and sufficient conditions for positive definiteness. Special cases of this class will also be of interest. In particular, $C_{\mathcal{C}}(\cdot, 2, \gamma)$ is the characteristic function of the symmetric Bessel distribution, $C_{\mathcal{C}}(\cdot, \alpha, \alpha)$ is the characteristic function of the Linnik distribution, and $C_{\mathcal{C}}(\cdot, 1, \gamma)$ is the symmetric generalized Linnik characteristic function [Ruiz-Medina et al. 2011].

- (v) *Dagum* [Porcu et al. 2007]. In this case,

$$C_{\mathcal{D}}(r; \delta, \epsilon) := 1 - (1 + r^{-\delta})^{-\epsilon/\delta}, \quad (11)$$

where $0 < \epsilon < \delta$ and $0 < \delta \leq 2$ are sufficient conditions for positive definiteness.

Some comments are in order. The Cauchy and Dagum models have been chosen for the present study because they allow us to treat independently the fractal dimension D and the Hurst effect H of their associated random process F . In particular, it can be shown [Gneiting and Schlather 2004] that the Cauchy covariance in (10) behaves like (5) for $\theta \in (0, 2]$ and like (6) for $\eta \in (0, 1)$, whilst the Dagum model in (11) behaves like (5) for $\epsilon \in (0, 2]$ and like (6) for $\delta \in (0, 1)$, although some caution is needed because we work under the restriction $\epsilon \leq \delta$. Anyway, another sufficient condition is $\delta \in (0, 2]$ and $\epsilon \in (0, 1]$ [Mateu et al. 2007]. Another useful

sufficient condition in \mathbb{R}^3 is $\theta < (7 - \epsilon)/(1 + 5\epsilon)$ and $\epsilon < 7$. Since these two models decouple (D, H) , the associated random process will not be self similar in the sense of Mandelbrot, and in general we shall have $D + H \neq 2$ (recall that we are working with profiles here).

The Matérn covariance in (9) indexes the fractal dimension D but has light tails, so that it is not useful for indexing phenomena with long-range dependence.

3. The variance of $X(\cdot)$

Equation (4) implicitly shows that the variance of the response X is evolutionary in time (that is, nonstationary). Assuming $\beta = 1$ and $\gamma = 0$, we have

$$\mathbb{E}[X^2(t)] = \int_0^t \int_0^t C_F(t_1 - t_2) h_a(t - t_1) h_a(t - t_2) dt_1 dt_2, \quad (12)$$

with h_a defined through (4) and where C_F is the covariance function associated with F , which can be one of the five choices proposed in previous section.

Let us now show how these variances vary from one case to another.

(i) *White noise*. If $C_F = C_{\text{WN}}$, the calculation of the variance in (4) is straightforward. In fact, if $F = \text{WN}$ we have $\mathbb{E}[F] = 0$ and $S(\omega) = S_0 < \infty$, where S denotes the Fourier transform of C_{WN} and S_0 is an arbitrary constant. Without loss of generality, we let $S_0 = 1/(2\pi)$ so that

$$\int_{-\infty}^{+\infty} C_{\text{WN}}(t) dt = 1.$$

We thus have (see [Elishakoff 1983, Equation (9.104), p. 348])

$$\mathbb{E}[X^2(t)] = 2\pi S_0 e^{-2at} \left\{ \frac{\beta^2}{2a} (e^{2at} - 1) + 2\beta\gamma \left[\frac{e^{2at}}{4a^2} (2at - 1) + \frac{1}{4a^2} \right] + \frac{\gamma^2}{4a^3} (e^{2at} (2a^2 t^2 - 2at + 1) - 1) \right\}.$$

(ii) *Ornstein–Uhlenbeck*. In the case $F = \text{OU}$, the variance of $X(t)$ is

$$\mathbb{E}[X^2(t)] = \int_0^t \int_0^t C_{\text{OU}}(t_1 - t_2) h_a(t - t_1) h_a(t - t_2) dt_1 dt_2.$$

Direct computation yields the following special cases:

$$\begin{aligned} \text{if } a = \nu = 1, \quad & \mathbb{E}[X^2(t)] = \frac{1}{4} - \frac{1}{4} e^{-2t} (1 + e^{2t}), \\ \text{if } a = 1, \nu \neq 1, \quad & \mathbb{E}[X^2(t)] = \frac{1}{-1 + \nu} e^{-t\nu} \sinh(t), \\ \text{if } a \neq 1, a \neq \nu, \quad & \mathbb{E}[X^2(t)] = \frac{\nu}{2(a^3 - a\nu^2)} [a - \nu + (a + \nu)e^{-2at} - 2ae^{-(a+\nu)t}]. \end{aligned}$$

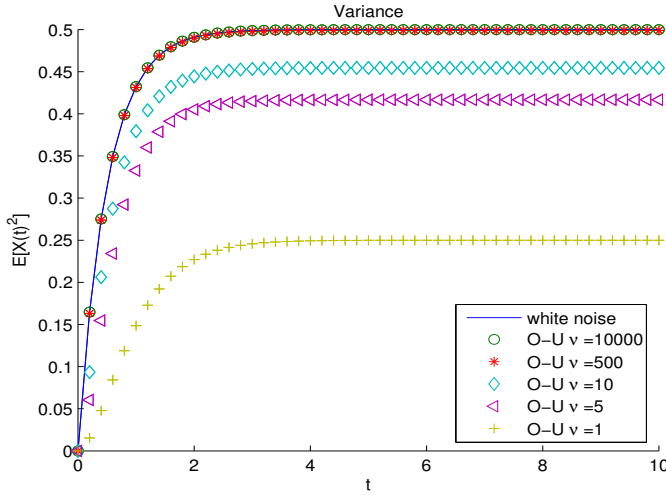


Figure 1. The variances of the response $X(t)$ under white noise and Ornstein–Uhlenbeck (OU) forcings. The white noise curve overlaps with the OU process curves for $\nu = 10,000$ and $\nu = 500$.

Figure 1 depicts $\mathbb{E}[X^2(t)]$ with different values of ν and compares it with the variance from the white noise. Here we let $a = 1$. Note that the variance caused by the OU process goes to the variance caused by the white noise when ν is large enough for $F(t)$ approaching white noise.

(iii) *Matérn*. If $C_F = C_M$, the calculation of the variance is not available in a closed form due to the presence of the modified Bessel function \mathcal{K} in (9). Thus, we choose the case $C_F = C_M(\cdot; 3/2)$ so that, for $a \neq 1$,

$$\begin{aligned} \mathbb{E}[X^2(t)] &= \int_0^t \int_0^t C_M(t_1 - t_2; 3/2) h_a(t - t_1) h_a(t - t_2) dt_1 dt_2 \\ &= \int_0^t \left(\int_0^{t_2} + \int_{t_2}^t \right) C_M(t_1 - t_2; 3/2) e^{-a(t-t_1)} e^{-a(t-t_2)} dt_1 dt_2 \\ &= \frac{a}{(a^2 - 1)^2} [2 - 3a + a^3 \\ &\quad + e^{-2t}(-2 - 3a + a^3) + e^{-t-t/a}(6a - 2a^3 + 2t - 2a^2t)]. \end{aligned}$$

For $a = 1$, a straightforward computation gives

$$\mathbb{E}[X^2(t)] = \frac{1}{4} (3 + e^{-2t}(-2t^2 - 6t - 3)).$$

The same calculations can be performed using the Fourier transform of the Matérn function and then invoking basic Fourier calculus; the details are omitted for the sake of simplicity.

(iv) *Generalized Cauchy*. If $C_F(\cdot) = C_{\mathcal{C}}(\cdot, \theta, \eta)$ then

$$\mathbb{E}[X^2(t)] = \int_0^t \int_0^t C_{\mathcal{C}}(t_1 - t_2; \theta, \eta) h_a(t - t_1) h_a(t - t_2) dt_1 dt_2.$$

For $\theta = \eta = 1$, we get

$$\begin{aligned} \mathbb{E}[X^2(t)] &= \frac{1}{2a} e^{-a(2t+1)} \\ &\quad \times \left[\mathbb{E}_1(-2a(t+1)) - \mathbb{E}_1(-2a) - 2e^{2a(t+1)} (\text{Ei}(-a) - \text{Ei}(-a(t+1))) \right. \\ &\quad \left. - 2\text{Ei}(a(t+1)) + \text{Ei}(2a(t+1)) + 2\text{Ei}(a) - \text{Ei}(2a) \right], \end{aligned}$$

where

$$\text{Ei}(z) := - \int_{-z}^{\infty} e^{-t}/t dt, \quad \mathbb{E}_n(z) := \int_1^{\infty} e^{-zt}/t^n dt.$$

For $\theta = \eta = a = 1$, we obtain

$$\mathbb{E}[X^2(t)] = e(-\text{Ei}(-1) + \text{Ei}(-1-t)) + e^{-(1+2t)}(\text{Ei}(1) - \text{Ei}(1+t)).$$

(v) *Dagum*. If $C_F(\cdot) = C_{\mathcal{D}}(\cdot; \delta, \epsilon)$, we cannot get an explicit formula for $\mathbb{E}[X^2(t)]$, but by numerical computation of (12) using Matlab we obtain the plots in Figure 2.

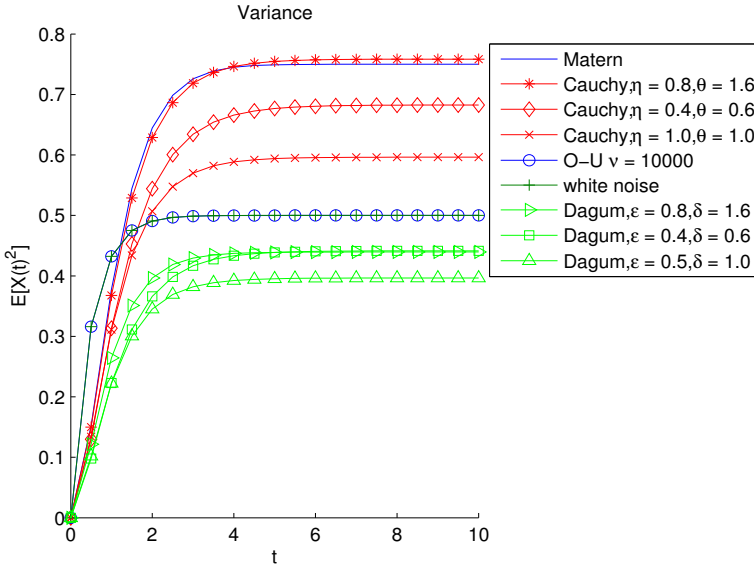


Figure 2. Variances under various forcings: Matérn, Cauchy ($\eta = 0.8$, $\theta = 1.6$; $\eta = 0.4$, $\theta = 0.6$; and $\eta = 1.0$, $\theta = 1.0$), Ornstein–Uhlenbeck ($\nu = 10,000$), white noise, and Dagum ($\epsilon = 0.8$, $\delta = 1.6$; $\epsilon = 0.4$, $\delta = 0.6$; and $\epsilon = 0.5$, $\delta = 1.0$).

4. Correlation structure of the response $X(\cdot)$

The correlation function of the response can be readily calculated as follows (recall that, by construction, $\mathbb{E}[X(\cdot)] = 0$):

$$\begin{aligned}
 C_X(t_1, t_2) &:= \mathbb{E}[X(t_1)X(t_2)] \\
 &= \mathbb{E}\left[\int_0^{t_1} Y(\tau_1)h_a(t_1 - \tau_1) d\tau_1 \int_0^{t_2} Y(\tau_2)h_a(t_2 - \tau_2) d\tau_2\right] \\
 &= \int_0^{t_2} \int_0^{t_1} \mathbb{E}[Y(\tau_1)Y(\tau_2)]h_a(t_1 - \tau_1)h_a(t_2 - \tau_2) d\tau_1 d\tau_2 \\
 &= \int_0^{t_2} \int_0^{t_1} \Psi(\tau_1, \tau_2)C_F(\tau_1, \tau_2)h_a(t_1 - \tau_1)h_a(t_2 - \tau_2) d\tau_1 d\tau_2, \quad (13)
 \end{aligned}$$

where $C_F(\tau_1, \tau_2)$ is the covariance function of $F(t)$ and where

$$\Psi(t_1, t_2) := (\beta + \gamma t_1)(\beta + \gamma t_2)U(t_1)U(t_2).$$

(i) *White noise.* If $C_F = C_{\text{WN}}$, the calculation of C_X can be deduced from (13) and the fact that

$$C_Y(t_1, t_2) = \Psi(t_1, t_2)C_{\text{WN}}(t_1, t_2).$$

Also, keeping in mind that

$$\delta(\tau_1 - \tau_2) = 0 \quad \text{if} \quad \tau_1 \neq \tau_2$$

if $t_1 > t_2$, we see that

$$\begin{aligned}
 C_X(t_1, t_2) &= \int_0^{t_2} \int_0^{t_1} C_Y(\tau_1, \tau_2)h_a(t_1 - \tau_1)h_a(t_2 - \tau_2) d\tau_1 d\tau_2 \\
 &= e^{-a(t_1+t_2)} \int_0^{t_2} (\beta + \gamma \tau_2)^2 e^{2a\tau_2} d\tau_2 \\
 &= e^{-a(t_1+t_2)} \left\{ \frac{\beta^2}{2a}(e^{2at_2} - 1) + 2\beta\gamma \left[\frac{e^{2at_2}}{4a^2}(2at_2 - 1) + \frac{1}{4a^2} \right] \right. \\
 &\quad \left. + \frac{\gamma^2}{4a^3}(e^{2at_2}(2a^2t_2^2 - 2at_2 + 1) - 1) \right\} \\
 &= e^{-a(t_1-t_2)} \mathbb{E}[X(t_2)^2].
 \end{aligned}$$

We can then repeat the same procedure when $t_1 < t_2$ in order to deduce

$$C_X(t_1, t_2) = \begin{cases} e^{-a(t_1-t_2)} \mathbb{E}[X(t_2)^2] & \text{if } t_1 \geq t_2, \\ e^{-a(t_2-t_1)} \mathbb{E}[X(t_1)^2] & \text{if } t_1 < t_2. \end{cases}$$

From the equations above, if we let $\gamma = 0$, we can see that when t_1 and t_2 are large enough,

$$C_X(t_1, t_2) \approx C_X(t_2, t_1) \approx e^{-a|t_1-t_2|} \frac{\beta^2}{2a},$$

which shows that the random process is homogeneous (that is, WSS). We see that this correlation function is different from the correlation function of white noise.

(ii) *Ornstein–Uhlenbeck*. In the case $F = OU$, we determine the correlation function of $X(t)$ as follows.

If $a = \nu = 1$,

$$C_X(t_1, t_2) = \begin{cases} \frac{1}{4} [e^{-t_1+t_2}(t_1 - t_2 + 1) + e^{-t_1-t_2}(-t_1 - t_2 - 1)] & \text{if } t_1 \geq t_2, \\ \frac{1}{4} [e^{-t_2+t_1}(t_2 - t_1 + 1) + e^{-t_2-t_1}(-t_2 - t_1 - 1)] & \text{if } t_1 < t_2, \end{cases}$$

which shows that C_X is symmetric.

If $a = 1$, $\nu \neq 1$, we get

$$C_X(t_1, t_2) = \begin{cases} \frac{\nu e^{-(1+\nu)(t_1+t_2)}}{2(-1+\nu^2)} [e^{\nu t_1+t_2} + e^{t_1+\nu t_2} - e^{t_1+t_2+2\nu t_2} \\ \quad + e^{\nu(t_1+t_2)}(-1-\nu+\nu e^{2t_2})] & \text{if } t_1 \geq t_2, \\ C_X(t_2, t_1) & \text{if } t_1 < t_2. \end{cases}$$

Finally, if $a \neq 1$ and $a \neq \nu$,

$$C_X(t_1, t_2) = \frac{\nu}{2a(a^2 - \nu^2)} [a(e^{-a(t_1+t_2)} - e^{-\nu t_1 - at_2} - e^{-at_1 - \nu t_2} + e^{-\nu(t_1-t_2)}) \\ + \nu(e^{-a(t_1+t_2)} - e^{-a(t_1-t_2)})] \quad \text{if } t_1 \geq t_2,$$

and the symmetric extension follows when $t_1 < t_2$.

Figure 3 shows the correlation function of the response from the OU process. Note that, as ν becomes large, the correlation function of $X(t)$ approaches the covariance of the response to the white noise excitation.

(iii) *Matérn*. If $C_F = C_{\mathcal{M}}(\cdot; \nu = 3/2)$, we can find the autocorrelation function of $X(t)$ by direct inspection. The correlation is symmetric, so we do not give the symmetry extensions for all the cases.

If $a \neq 1$, we easily get

$$C_X(t_1, t_2) = \frac{1}{2a(-1+a^2)^2} \{(-2+a)(1+a)^2 [e^{-2at_2} + e^{-a(t_1+t_2)} - 1] \\ + (-1+a)^2(2+a)e^{-a(t_1-t_2)} - 2a(-3-t_1+a^2(1+t_1))e^{(-1+a)t_1-2at_2} \\ - 2a[-3-t_2+a^2(1+t_2)]e^{-(at_1+t_2)} \\ - 2a[3+t_1-t_2+a^2(-1-t_1+t_2)]e^{(-1+a)(t_1-t_2)}\} \quad \text{if } t_1 \geq t_2.$$

If $a = 1$,

$$C_X(t_1, t_2) = \frac{1}{4} \{ e^{-t_1-t_2} [-3 - 3(t_1 + t_2) - (t_1^2 + t_2^2)] + \frac{1}{4} e^{-(t_1-t_2)} [3 + 3(t_1 - t_2) + (t_1 - t_2)^2] \} \quad \text{if } t_1 \geq t_2.$$

If t_1 and t_2 are large enough,

$$C_X(t_1, t_2) \approx \frac{1}{4} e^{-(t_1-t_2)} [3 + 3(t_1 - t_2) + (t_1 - t_2)^2] \quad \text{if } t_1 \geq t_2,$$

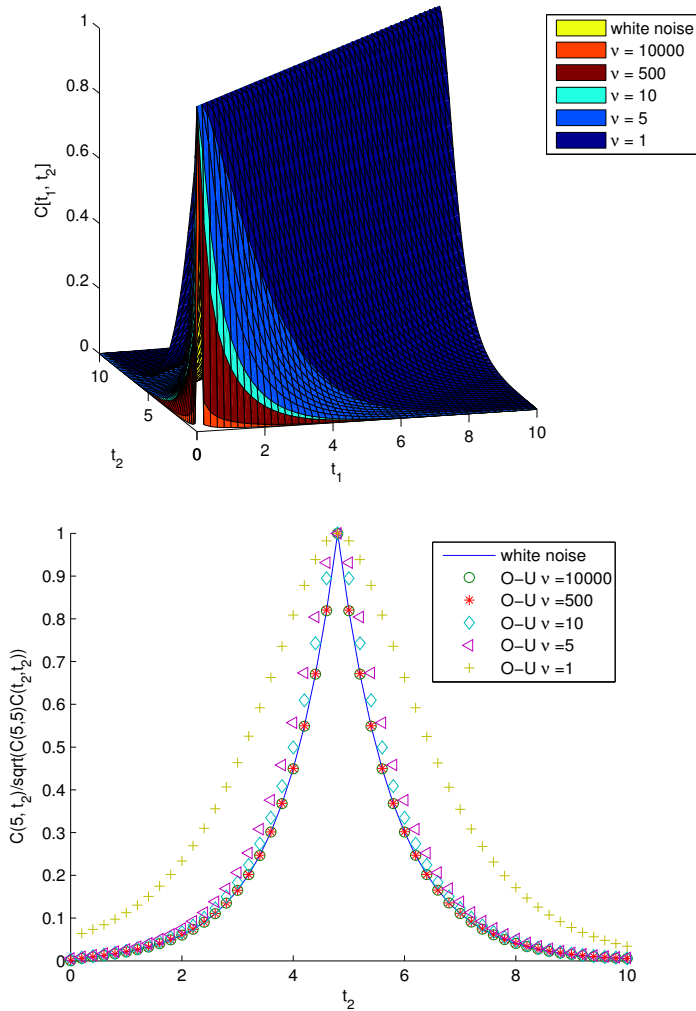


Figure 3. The correlation function under the OU forcings at various ν values (top) and the correlation functions of response $X(t)$ at $t_1 = 5$ under white noise and OU forcings (bottom). The white noise curve overlaps with the OU process curves for $\nu = 10,000$ and 500 .

and the random process is homogeneous, that is, $C_X(t_1, t_2) = C_X(|t_2 - t_1|)$. We also observe that, if the excitation correlation function is Matérn, the correlation function of the response is approximately Matérn.

(iv) *Generalized Cauchy*. If $C_F(\cdot) = C_{\mathcal{C}}(\cdot, \theta, \eta)$ then, if the correlation function of $F(t)$ is Cauchy, we can find the correlation function of $X(t)$ by direct inspection:

$$\begin{aligned} C_X(t_1, t_2) &= \frac{1}{2} e^{-1-t_1-t_2} [2\text{Ei}(1) - \text{Ei}(1+t_2) - \text{Ei}(1+t_1)] \\ &\quad + \frac{1}{2} e^{1-(t_1-t_2)} [-\text{Ei}(-1) + \text{Ei}(-1-t_2)] \\ &\quad + \frac{1}{2} e^{-1-(t_1-t_2)} [-\text{Ei}(1) + \text{Ei}(1+t_1-t_2)] \\ &\quad + \frac{1}{2} e^{1+(t_1-t_2)} [\text{Ei}(-1-t_1) - \text{Ei}(-1-t_1+t_2)] \quad \text{if } t_1 \geq t_2. \end{aligned}$$

Once again, we omit the case $t_1 < t_2$ since it can be deduced by a symmetry extension. Note that, although $\text{Ei}(1+t_1)$ and $\text{Ei}(1+t_2)$ go to $+\infty$ when $t_1, t_2 \rightarrow +\infty$, the function $e^{-1-t_1-t_2}$ decreases more rapidly. Hence, when t_1 and t_2 are large enough, the first term goes to zero. When $t_1, t_2 \rightarrow +\infty$, the functions $\text{Ei}(-1-t_1)$ and $\text{Ei}(-1-t_2)$ are close to zero as well. Therefore, we have

$$\begin{aligned} C_X(t_1, t_2) &\approx \frac{1}{2} e^{1-(t_1-t_2)} [-\text{Ei}(-1)] + \frac{1}{2} e^{-1-(t_1-t_2)} [-\text{Ei}(1) + \text{Ei}(1+t_1-t_2)] \\ &\quad + \frac{1}{2} e^{1+(t_1-t_2)} [-\text{Ei}(-1-t_1+t_2)] \quad \text{if } t_1 \geq t_2. \end{aligned}$$

Now we see that

$$\begin{aligned} C_X(t_1, t_2) &= C_X(t_2, t_1) \approx C_X(|t_1 - t_2|) \\ &= \frac{1}{2} e^{1-|t_1-t_2|} [-\text{Ei}(-1)] + \frac{1}{2} e^{-1-|t_1-t_2|} [-\text{Ei}(1) + \text{Ei}(1+|t_1-t_2|)] \\ &\quad + \frac{1}{2} e^{1+|t_1-t_2|} [-\text{Ei}(-1-|t_1-t_2|)], \end{aligned}$$

or

$$\begin{aligned} C_X(t_1, t_2) &= C_X(t_2, t_1) \approx C_X(r) \\ &= \frac{1}{2} e^{1-r} [-\text{Ei}(-1)] + \frac{1}{2} e^{-1-r} [-\text{Ei}(1) + \text{Ei}(1+r)] \\ &\quad + \frac{1}{2} e^{1+r} [-\text{Ei}(-1-r)], \end{aligned} \tag{14}$$

which means that, when t_1 and t_2 are large enough, the response is homogeneous. Finally, if $r \rightarrow 0$, from Taylor's formula we have

$$\begin{aligned} C_X(r) &= -e\text{Ei}(-1) + \left(-\frac{1}{2} - \frac{1}{2} e\text{Ei}(-1)\right)r^2 + \frac{1}{6}r^3 + \left(-\frac{1}{8} - \frac{1}{24} e\text{Ei}(-1)\right)r^4 + \frac{7}{120}r^5 + O(r^6). \end{aligned}$$

Comparing with the Cauchy function,

$$\frac{1}{1+r} = 1 - r + r^2 - r^3 + r^4 - r^5 + O(r^6),$$

we see that the response from Cauchy excitation is not Cauchy.

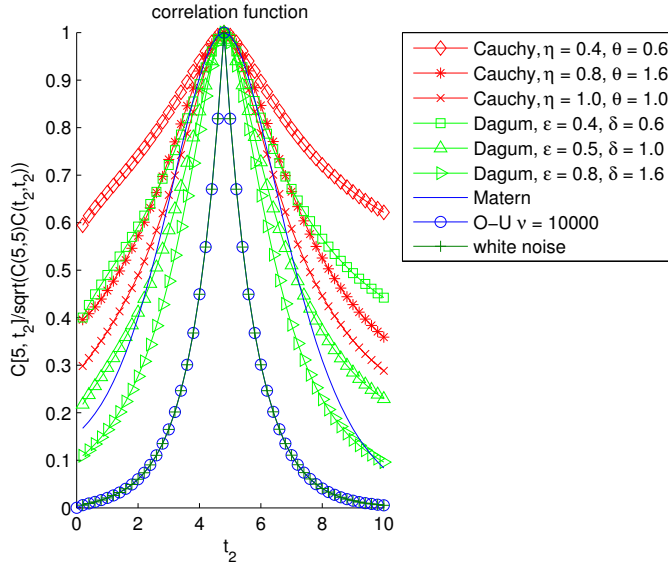


Figure 4. The correlation functions of response $X(t)$ at $t_1 = 5$ under various forcings: Cauchy ($\eta = 0.4, \theta = 0.6$; $\eta = 0.8, \theta = 1.6$; and $\eta = 1.0, \theta = 1.0$), Dagum ($\epsilon = 0.4, \delta = 0.6$; $\epsilon = 0.5, \delta = 1.0$; and $\epsilon = 0.8, \delta = 1.6$), Matérn, Ornstein–Uhlenbeck ($\nu = 10,000$), and white noise.

(v) *Dagum*. In this case no explicit analytical formula for the correlation function of $X(t)$ can be obtained and one has to proceed by numerical integration of (13). Figure 4 shows the resulting correlation function compared to those due to the four other excitations. Since there is no formula analogous to (14), we cannot say whether the response from Dagum-type excitation is Dagum or not.

5. Conclusions

A study has been conducted of the responses of first-order, linear dynamical systems under time-stationary random forcings of Cauchy and Dagum types. These forcings lack explicit parametric spectral densities, yet they allow the decoupling of the fractal dimension and Hurst effect. Working directly in the time domain, we find transient second-order characteristics of responses and, for comparison, we also examine the effects of Gaussian white noise, Ornstein–Uhlenbeck (which in the limit becomes white noise), and Matérn forcings. Overall, given the same variance on input, the variance on output is strongest for Matérn, then Cauchy, then white noise, and finally Dagum forcing. We also find that, if the excitation correlation function is Matérn, the correlation function of the response is approximately Matérn. On the other hand, the response due to the Cauchy excitation is not Cauchy, but, at this stage, we cannot say whether the response due to the Dagum

excitation (with its fractal and Hurst effects) is Dagum or not. The latter issue will require further research. An analogous study of the responses of second-order, linear dynamical systems subjected to Cauchy and Dagum excitations is presently underway [Shen et al. 2014b].

While the studies reported in the aforementioned paper and in the present work focused on randomness in the time domain for a one-degree-of-freedom system, similar studies have been conducted in the spatial domain for static systems. Namely, responses of elastic rods (or, equivalently, shear beams) [Shen et al. 2015] and Bernoulli-Euler beams [Shen et al. 2014a] with random field properties and, also possibly, under random field forcings of either Cauchy or Dagum type have been compared with those of either linear, exponential, or Matérn. Typically, given the same variance of the random field, the variance on output is strongest for Matérn. However, the relative effects of Dagum, Cauchy, linear, and exponential models depend on the particular loading situation. In a number of cases, the results may be obtained in explicit (albeit very lengthy) analytical forms, but as Cauchy and Dagum models are introduced, one has to resort to numerics. Thus, while the introduction of fractal and Hurst effects brings more reality into models of randomness in time and space domains, it results in more challenging analyses.

Further research is needed in order to evaluate the impact of the proposed framework in terms of the fractal dimension and Hurst effect for the resulting stochastic structures. Analytically, this is not an easy task. From a statistical viewpoint, it would be of interest to follow along the lines of [Gneiting and Schlather 2004; Mateu et al. 2007]: first, simulating Gaussian random processes under the covariances obtained in the present paper, then estimating the fractal dimension and Hurst effect, and inspecting whether there is any tendency toward decoupling. This will be an important issue to address in the future.

Acknowledgements

Lihua Shen was partially supported by the National Science Foundation of China under Grant 11171232 and the Beijing Municipal Education Commission under Grant KZ201310028030. Martin Ostoja-Starzewski was partially supported by the NSF under grant CMMI-1030940, and Emilio Porcu by Proyecto Fondecyt Regular number 1130647.

References

- [Adler 1981] R. J. Adler, *The geometry of random fields*, Wiley, Chichester, 1981. Reprinted in *Classics in Applied Mathematics* **62**, SIAM, Philadelphia, 2010.
- [CFA 2008] CFA, Context free art: tutorials/fractals, 2008, <http://www.contextfreeart.org/mediawiki/index.php/Tutorials/Fractals>.

- [Christakos 2000] G. Christakos, *Modern spatiotemporal geostatistics*, Studies in Mathematical Geology **6**, Oxford University Press, New York, 2000.
- [Elishakoff 1983] I. Elishakoff, *Probabilistic methods in the theory of structures*, Wiley, New York, 1983. 2nd ed. published by Dover, Mineola, NY, 1999.
- [Gneiting and Schlather 2004] T. Gneiting and M. Schlather, “Stochastic models that separate fractal dimension and the Hurst effect”, *SIAM Rev.* **46**:2 (2004), 269–282.
- [Hall and Wood 1993] P. Hall and A. Wood, “On the performance of box-counting estimators of fractal dimension”, *Biometrika* **80**:1 (1993), 246–252.
- [Matérn 1986] B. Matérn, *Spatial variation*, 2nd ed., Lecture Notes in Statistics **36**, Springer, Berlin, 1986.
- [Mateu et al. 2007] J. Mateu, E. Porcu, and O. Nicolis, “A note on decoupling of local and global behaviours for the Dagum random field”, *Probab. Eng. Mech.* **22**:4 (2007), 320–329.
- [Matheron 1965] G. Matheron, *Les variables régionalisées et leur estimation*, Masson, Paris, 1965.
- [Porcu and Stein 2012] E. Porcu and M. L. Stein, “On some local, global and regularity behaviour of some classes of covariance functions”, pp. 221–238 in *Advances and challenges in space-time modelling of natural events*, edited by E. Porcu et al., Lecture Notes in Statistics **207**, Springer, Heidelberg, 2012.
- [Porcu et al. 2007] E. Porcu, J. Mateu, A. Zini, and R. Pini, “Modelling spatio-temporal data: a new variogram and covariance structure proposal”, *Stat. Probab. Lett.* **77**:1 (2007), 83–89.
- [Ruiz-Medina et al. 2011] M. D. Ruiz-Medina, E. Porcu, and R. Fernandez-Pascual, “The Dagum and auxiliary covariance families: towards reconciling two-parameter models that separate fractal dimension and the Hurst effect”, *Probab. Eng. Mech.* **26**:2 (2011), 259–268.
- [Shen et al. 2014a] L. Shen, M. Ostoja-Starzewski, and E. Porcu, “Bernoulli–Euler beams with random field properties under random field forcings: fractal and Hurst effects”, *Arch. Appl. Mech.* **84** (2014), 1595–1626.
- [Shen et al. 2014b] L. Shen, M. Ostoja-Starzewski, and E. Porcu, “Harmonic oscillator driven by random processes with fractal and Hurst effects”, submitted, 2014.
- [Shen et al. 2015] L. Shen, M. Ostoja-Starzewski, and E. Porcu, “Elastic rods and shear beams with random field properties under random field loads: fractal and Hurst effects”, *J. Engin. Mech. (ASCE)* (2015).
- [Stein 1999] M. L. Stein, *Interpolation of spatial data: some theory for Kriging*, Springer, New York, 1999.

Received 15 Apr 2013. Revised 14 Sep 2013. Accepted 17 Nov 2013.

LIHUA SHEN: shenlh@lsec.cc.ac.cn

Department of Computational Mathematics, Capital Normal University, Beijing, 100037, China

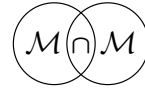
MARTIN OSTOJA-STARZEWSKI: martinost@illinois.edu

Department of Mechanical Science and Engineering, University of Illinois at Urbana-Champaign, 1206 W. Green Street, Urbana, IL 61801-2906, United States

EMILIO PORCU: emilio.porcu@usm.cl

Department of Mathematics, University Federico Santa Maria, 2360102 Valparaíso, Chile





REFLECTIONS ON MATHEMATICAL MODELS OF DEFORMATION WAVES IN ELASTIC MICROSTRUCTURED SOLIDS

JÜRI ENGELBRECHT AND ARKADI BEREZOVSKI

This paper describes the mathematical models derived for wave propagation in solids with internal structure. The focus of the overview is on one-dimensional models which enlarge the classical wave equation by higher-order terms. The crucial parameter in models is the ratio of characteristic lengths of the excitation and the internal structure. Novel approaches based on the concept of internal variables permit one to take the thermodynamical conditions into account directly. Examples of generalisations include frequency-dependent multiscale models, nonlinear models and thermoelasticity. The substructural complexity within the framework of elasticity gives rise to dispersion of waves. Dispersion analysis shows that acoustic and optical branches of dispersion curves together describe properly wave phenomena in microstructured solids. In the case of nonlinear models, the governing equations are of the Boussinesq type. It is argued that such models of waves in solids with microstructure display properties that can be analysed as phenomena of complexity.

1. Introduction

Waves are not only carriers of energy; they are also carriers of information. This means that waves generated by certain initial and boundary conditions carry the information not only from those conditions, but the information about the properties of the media they meet in their course of propagation as well. This information is reflected in changes of the wave profiles or, in other words, in changes of their spectra. In the present overview we focus on the influence of microstructure of solids on the macrobehaviour of deformation waves. Although deformation waves in solids have been studied for over a century, new and intriguing applications continue to arise in contemporary engineering problems. Solids with unconventional

Communicated by Francesco dell'Isola.

This research was supported by the EU through the European Regional Development Fund and by the Estonian Ministry of Education and Research (SF 0140077s08). The authors would like to thank all their coauthors and colleagues for valuable discussions.

MSC2010: 74A30, 74J99, 74E05, 74H99.

Keywords: wave motion, microstructured solids, internal variables, dispersion, nonlinearity.

properties resulting from their composition and internal architecture and their wave propagation characteristics will be of interest along with the novel technologies that they inspire. Of particular interest are multiscale wave processes in solids characterised by hierarchical structures, with nested levels of geometric and/or material complexity, as well as multiphysics phenomena due to coupled mechanical, thermal and electromagnetic effects. Besides, deformation waves can be regarded as attractive characterisation tools, due to their sensitivity to small-scale structural features, such as discontinuities, interphases and defects.

Every material body has actually a microstructure at a smaller scale. Take for example alloys, polycrystalline solids, ceramic composites, functionally graded materials, granular materials, etc. From this viewpoint, there exists an intrinsic space-scale which should be taken into account in deriving the governing equation of motion. The natural question is: when is it needed? Clearly one should pay attention to two characteristic lengths: the characteristic length L_0 of an external excitation (the wavelength) and the internal characteristic length l . When $L_0/l \geq 1$, the conventional theories and corresponding mathematical models can be effectively used because the microstructure acts collaboratively. When $L_0/l \approx 1$, the influence of a microstructure becomes important, which demonstrates the nonlocality of the wave propagation [Engelbrecht and Braun 1998]. In terms of time-scale, the high-frequency excitations (corresponding to short wavelengths) should also strongly be influenced by the presence of the microstructure. All this calls for more sophisticated and physically well-grounded modelling where the conventional assumptions for constructing the theories might not work, and attention should be focussed on catching effects caused by the internal structure of materials. Although there are many theoretical studies in this field, the space-scale in real dimensions is not always introduced. That is why some estimates should here be given. The internal characteristic lengths certainly vary largely in scale [Gates et al. 2005]. If we take a characteristic size of a structural element of 10^0 m, then in typical materials the characteristic internal lengths are between 10^{-3} m and 10^{-6} m. However, in concrete, for example, the internal lengths can be around 10^{-2} m. We leave aside here smaller and larger internal lengths like in nanostructured materials (in nm) or seismology (in km).

As mentioned by Eringen [1999], “the published work in microcontinuum mechanics is so large” that we do not aim to present an overwhelming review, but shall concentrate our attention on the mathematical modelling of elastic deformation waves. Even more, in order to explain the various models, we limit ourselves to the analysis of one-dimensional longitudinal waves as a benchmark, although in most cases the more general three-dimensional theories exist as a basis for deriving them. This gives a possibility to compare the interaction effects between macro- and microstructure in a simple and transparent manner and find unified patterns.

In addition, it gives a possibility to analyse the changes which occur to one of the three cornerstones of mathematical physics — to the classical wave equation — which will turn into an equation with higher-order terms governing the dispersion effects. Some basic concepts should be reviewed in order to explain descriptions used in various studies:

- Microstructured solids display “material substructural complexity” [Mariano and Stazi 2005] because of interaction between their constituents.
- Substructural complexity can be characterised as “complexity of particles” [Kröner 1968], which leads to nonlocality and wave dispersion.
- In mathematical models for waves, higher-order spatial gradients should be accompanied by higher-order time derivatives [Metrikine 2006] and be dynamically consistent [Askes and Aifantis 2006].

An overview is needed for summing up the previous research on models of waves in microstructured solids and demonstrating their essential features. The present overview is initiated by many others, which sometimes are selective, emphasising the author’s sympathies. We tried to pay due attention to all essential results, to the best of our knowledge.

The paper is organised as follows. In Section 2, a brief description of basic theories is presented, including discrete and continuum theories and links between them. This is the basis for Section 3, where various one-dimensional mathematical models are presented and compared. Section 4 is devoted to the generalisation of models involving multiscale and multifield cases, and in Sections 5 to 7 the analysis of physical effects observed in the macro- and microbehaviour of waves in microstructured solids is presented. Finally, in Section 8 a summary of results and further discussion are given.

2. Theoretical landscape of modelling

The idea of theories relies on the mathematical modelling of phenomena under consideration. This was already known to Leonardo da Vinci: observe the phenomenon, and list quantities having numerical magnitude that seem to influence it. Although the great master recommended setting up linear relations among the pairs of these quantities, it was a considerable step forward to contemporary physical sciences. Nowadays we certainly know about the importance of being nonlinear, but in many cases the basic concepts follow the advice of Leonardo da Vinci, as will be explicitly seen from what follows.

In the case of microstructured solids, the deformation waves, as said in Section 1, are influenced by the microstructure. In an ideal case, the behaviour of materials should be simulated, with only the constitutive law describing interactions between

atoms. However, explicit calculation of all of the atomic degrees of freedom will never be feasible due to the scales of deformation that are important in realistic problems. The only possibility is to selectively remove most of these degrees of freedom to make the problem tractable [Curtin and Miller 2003]. Thus, the crucial point in modelling wave phenomena is to choose the starting point: either to start from a discrete (lattice structure) or from a continuous (continuum) model in order to capture size effects of the microstructure. Here one should remember that “mass point and continuum theories have equal rights in the classical mechanics of matter” [Kr ner 1968].

So, attention should be paid to (i) discrete models (bottom-up approach); (ii) continuum models (top-down approach); and (iii) links between discrete and continuum models.

2.1. Discrete models. A discrete model takes into account all the constituents of a solid by treating them as point-like masses. For example, the monocrystalline solids have a regular arrangement of their constituents; in polycrystalline solids the arrangements are more complicated [Maugin 1999]. We leave aside here amorphous materials and liquid crystals. The most intriguing question is how to establish (postulate) the interactive forces between the constituents which are included into the equations of motion for every point-like mass (usually Newton’s law).

The well-known studies of Brillouin [1946] and Askar [1986] have analysed the basic cases, including diatomic and polyatomic chains. Kunin [1975] has derived the governing equations for a diatomic chain with an additional average relative deformation (called microdeformation) of the elementary cell together with a deep mathematical analysis of corresponding models. Maugin [1999] has presented a contemporary description of waves in elastic crystals (lattice dynamics).

Probably, the best-known discrete model for waves in a one-dimensional lattice is the Born–von K rm n model [1912], (see also [Maugin 1999]). This model and its counterparts for more complicated cases form the basis for the derivation of the higher-order dispersive wave equation by continualisation procedures; see for example [Maugin 1999; Askes and Metrikine 2005; Askes et al. 2008; Andrianov et al. 2010]. However, as remarked in [Seeger 2010], the explicit solution of the Born–von K rm n model derived by Schr dinger [1914] predicts that very distant particles start to move, even at arbitrarily small time after any localised perturbation. This physically inconsistent situation can be avoided by taking inertia of particles into account and using more complicated continualisation techniques. There are several studies along this line [Metrikine and Askes 2002; Askes and Aifantis 2006; Polyzos and Fotiadis 2012] resulting in strain-gradient models. This means actually following the principle of dynamic consistency [Metrikine 2006].

Besides one-dimensional chains, also two-dimensional structures are analysed; see [Maugin 1999; Pichugin et al. 2008; Andrianov et al. 2010]. The studies of

granular media include also the modelling of granular lattices, i.e., chains of beads under Hertz contact [Coste et al. 1997; Porter et al. 2009].

2.2. Continuum models. Looking back in history, the important generalisation to account for the influence of a microstructure into the continuum theory was made by E. Cosserat and F. Cosserat [1909], who elaborated a theory with microrotations at each material point of a continuum. The degrees of freedom are then characterised by three rigid directors and the corresponding theory is nowadays called micropolar. If these directors are deformable, then the result is the micromorphic theory [Eringen and Suhubi 1964a; Eringen and Suhubi 1964b; Mindlin 1964; Eringen 1999]. When the directors are constrained in a special way (three microrotations and one microstretch), then the result is the microstretch theory [Eringen 1969]. Detailed descriptions of these theories can be found in the monographs [Eringen 1999; Capriz 1989; Maugin 2013]. In what follows we limit ourselves to one-dimensional micromorphic theory and leave aside the Cosserat-type microrotation. Analysis of the latter theory in the contemporary framework can be found in [Neff 2006; Neff and Jeong 2009].

Another avenue to generalisation is the inclusion of higher-order gradients of strain into the free energy function, as compared with the classical Cauchy theory, which accounts only for strains in constitutive equations; see [dell’Isola et al. 2009], for example. Such a possibility was pointed out already by Kröner [1968], and a detailed overview on gradient theories is given by Maugin [2013]. There are several studies on waves using this idea [Metrikine and Askes 2002; Papargyri-Beskou et al. 2009; Polyzos and Fotiadis 2012]. A comparison of gradient and micromorphic theories is given by Kirchner and Steinmann [2004].

According to Kröner [1968], the complexity of particles in a solid plays a decisive role in deriving the mathematical models. This concept is explicitly used by Mindlin [1964], who has introduced a unit cell which “may also be interpreted as a molecule of a polymer, a crystallite of a polycrystal or a grain of a granular material”. Such an approach is used in many later studies for deriving the governing equations of waves [Engelbrecht et al. 2005; Papargyri-Beskou et al. 2009; Porubov et al. 2009; Polyzos and Fotiadis 2012; Berezovski et al. 2013]. Mariano [2002] has used order parameters for describing, as he said, “the substructural configuration”.

As far as our knowledge on internal structure of solids is not always explicitly described, one should think about replacing the physical structure by a certain field. Then the concept of internal variables has proved to be useful. Proposed originally to describe dissipative processes, and traced back to [Duhem 1911a; Duhem 1911b], the modern understanding is presented by Maugin and Muschik [1994]. The generalisation of this concept by introducing dual internal variables has made it possible to use for describing wave processes [Ván et al. 2008; Berezovski

et al. 2011b]. This approach has a clear thermodynamic background, although the microstructure itself becomes latent and its influence can be considered as an additional field. Such a possibility is also mentioned by Capriz [1989] and Mariano [2002]. Germain [1973] has noted a possibility to introduce “hidden parameters” into the function of internal energy.

The separation of the macro- and microstructure in a continuum leads, in general terms, to the formulation of separate balance laws for each [Eringen and Suhubi 1964a; Eringen and Suhubi 1964b; Mindlin 1964; Eringen 1999; Mariano 2002]. Maugin [1993; 2011a] has proposed using the material formulation to represent the balance law of the macrostructure, which includes all the interaction forces within the solid, accounting for microstructural effects. Such an approach becomes very useful, when internal variables are introduced, for describing the effects due to the presence of the microstructure. Namely, the evolution of internal variables needed for determining the internal forces is then governed not by a balance law but by satisfying thermodynamical considerations [Ván et al. 2008; Berezovski et al. 2011b].

2.3. Links between lattice dynamics and continua. Calculation of values of continuum variables based on atomistic models has a long and rich history (see, for example, reviews by Goddard [1986], Zimmerman et al. [2002] and Webb et al. [2008]). Contemporary contributions include the thermomechanical equivalent continuum [Zhou 2005], generalised mathematical homogenisation method [Fish et al. 2005], and scale-dependent molecular averages [Murdoch 2010]. As concerns wave propagation, Chen et al. [2003; 2004] have justified applicability of micro-continuum theories from the atomistic viewpoint, and they stress the importance of size effects and phonon dispersion relation; see also [Chen and Lee 2003].

From the physical viewpoint, an extremely important question is how to establish the material parameters from discrete (atomic) models at the microscale. There are several studies in this direction based on experiments. Maranganti and Sharma [2007] have established strain-gradient elastic constants for various metals, semiconductors, silica and polymers by relating them to the atomic displacement correlations in a molecular dynamics computational ensemble (see also a long list of references on studies in this field). Zeng et al. [2006] have proposed to determine the dispersive elastic constants by using phonon dispersion relations. Dispersive phonon imaging is used by Jakata and Every [2008] for the cubic crystals Ge, Si, GaAs, and InSb.

Remark 1. We do not go into details for describing the homogenisation methods, which basically deal with averaged physical parameters, and serve well for static problems. But an important idea for describing waves in periodic structures must be stressed. The studies by Achenbach et al. [1968] and Sun et al. [1968]

analysed dynamic behaviour of laminated composites by introducing the effective stiffness theory capable to describe dispersive effects. Later, a similar problem was studied by Ziegler [1977], who explained the mechanism of emerging stopping bands for harmonic waves as a result of combination of Floquet waves. Santosa and Symes [1991] derived a governing equation for waves in periodic composites which includes higher-order terms responsible for dispersion, like simple governing equations derived from lattice dynamics [Maugin 1999]. A similar problem for bilaminates is studied by Fish et al. [2002]. Nowadays, the homogenisation approach for such periodic composites is well developed; see for example [Craster et al. 2010].

Remark 2. In modelling of waves in microstructured solids, the inertial effects caused by the microstructure must be taken into account. This has been stressed already by Eringen [1964], who introduced the law of conservation of microinertia. This is characteristic to micromorphic models, strain gradient models, etc. In other words, kinetic energy must be attributed also to the microstructure, as in [Mindlin 1964; Mariano 2002; Engelbrecht et al. 2005].

3. Models of waves in microstructured solids

The diversity of models presented in the previous section means that “ a unified continuum-mechanical description of materials with inherent microstructure is to date not available” [Kirchner and Steinmann 2004]. Nevertheless, there exists a guiding tool for the selection of a proper model: optical modes should be taken into account together with acoustic modes. As mentioned in [Chen et al. 2003],

The absence of optical branch is due to the neglecting of the atomic structure of crystal. From this viewpoint, classical continuum theory, the gradient theories, and the couple stress theories do not stem from the considerations of microstructure or micromotion and as a consequence, would break down if the micromotion and/or the microstructure become too significant to be neglected.

This is why we consider mainly approaches that include optical modes, at least in principle.

3.1. General frameworks. We start with most characteristic examples in the general setting.

3.1.1. Micromorphic solids. Mindlin [1964] formulated the linear micromorphic theory using two balance laws: one for macrostructure, another for microstructure. In the case of centrosymmetric, isotropic materials, these laws are

$$\rho \dot{\mathbf{v}} = \operatorname{div}(\boldsymbol{\sigma} + \boldsymbol{\tau}) + \mathbf{f}, \quad (1)$$

$$\mathbf{I} \ddot{\boldsymbol{\psi}} = \operatorname{div} \boldsymbol{\mu} + \boldsymbol{\tau} + \Phi, \quad (2)$$

where ρ is the density, \mathbf{v} is the particle velocity, \mathbf{I} is a microinertia tensor, $\boldsymbol{\psi}$ is the microdeformation tensor, \mathbf{f} is the body force, and Φ is the double force per unit volume. The corresponding stress tensors, namely, the Cauchy stress $\boldsymbol{\sigma}$, the relative stress $\boldsymbol{\tau}$, and the double stress $\boldsymbol{\mu}$,

$$\boldsymbol{\sigma} \equiv \frac{\partial W}{\partial \boldsymbol{\varepsilon}}, \quad \boldsymbol{\tau} \equiv \frac{\partial W}{\partial \boldsymbol{\gamma}}, \quad \boldsymbol{\mu} \equiv \frac{\partial W}{\partial \boldsymbol{\kappa}}, \quad (3)$$

are defined, respectively, as derivatives of the free energy W with respect to the classical strain tensor $\boldsymbol{\varepsilon}$, the relative deformation tensor $\boldsymbol{\gamma}$, and the microdeformation gradient $\boldsymbol{\kappa}$ [Mindlin 1964],

$$\boldsymbol{\varepsilon} \equiv \frac{1}{2}(\nabla \mathbf{u} + (\nabla \mathbf{u})^T), \quad \boldsymbol{\gamma} \equiv \nabla \mathbf{u} - \boldsymbol{\psi}, \quad \boldsymbol{\kappa} \equiv \nabla \boldsymbol{\psi}. \quad (4)$$

In terms of the macrodisplacement \mathbf{u} , after choosing the quadratic free energy function W , Mindlin's model (1)–(2) results in

$$\begin{aligned} (\lambda + 2\mu)(1 - l_1^2 \nabla^2) \nabla \nabla \cdot \mathbf{u} - \mu(1 - l_2^2 \nabla^2) \nabla \times \nabla \times \mathbf{u} \\ = \rho(\ddot{\mathbf{u}} - h_1^2 \nabla \nabla \cdot \ddot{\mathbf{u}} + h_2^2 \nabla \times \nabla \times \ddot{\mathbf{u}}), \end{aligned} \quad (5)$$

where l_1^2, l_2^2 describe the elastic microstructural parameters and h_1^2, h_2^2 the microinertia, while λ and μ are the Lamé parameters as in the classical theory of elasticity. This is known as Form I, in Mindlin's notation. Papargyri-Beskou et al. [2009] have followed [Mindlin 1964], and after certain simplifications get

$$(1 - g^2 \nabla^2)[(\lambda + \mu) \nabla \nabla \cdot \mathbf{u} + \mu \nabla^2 \mathbf{u}] = \rho(\ddot{\mathbf{u}} - h^2 \nabla^2 \ddot{\mathbf{u}}), \quad (6)$$

where $g^2 = l_1^2 = l_2^2$ and $h^2 = h_1^2 = h_2^2$ govern the elastic microstructural and microinertia terms.

A more general model than that of [Mindlin 1964] is described in [Mariano 2002], with the effects of microstructure embedded into order parameters as

$$\operatorname{Div} \mathbf{T} + \mathbf{b}^{\text{ni}} = \rho \ddot{\mathbf{x}}, \quad (7)$$

$$\operatorname{Div} S - \mathbf{z} + \boldsymbol{\beta}^{\text{ni}} = \frac{d}{dt} \frac{\partial \chi}{\partial \dot{\varphi}} - \frac{\partial \chi}{\partial \varphi}, \quad (8)$$

where \mathbf{x} is the placement field, φ is the order parameter, $\mathbf{T} = \partial W / \partial \mathbf{F}$ is the first Piola–Kirchhoff stress tensor, $S = \partial W / \partial \nabla \varphi$ is the microstress tensor, \mathbf{b}^{ni} is the noninertial bulk force, $\mathbf{z} = \partial W / \partial \varphi$ is the internal self-force, $\boldsymbol{\beta}^{\text{ni}}$ is the noninertial external bulk interaction force, χ is the substructural kinetic coenergy density (the Legendre transform with respect to $\dot{\varphi}$ of the substructural kinetic energy density), and ρ is the density of the macrostructure. The model is presented here in its original form [Mariano 2002], and all the notation can be found in the original paper.

In the micromorphic theory of Mindlin, as well as in the multifield Mariano model, the balances of linear momentum for macroscale and microscale are introduced independently. This means that the introduced microdeformation or the corresponding order parameter play the role of an additional degree of freedom, causing obvious problems with boundary conditions.

3.1.2. Material formulation and internal variables. An alternative framework is provided by the internal variable approach. This approach is based on the canonical (or material) formulation of continuum mechanics. Following [Maugin 2006], we represent the canonical (material) momentum balance in the form

$$\left. \frac{\partial \mathbf{P}}{\partial t} \right|_X - \operatorname{div}_R \mathbf{b} = \mathbf{f}^{\text{int}} + \mathbf{f}^{\text{ext}} + \mathbf{f}^{\text{inh}}, \quad (9)$$

where \mathbf{P} is material momentum, \mathbf{b} the material Eshelby stress, and \mathbf{f}^{int} , \mathbf{f}^{ext} , and \mathbf{f}^{inh} are the material internal force, material external (body) force and the material inhomogeneity force, respectively. They are defined by

$$\mathbf{P} = -\rho_0 \mathbf{v} \cdot \mathbf{F}, \quad \mathbf{b} = -(\mathcal{L} \mathbf{I}_R + \mathbf{T} \cdot \mathbf{F}), \quad \mathcal{L} = K - W, \quad (10)$$

$$\mathbf{f}^{\text{inh}} = \left(\frac{1}{2} v^2 \right) \nabla_R \rho_0 - \left. \frac{\partial W}{\partial X} \right|_{\text{expl}}, \quad (11)$$

$$\mathbf{f}^{\text{ext}} = -\mathbf{f}_0 \cdot \mathbf{F}, \quad \mathbf{f}^{\text{int}} = \mathbf{T} : (\nabla_R \mathbf{F})^T - \nabla_R W|_{\text{impl}}, \quad (12)$$

where \mathbf{F} is the deformation gradient, ρ_0 is the matter density in the reference configuration, \mathbf{v} is the velocity vector, K is the kinetic energy density, W is the free energy per unit reference volume, \mathbf{T} is again the first Piola–Kirchhoff stress tensor, \mathbf{f}_0 is the body force in the reference configuration. The subscript expl means taking the material gradient keeping the fields fixed (and thus extracting the explicit dependence on \mathbf{X}), while the subscript impl means taking the material gradient only through fields present in the function. The “dot” notation is used for the product of two tensors and colon denotes the tensor contraction. Equation (9) is called the pseudomomentum balance [Maugin 1993].

The canonical form of the energy conservation at any regular material point \mathbf{X} in the body, for sufficiently smooth fields, has the form

$$\left. \frac{\partial (S\theta)}{\partial t} \right|_X + \nabla_R \cdot \mathbf{Q} = h^{\text{int}}, \quad h^{\text{int}} = \mathbf{T} : \dot{\mathbf{F}} - \left. \frac{\partial W}{\partial t} \right|_X, \quad (13)$$

where \mathbf{Q} is the material heat flux, S is the entropy density per unit reference volume, and θ is the absolute temperature. In addition, the Clausius–Duhem inequality is to be satisfied as

$$-\left(\frac{\partial W}{\partial t} + S \frac{\partial \theta}{\partial t} \right)_X + \mathbf{T} : \dot{\mathbf{F}} + \nabla_R (\theta \mathbf{J}) - \mathbf{S} \cdot \nabla_R \theta \geq 0, \quad (14)$$

where \mathbf{S} is the entropy flux and \mathbf{J} is the “extra entropy flux”, which vanishes in most cases. Berezovski et al. [2011b] have used the dual internal variable concept [Ván et al. 2008] in addition to canonical equations (9) and (13). In this case, for example, the governing equation for the internal variable α (identified as the microdeformation tensor) is obtained by satisfying inequality (14) [Engelbrecht and Berezovski 2012]:

$$\mathbf{I}_m \ddot{\alpha} = \left(-\frac{\partial W}{\partial \alpha} + \operatorname{div}_R \frac{\partial W}{\partial (\nabla \alpha)} \right), \quad (15)$$

where \mathbf{I}_m can be identified as the microinertia, calculated from geometry and state variables (for details, see [ibid.]).

In order to go further, the free energy function W must be specified. The constraints for W require positive definiteness for uniqueness and stability; it should be homogeneous and polyconvex in terms of the deformation gradient. In linear theory W is a quadratic function; in the simplest version of nonlinear theory it is a cubic function. The regularity of energy densities is analysed in [Mariano 2002]. The specific question is how microdeformations (or the order parameter or internal variables) are described in the function W . This question must be answered with a full confidence about the internal structure but at the same time offers several opportunities for respective models (see below). For the description of deformation waves in microstructured solids, the inertia of the microstructure should be taken into account [Mindlin 1964; Mariano 2002].

Remark 3. Mindlin [1964] used Hamilton’s principle for deriving the equations of motion combining total kinetic and potential energies and the work done by external forces. It is possible also to directly use the Euler–Lagrange formulation [Engelbrecht et al. 2005; Casasso and Pastrone 2010]. The two approaches yield the same equations of motion and the same pseudomomentum balance [Engelbrecht et al. 2006].

3.2. One-dimensional models. The classical one-dimensional wave equation possesses the well-known d’Alembert solution. It is of considerable interest to use the one-dimensional setting also for describing microstructured solids in order to understand possible effects in the most transparent way. Certainly, one notes the price of simplifications compared with three-dimensional models: the oversimplified description of rotational effects, as in the Cosserats’ model, the emerging artefact between scalar and covectorial character of energy equation and the balance of momentum [Maugin 2011a] and simplification of geometry of solids. On the other hand, the appearance of new terms in the wave equation can cast more light on dispersive, nonlinear, and other effects. A typical example in this sense is the Boussinesq-type equation [Christov et al. 2007; Engelbrecht et al. 2011].

3.2.1. Structure of equations. The models briefly described in Section 3.1 result in systems of partial differential equations. In the one-dimensional case with a single microstructure, this means that one obtains a system of two equations. If we now take displacement $u = u_1$ and the microdeformation $\varphi = \varphi_{11}$ according to the Mindlin model [1964], then the kinetic energy density K and the potential energy density W are

$$K = \frac{1}{2}\rho u_t^2 + \frac{1}{2}I\varphi_t^2, \quad W = W(u_x, \varphi, \varphi_x), \quad (16)$$

where ρ and I denote macroscopic density and microinertia, respectively, and indices denote derivatives. The corresponding Euler–Lagrange equations have the general form

$$\left(\frac{\partial \mathcal{L}}{\partial u_t}\right)_t + \left(\frac{\partial \mathcal{L}}{\partial u_x}\right)_x - \frac{\partial \mathcal{L}}{\partial u} = 0, \quad (17)$$

$$\left(\frac{\partial \mathcal{L}}{\partial \varphi_t}\right)_t + \left(\frac{\partial \mathcal{L}}{\partial \varphi_x}\right)_x - \frac{\partial \mathcal{L}}{\partial \varphi} = 0, \quad (18)$$

where the Lagrangian density is given by $\mathcal{L} = K - W$. The simplest potential energy function is a quadratic function

$$W = \frac{1}{2}(\lambda + 2\mu)u_x^2 + A\varphi u_x + \frac{1}{2}B\varphi^2 + \frac{1}{2}C\varphi_x^2, \quad (19)$$

where λ , μ are Lamé parameters (in order to keep notations from classical elasticity) and A , B , C are other material constants.

The governing equations are now [Engelbrecht et al. 2005]

$$\rho u_{tt} = (\lambda + 2\mu)u_{xx} + A\varphi_x, \quad (20)$$

$$I\varphi_{tt} = C\varphi_{xx} - Au_x - B\varphi, \quad (21)$$

which is the simplest Mindlin-type (micromorphic) model. A similar model is used in [Porubov et al. 2009; Casasso and Pastrone 2010]. Huang and Sun [2008] have derived the governing equations for waves along the layers of a bimaterial layered medium. In terms of the displacement U and “kinematic variable” Φ , the governing system of equations in a micromorphic case is

$$k_1 U_{tt} = k_2 U_{xx} + k_2 \Phi_x, \quad (22)$$

$$k_3 \Phi_{tt} = k_4 \Phi_{xx} - k_2 U_x - k_2 \Phi, \quad (23)$$

where k_1 , k_2 , k_3 , k_4 reflect elastic and geometric characteristics of layers. The system of equations (20)–(21) is very similar to the system (22)–(23).

Maugin [1999] has derived a model of a chain of dumbbells (see also [Askar 1986]) which exhibits transverse displacements U and rotations ψ . After continuation, the governing equations are

$$\rho_0 U_{tt} = (\mu + \chi) U_{xx} + \chi \psi_x, \quad (24)$$

$$j \psi_{xx} = \alpha \psi_{xx} - \chi U_x - \chi \psi, \quad (25)$$

where coefficients are related to the mass m , chain scale a and stiffness k . Note that here j is the microinertia density and χ and α are micropolar coefficients.

Again, the structure of the equations is the same as above. In order to compare these (and other) results within one framework, we shall focus now on models in the form of single equation, derived directly from three-dimensional models (5) or (6), or from systems of equations like (20)–(21) or (22)–(23). Let us introduce a wave operator

$$\mathcal{L}_w = u_{tt} - c_i^2 u_{xx}, \quad (26)$$

where c_i is a velocity, and the function

$$\mathcal{F}_w = \mathcal{F}_w(u_{xx}, u_{xxxx}, u_{xxtt}, \dots), \quad (27)$$

leaving the coefficients of derivative aside. Then the models derived for describing the one-dimensional wave propagation in microstructured solids can be summarised by either

$$\mathcal{L}_w = \mathcal{F}_w(\cdot) \quad (28)$$

or, more explicitly,

$$\mathcal{L}_w = (\mathcal{L}_{jw})_{xx} + (\mathcal{L}_{kw})_{tt} + \mathcal{F}_w(\cdot), \quad (29)$$

where \mathcal{L}_{jw} , \mathcal{L}_{kw} have velocities c_j , c_k , respectively (see Whitham [1974]). The presentation (29) can be called hierarchical since it involves several wave operators, and in general $\mathcal{L}_{iw} = \mathcal{O}(\epsilon)$, where ϵ is a small parameter. In general terms, \mathcal{F}_w is also of accuracy $\mathcal{O}(\epsilon)$.

3.2.2. Classification of models. Models of dispersive waves in terms of \mathcal{L}_w and \mathcal{F}_w are collected in Table 1, and the corresponding models in terms of \mathcal{L}_w and \mathcal{L}_{jw} are presented in Table 2.

The models listed in Tables 1 and 2 are derived using various assumptions and procedures, but they all include higher-order derivatives in space and/or in time, or mixed space-time ones. All these derivatives are even, which shows that the models are conservative and that they display dispersive effects (see Section 5). These effects are reflected first in phase and group velocities, and second in wave profiles.

Table 2 demonstrates the structures of models using the wave operators (26). The basic idea behind introducing such operators is the possibility to stress the importance of scaling [Engelbrecht et al. 2006]. Namely, in this case the wave hierarchies can be formulated [Whitham 1974]. The general structure of models is then

$$\mathcal{L}_{1w} = \delta(\mathcal{L}_{1w})_{xx} + \delta^2(\mathcal{L}_{2w})_{xxxx} + \dots, \quad (30)$$

$\mathcal{F}_w(\cdot)$	Sources
0	Classical wave equation
u_{xxxx}	[Santosa and Symes 1991], [Maugin 1995], [Erofeyev 2003], [Andrianov et al. 2010], [dell’Isola et al. 2012], [Andrianov et al. 2013]
u_{xxxx}, u_{6x}	[Pichugin et al. 2008], [Andrianov et al. 2011]
u_{xxtt}	[Love 1944], [Maugin 1995], [Wang and Sun 2002]
u_{xxxx}, u_{xxtt}	[Askes and Metrikine 2002], [Pastrone et al. 2004], [Metrikine 2006], [Papargyri-Beskou et al. 2009], [Porubov et al. 2009], [Challamel et al. 2009], [Polyzos and Fotiadis 2012]
$u_{xxxx}, u_{xxtt}, u_{xx}$	[Engelbrecht and Pastrone 2003],
$u_{xxxx}, u_{xxtt}, u_{tttt}$	[Metrikine 2006], [Polyzos and Fotiadis 2012], [Pichugin et al. 2008]
u_{xxtt}, u_{tttt}	[Pichugin et al. 2008]
$u_{xxxx}, u_{xxtt}, u_{6x}$	[Polyzos and Fotiadis 2012]

Table 1. Models of dispersive waves in the form $\mathcal{L}_w = \mathcal{F}_w$, $\mathcal{L}_w = u_{tt} - c_0^2 u_{xx}$.

(\mathcal{L}_{jw})	(\mathcal{L}_{kw})	\mathcal{F}_w	Source
$(u_{tt} - c_j^2 u_{xx})_{xx}$		u_{xx}	[Engelbrecht et al. 2005] [Engelbrecht and Salupere 2014]
	$(u_{tt} - c_i^2 u_{xx})_{tt}$		[Maugin 1995] (here $c_k = c_i$)
$(u_{tt} - c_i^2 u_{xx})_{xx}$	$(u_{tt} - c_i^2 u_{xx})_{tt}$	u_{xx}	[Engelbrecht et al. 2005] [Berezovski et al. 2011b]
$(u_{tt} - c_i^2 u_{xx})_{xx}$		u_{xxxx}	[Berezovski et al. 2011b]
$(u_{tt} - c_i^2 u_{xx})_{xx}$	$(u_{tt} - c_i^2 u_{xx})_{tt}$	u_{xx}, u_{xxxx}	[Berezovski et al. 2011b]
$(u_{tt} - c_i^2 u_{xx})_{xx}$	$(u_{tt} - c_i^2 u_{xx})_{tt}$	u_{xxxx}	[Engelbrecht et al. 2005]

Table 2. Models of dispersive waves in the form $\mathcal{L}_w = (\mathcal{L}_{jw})_{xx} + (\mathcal{L}_{kw})_{tt} + \mathcal{F}_w$.

where δ is related to the ratio L_0/l . Such a hierarchy explicitly demonstrates the dependence of the macrobehaviour on microstructure. If δ is small then waves “feel” more the properties of the macrostructure, and the influence of the microstructure is of a perturbative character. If, however, δ is large, then waves “feel” more the properties of the microstructure. The wave hierarchies are analysed in several

studies [Whitham 1974; Engelbrecht et al. 2006; Casasso and Pastrone 2010] and an overview presented by Engelbrecht and Salupere [2014].

The most complicated case — model 5 of Table 2 — has been derived by Berezovski et al. [2011a] by using the concept of dual internal variables φ_1 and φ_2 [Ván et al. 2008]. Here, φ_1 is identified as a microdeformation and φ_2 as its rate. The energy function has the quadratic form

$$W = \frac{1}{2}\rho c^2 u_x^2 + Au_x \varphi_1 + A' u_x \varphi_2 + \frac{1}{2}B\varphi_1^2 + \frac{1}{2}C(\varphi_1^2)_x + \frac{1}{2}D\varphi_2^2, \quad (31)$$

where ρ is the density and c is the velocity in the macrostructure; the coefficients A and A' characterise coupling, and B , C , D the microstructure. The corresponding dispersive wave equation has the form

$$u_{tt} - c^2 u_{xx} = \frac{C}{B}(u_{tt} - c^2 u_{xx})_{xx} - \frac{I}{B}(u_{tt} - c^2 u_{xx})_{tt} + \frac{A'^2}{\rho B} u_{xxxx} - \frac{A^2}{\rho B} u_{xx}. \quad (32)$$

The right-hand side of (32) includes the space and time derivatives of the wave operator $\mathcal{L}_w = u_{tt} - c^2 u_{xx}$ and additional terms with coupling coefficients. Note that (32) can be rewritten in terms of different wave operators as

$$u_{tt} - (c^2 - c_A^2)u_{xx} = \frac{C}{B}(u_{tt} - (c^2 - c_c^2)u_{xx})_{xx} - \frac{I}{B}(u_{xx} - c^2 u_{xx})_{tt}, \quad (33)$$

where $c_A^2 = A^2/\rho B$, $c_c^2 = A'^2/\rho C$. If $A' = 0$ then (32) yields, in a shorter form obtained by asymptotic analysis [Engelbrecht et al. 2005],

$$u_{tt} - (c^2 - c_A^2) u_{xx} = p^2 c_A^2 (u_{tt} - c_1^2 u_{xx})_{xx}, \quad (34)$$

where $c_1^2 = C/IB$, $p^2 = I/B$.

Remark 4. The models in Section 3.2 are one-dimensional with a clear three-dimensional background. Similar models are known for rods [Samsonov 2001; Porubov 2003], where the higher-order derivatives in governing equations in terms of the displacement appear due to geometrical considerations (effects of the transverse displacement). As far as dispersive effects are of a different character, the governing equation is called the “double” dispersion equation [Samsonov 2001]. The combination of microstructural effects and geometrical characteristics of rods is studied in [Porubov 2000].

4. Generalisation of models

The mathematical models described in Section 3 involved one microstructure beside the macrostructure; this microstructure is homogeneously distributed over the space, the dissipative effects are not accounted for, and the governing equations are linear. Clearly, these assumptions need more attention and, if needed, to be

changed. In what follows, possible generalisations are described. Dissipative models will not be considered here; attention is paid to thermoelasticity, i.e., to coupled fields with energy transfer.

4.1. Multiscale models. In reality, there are cases when a microstructure includes another microstructure at a smaller scale [Engelbrecht et al. 2006], or there are two microstructures in parallel with different properties [Berezovski et al. 2010]. The first case (a scale within a scale) may be called hierarchical microstructures and the second case concurrent microstructures.

For a hierarchical microstructure, the free energy function is taken in the form [Engelbrecht et al. 2006; Berezovski et al. 2010]

$$W = \frac{1}{2}(\lambda + 2\mu)u_x^2 + A_1\varphi_1 u_x + \frac{1}{2}B_1\varphi_1^2 + \frac{1}{2}C_1(\varphi_1)_x^2 + \frac{1}{2}A_{12}(\varphi_1)_x\varphi_2 + \frac{1}{2}B_2\varphi_2^2 + \frac{1}{2}C_2(\varphi_2)_x^2, \quad (35)$$

where φ_1 and φ_2 are microdeformations (φ_2 within φ_1) and $A_1, B_1, B_2, C_1, C_2, A_{12}$ are coefficients. Then the governing equations are (see also [Casasso and Pastrone 2010])

$$\rho u_{tt} = (\lambda + 2\mu)u_{xx} + A_1(\varphi_1)_x, \quad (36)$$

$$I_1(\varphi_1)_{tt} = C_1(\varphi_1)_{xx} - A_1u_x - B_1\varphi_1 + A_{12}(\varphi_2)_x, \quad (37)$$

$$I_2(\varphi_2)_{tt} = C_2(\varphi_2)_{xx} - A_{12}(\varphi_1)_x - B_2\varphi_2, \quad (38)$$

where I_1 and I_2 are the corresponding microinertias.

For a concurrent microstructure, the free energy is [Berezovski et al. 2010]

$$W = \frac{1}{2}(\lambda + 2\mu)u_x^2 + A_1\varphi_1 u_x + \frac{1}{2}B_1\varphi_1^2 + \frac{1}{2}C_1(\varphi_1)_x^2 + A_{12}(\varphi_1)_x\varphi_2 + \frac{1}{2}B_2\varphi_2^2 + \frac{1}{2}C_2(\varphi_2)_x^2 + A_2\varphi_2 u_x, \quad (39)$$

where now φ_1 and φ_2 are parallel microstructure (the same scale). The governing equations become

$$\rho u_{tt} = (\lambda + 2\mu)u_{xx} + A_1(\varphi_1)_x + A_2(\varphi_2)_x, \quad (40)$$

$$I_1(\varphi_1)_{tt} = C_1(\varphi_1)_{xx} + A_{12}(\varphi_2)_x - A_1u_x - B_1\varphi_1, \quad (41)$$

$$I_2(\varphi_2)_{tt} = C_2(\varphi_2)_{xx} - A_{12}(\varphi_1)_x - A_2u_x - B_2\varphi_2. \quad (42)$$

If $A_{12} \neq 0$ then the microstructures are coupled; if, however, $A_{12} = 0$, then both microstructures are coupled with the macrostructure but not coupled with each other [Berezovski et al. 2010]. In the latter case, after reformulating the system of equations (36)–(38) in the form of a single equation and using asymptotic analysis, the analogue to (33) can be obtained as [Engelbrecht et al. 2006]

$$\begin{aligned}
u_{tt} - (c_0^2 - a_{A1}^2)u_{xx} \\
= p_1^2 c_{A1}^2 [u_{tt} - (c_1^2 - c_{A2}^2)u_{xx}]_{xx} - p_1^2 c_{A1}^2 c_{A2}^2 (u_{tt} - c_2^2 u_{xx})_{xxxx}, \quad (43)
\end{aligned}$$

where $c_{A1}^2 = A_1^2/\rho B_1$, $c_{A2}^2 = A_2^2/\rho B_2$, $c_1^2 = C_1/I_1$, $p_1^2 = I_1/B_1$, $p_2^2 = I_2/B_2$. One should note the appearance of the sixth-order derivatives in (43), as in the model derived from lattice dynamics in the continuum limit [Maugin 1999]. However, here u_{ttxxxx} is also involved because of the inertia of the second microstructure.

There are many studies concerning multiscales in terms of building of atomistic-continuum models (see, for example, [Liu et al. 2010] and the references therein). Such an approach is needed because, in design of structural elements, some areas like crack tips, plastic zones, thin layers, etc., need smaller spatial scales compared with the whole. That is why mixed atomistic-continuum models are derived. Here, however, multiscale is understood as excitation-dependent (i.e., frequency-dependent). The governing parameter is L_0/l , which gives the weight to different terms in models, and consequently is the reason for the appearance of different physical effects.

4.2. Nonlinear models. Contemporary technology is often characterised by intensive and high-speed impacts. That is why nonlinearities should be accounted for in mathematical models. This means that the full deformation tensor involves nonlinear terms and the stress-strain should also be nonlinear [Eringen 1962]. As shown by Engelbrecht [1997], the physical nonlinearities (stress-strain relations) for most materials are stronger than geometrical (deformation tensor), and, therefore, we limit ourselves here to physical nonlinearities only. This is easily formulated in terms of the free energy function W . Note, however, that we deal with one-dimensional problems, and for three-dimensional problems such an assumption needs careful analysis. Following the model (20)–(21), instead of the free energy function (18), we can postulate [Engelbrecht et al. 2005]

$$W = \frac{1}{2}(\lambda + 2\mu)u_x^2 + A\varphi u_x + \frac{1}{2}B\varphi^2 + \frac{1}{2}C\varphi_x^2 + \frac{1}{6}Nu_x^3 + \frac{1}{6}M\varphi_x^3, \quad (44)$$

where now N and M are nonlinear parameters for macro- and microstructure, respectively. In this case, the governing equations are

$$\rho u_{tt} = (\lambda + 2\mu)u_{xx} + Nu_x u_{xx} + A\varphi_x, \quad (45)$$

$$I\varphi_{tt} = C\varphi_{xx} + M\varphi_x\varphi_{xx} - Au_x - B\varphi. \quad (46)$$

Porubov et al. [2009] have derived the same model, linking N and M to Murnaghan's moduli. From (45) and (46) we get

$$u_{tt} - (c^2 - c_A^2)u_{xx} - k_1(u_x^2)_x = p^2 c_A^2 (u_{tt} - c_1^2 u_{xx})_{xx} + k_2(u_{xx}^2)_{xx}, \quad (47)$$

where k_1 and k_2 are coefficients (compare with (33)). Equation (47) in terms of

the deformation $v = u_x$ reads

$$v_{tt} - (c^2 - c_A^2)v_{xx} - k_1(v^2)_{xx} = p^2c_A^2(v_{tt} - c_1^2v_{xx})_{xx} + k_2(v_x^2)_{xxx}. \quad (48)$$

This equation will be analysed later.

Several modifications of (47) are derived under various assumptions. Maugin [1999] has described the continualisation of discrete lattices and obtained

$$u_{tt} - c^2u_{xx} + c^2\beta au_xu_{xx} - \frac{c^2a^2}{12}u_{xxxx} = 0, \quad (49)$$

where a is lattice spacing and β is related to the potential. Andrianov et al. [2013] have derived a similar model for a layered composite and Erofejev [2003] for a medium with coupled stresses. In these models, nonlinear terms stem from the macrostructure. It is certainly possible to assume that nonlinearity is essential only at the level of the microstructure. Then the corresponding governing equation reads [Engelbrecht and Pastrone 2003]

$$u_{tt} - (c^2 - c_A^2)u_{xx} = p^2c_A^2(u_{tt} - c_1^2u_{xx})_{xx} + k_2(u_{xx}^2)_{xx}. \quad (50)$$

All models (47)–(50) are of the Boussinesq-type. Christov et al. [1996; 2007] have stated that the Boussinesq paradigm grasps the following effects: (a) bidirectionality of waves; (b) nonlinearity (of any order); (c) dispersion (of any order, modelled by space and time derivatives of the fourth order at least). The recent results of studies are summarised by Christov et al. [2007], and with a special attention to microstructured solids by Engelbrecht et al. [2011].

Remark 5. The nonlinear governing equation for rods derived by Samsonov [2001] and Porubov [2003] belong also to the family of Boussinesq equations. In this case the nonlinearity is quadratic, like the nonlinearity of the macrostructure (equations (47) and (48)) in microstructured materials, but it may also be cubic [Porubov and Maugin 2005].

4.3. Thermoelastic models. The classical thermoelastic theory combines the elastic behaviour of homogeneous media with heat conduction, which is usually governed by Fourier's law (see, for example, [Nowacki 1972]). The difference between elastic deformation of a solid and heat conduction consists in that the former is a conservative process without dissipation, whereas the latter is a dissipative one. Bearing in mind microstructured materials, it is possible to use the concept of internal variables to construct mathematical models for governing the wave motion. This is achieved by the dual internal variable theory [Ván et al. 2008], which permits modelling of the dissipation effects due to the microstructure in thermoelastic solids [Berezovski et al. 2011b; Engelbrecht and Berezovski 2012]. The dissipation is associated with microtemperature, i.e., fluctuations of temperature due to the

difference of thermal characteristics of the macro- and microstructure in a solid. Here we present two models: the first one dealing with microtemperature only, and the second one with microdeformation and microtemperature simultaneously.

First, following [Berezovski et al. 2011b] and [Berezovski and Engelbrecht 2013], we postulate the free energy function W as

$$W = \frac{1}{2}(\lambda + 2\mu)u_x^2 - \frac{\rho c_p}{2\theta_0}(\theta - \theta_0)^2 + m(\theta - \theta_0)u_x + Q\varphi_x u_x + \frac{1}{2}P\varphi_x^2 + \frac{1}{2}D\psi^2, \quad (51)$$

where c_p is the heat capacity, $m = -\alpha(3\lambda + 2\mu)$, α is the dilatation coefficient, θ is the temperature, θ_0 is the reference temperature. The first internal variable φ is the microtemperature and the second internal variable ψ is the rate of the first one; Q , P , D_2 are, as before, the material parameters. Leaving aside the details (see references above), the governing equations are

$$\rho u_{tt} = (\lambda + 2\mu)u_{xx} + m\theta_x + Q\varphi_{xx}, \quad (52)$$

$$L\varphi_{tt} + R\varphi_t = P\varphi_{xx} + Qu_{xx}, \quad (53)$$

$$\rho c_p \theta_t - (k\theta_x)_x = m\theta_0 u_{xt} + R\varphi_t^2, \quad (54)$$

where k is the thermal conductivity and R , L are the material parameters related to conductance, which are obtained from satisfying the dissipation inequality. Note that the heat conduction is governed by the parabolic equation (54), while the microtemperature is governed by the hyperbolic equation (53).

Second, following Berezovski et al. [2011b], we use the dual internal variables; the first pair, φ_1 and φ_2 , are related to microdeformation, and the second pair, ψ_1 and ψ_2 , to microstructure. Then the free energy function W is

$$W = \frac{1}{2}(\lambda + 2\mu)u_x^2 - \frac{\rho c_p}{2\theta_0}(\theta - \theta_0)^2 + m(\theta - \theta_0)u_x + A\varphi_1 u_x + \frac{1}{2}B\varphi_1^2 + \frac{1}{2}C(\varphi_1^2)_x + \frac{1}{2}D_1\varphi_2^2 + Q(\psi_1)_x u_x + \frac{1}{2}P(\psi_1^2)_x + \frac{1}{2}D_2\psi_2^2, \quad (55)$$

where A , B , C , D_1 , Q , P , D_2 are, as before, the material parameters. Now the governing equations are

$$\rho u_{tt} = (\lambda + 2\mu)u_{xx} + m\theta_x + A(\varphi_1)_x + Q(\varphi_2)_{xx}, \quad (56)$$

$$I(\varphi_1)_{tt} = C(\varphi_1)_{xx} - Au_x - B\varphi_1, \quad (57)$$

$$L(\varphi_2)_{tt} + R(\varphi_2)_t = P(\varphi_2)_{xx} + Qu_{xx}, \quad (58)$$

$$\rho c_p \theta_t - (k\theta_x)_x = m\theta_0 u_{xt} + R(\varphi_2^2)_t. \quad (59)$$

For details of the derivation, see [Berezovski et al. 2014]. This model contains two hyperbolic equations for microeffects: Equation (57), for microinertia, and Equation (58), for microtemperature. These equations are not coupled, but both of them are coupled with the balance of momentum (56). The fourth equation, (59),

which models the heat conduction at the macrolevel, is parabolic and related only to the microtemperature, while microdeformation is nondissipative.

4.4. Models for inhomogeneous microstructure. Previous models were derived using the assumption of the homogeneity of the microstructure. In many practical application, this assumption must be refined. This is the case, for example, of functionally graded materials (FGMs) which are made up of two or more materials (constituent phases) combined in solid states [Birman and Byrd 2007; Mahamood et al. 2012]. The specimens made of FGMs can have a thin coating of a parent material or a special distribution within a bulk material [Yin et al. 2004]. Such inhomogeneities should be taken into account also in deriving the governing equations.

The simplest way to do that is to modify the well-known Mindlin model. In this case, starting from the conventional free energy function

$$W = \frac{1}{2}(\lambda + 2\mu)u_x^2 + A\varphi u_x + \frac{1}{2}B\varphi^2 + \frac{1}{2}C\varphi_x^2, \quad (60)$$

we assume that $A = A(x)$, $B = B(x)$, and $C = C(x)$. Then the governing equations yield (compare with equations (20) and (21))

$$\rho u_{tt} = (\lambda + 2\mu)u_{xx} + A\varphi_x + A_x\varphi, \quad (61)$$

$$I\varphi_{tt} = C\varphi_{xx} - Au_x - B\varphi + C_x\varphi_x. \quad (62)$$

Here, as before, φ denotes the microdeformation, the elements of the microstructure are of the same size ($I = \text{const}$), but the variation of the microstructure is emphasised by A_x and C_x .

5. Wave dispersion

The main aim of applying various theories to derive mathematical models is to get closer to reality. It has been shown in Sections 3 and 4 that inertia of microstructure(s) leads to higher-order time derivatives, the elasticity of microstructure(s) to higher-order space derivatives, and the coupling of macro- and microstructures results in the changes of velocities. The latter phenomenon is demonstrated also by numerical simulation of waves in metal-ceramic composites by using the finite volume method [Engelbrecht et al. 2005]. In this case, the physical parameters were assigned to every volume element in a material. The changes in the volume fraction $f = V_c/V$ are directly reflected in changes of velocities, where V_c is the volume of ceramic particles and V is the total volume.

In what follows, we explain how introduced microstructure models affect the macrobehaviour of waves: dispersion, wave profiles, frequencies, velocities, spectra, etc. As we have seen, the classical nondispersive wave equation is modified for processes in microstructured solids. The included even-order higher derivatives (fourth-order, sixth-order, etc.) lead to dispersion of waves. In discrete systems

the dispersion analysis is carried out by Brillouin [1946] and Askar [1986]. For diatomic chains they noticed the existence of acoustical and optical branches of the dispersion relation. Mindlin [1964] and Eringen [1972] have described the behaviour of the dispersion curves in microstructured materials, including also acoustical and optical branches. There are many studies to be noted [Huang and Sun 2008; Metrikine 2006; Andrianov et al. 2013] in dispersion analysis, but the most detailed studies are presented by Papargyri-Beskou et al. [2009] and Berezovski et al. [2013].

These studies demonstrate that the typical dispersion curves are convex. However, given the structural characteristics of solids, the periodic character of dispersion curves, as shown by Brillouin [1946] for a discrete chain, is not observed except in some limit cases [Pichugin et al. 2008]. In most models where the assumptions about length scales involve long waves (small wave numbers), the dispersion curves in a short-wave limit tend to some asymptotes corresponding to certain velocities [Engelbrecht et al. 2005; Metrikine and Askes 2002; Berezovski et al. 2011a]. This is explicitly seen from the analysis of group and phase velocities [Papargyri-Beskou et al. 2009; Berezovski et al. 2013]. If short waves are close to nanoscale in the length, then phonon-like dispersion curves are closer to the results of Brillouin [Maranganti and Sharma 2007].

5.1. Dispersion relations. Papargyri-Beskou et al. [2009] derived the following dispersion relation, following [Mindlin 1964] (see (6) in the one-dimensional setting):

$$\omega^2 = c^2 k^2 (1 + g^2 k^2) (1 + h^2 k^2)^{-1}, \quad c^2 = (\lambda + 2\mu) / \rho, \quad (63)$$

where ω , k are the frequency and the wave number, respectively, and g^2 , h^2 are the microstructural elasticity and microinertia coefficients. The corresponding dispersion curves are shown in Figure 1. It is concluded that the dispersion is physically acceptable only if $h^2 > g^2$. This conclusion stresses the importance of the microinertia. The main deficiency of the strain-gradient model is the absence of the optical branch of the dispersion curve.

A more realistic dispersion relation follows from (33), with $A' = 0$ for the sake of simplicity (see [Berezovski et al. 2013]):

$$\omega^2 = (c^2 - c_A^2) k^2 + p^2 (\omega^2 - c^2 k^2) (\omega^2 - c_1^2 k^2). \quad (64)$$

The corresponding dispersion curves are shown in Figure 2 [Berezovski et al. 2013]. In this figure, the dispersion curve computed from the relation

$$\omega^2 = (c^2 - c_A^2) k^2 - p^2 c_A^2 (\omega^2 - c_1^2 k^2)^2 \quad (65)$$

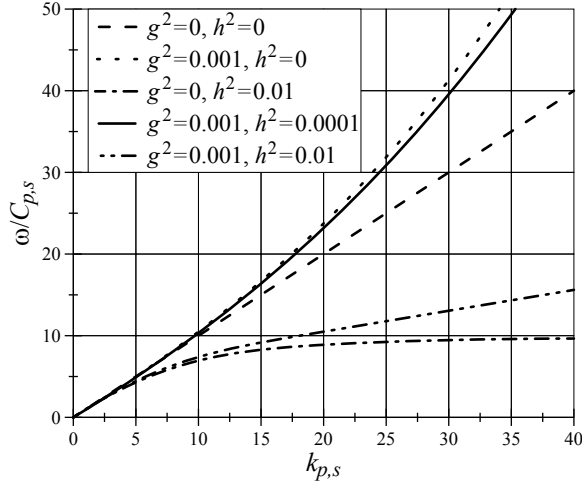


Figure 1. Dispersion curves of the $\omega/C_{p,s}$ versus wavenumber $k_{p,s}$ type for elastic medium with microstructure obeying Equation (63). Adapted from [Papargyri-Beskou et al. 2009].

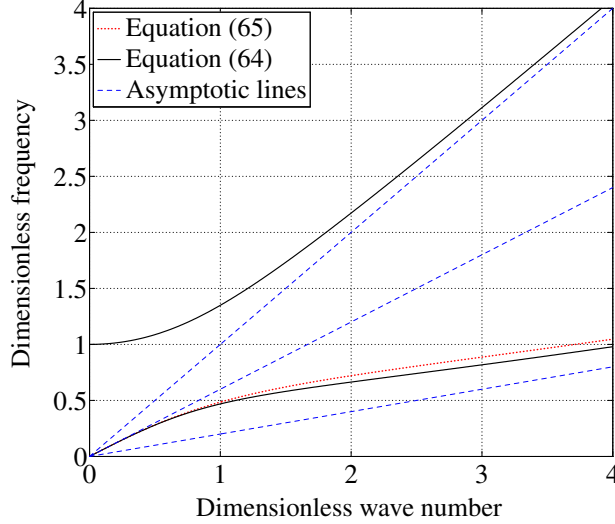


Figure 2. Dispersion curves in case of $c_{gr} < c_{ph}$ ($c_A = 0.8c$, $c_1 = 0.2c$).

following from (34) is also shown. The asymptotes in Figure 2 reflect the dimensionless velocities: $\omega = k$, $\omega = c_1 k/c$, $\omega = c_R k/c$, where $c_1^2 = C/I$, $c_R^2 = c^2 - c_A^2$. These velocities play a role in the case of shorter waves.

Dispersion relation (64), which reflects the behaviour of waves modelled by (33), leads to two dispersion curves — one branch is acoustic (lower branch), another one

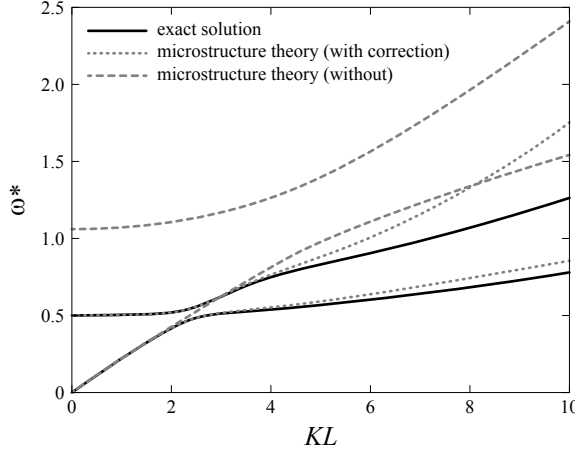


Figure 3. Comparison of the longitudinal dispersive curves with and without the correction factors. Adapted from [Huang and Sun 2008].

is optical (upper branch). Such a situation is noticed in many studies [Erofeyev 2003; Engelbrecht et al. 2005; Huang and Sun 2008; Berezovski et al. 2011a]. (As an example, the dispersion curves from the paper by Huang and Sun [2008] are shown in Figure 3.)

Direct calculations by the finite element method also display the changes in velocities due to dispersive effects [Gonella et al. 2011; Greene et al. 2012].

No band gaps are observed in the dispersion curves shown in Figures 2, 3. However, the existence of such band gaps has been demonstrated by Madeo et al. [2013] for unidirectional wave propagation in relaxed micromorphic media [Neff et al. 2014].

5.2. Phase and group velocities. The phase ($c_{\text{ph}} = \omega/k$) and group ($c_{\text{gr}} = \partial\omega/\partial k$) speeds corresponding to relation (64) are depicted in Figure 4. It must be noted that the asymptotic value of the acoustic phase speed approaches the value c_1/c monotonically, while the group speed changes faster and nonmonotonically. It is possible to determine the dimensionless parameters which govern the process as [Engelbrecht et al. 2013]

$$\gamma_A^2 = c_A^2/c^2, \quad \gamma_1^2 = c_1^2/c^2, \quad \Gamma = 1 - \gamma_A^2 - \gamma_1^2. \quad (66)$$

The parameter Γ is crucial for distinction between dispersion types. If $\Gamma \geq 0$ then the dispersion is normal ($c_{\text{gr}} < c_{\text{ph}}$) and if $\Gamma < 0$ then the dispersion is anomalous ($c_{\text{gr}} > c_{\text{ph}}$). In the dispersionless case $\Gamma = 0$. Following Papargyri-Beskou et al. [2009] (Figure 5), these conditions are related to the ratio h/g : if $h/g > 1$ then the dispersion is normal, and if $h/g < 1$ then the dispersion is anomalous.

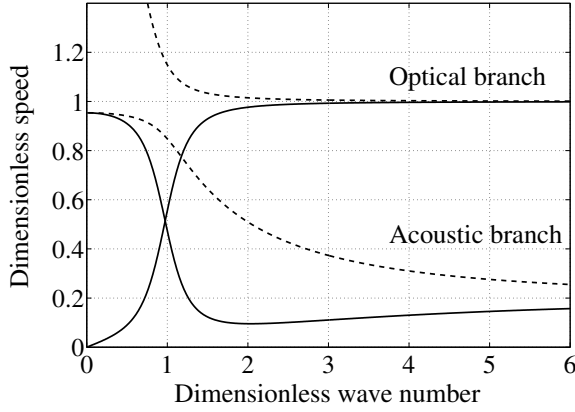


Figure 4. Group (solid line) and phase (dashed line) speed curves against the wave number, $c_A = 0.3c$, $c_1 = 0.2c$.

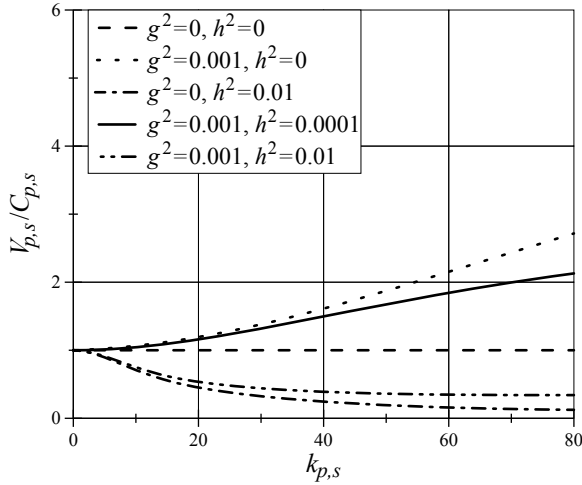


Figure 5. Dispersion curves of the $V_{p,s}/C_{p,s}$ versus $k_{p,s}$ type for elastic medium with microstructure obeying Equation (63). Adapted from [Papargyri-Beskou et al. 2009].

The parameter γ_A is related to coupling effects, and it defines the dimensionless speed of long waves. The greater the value of γ_A , the smaller the speed of long waves. The parameter γ_1 is actually the ratio of speeds in macro- and microstructures. The greater the value of γ_1 , the greater the speeds of short waves. The parameters γ_A and γ_1 can be used for determining the differences between the full equation (33) and its asymptotic presentation (34); see [Peets et al. 2008]. In addition, a dimensionless parameter γ_{AB} might be useful for asymptotic estimations,

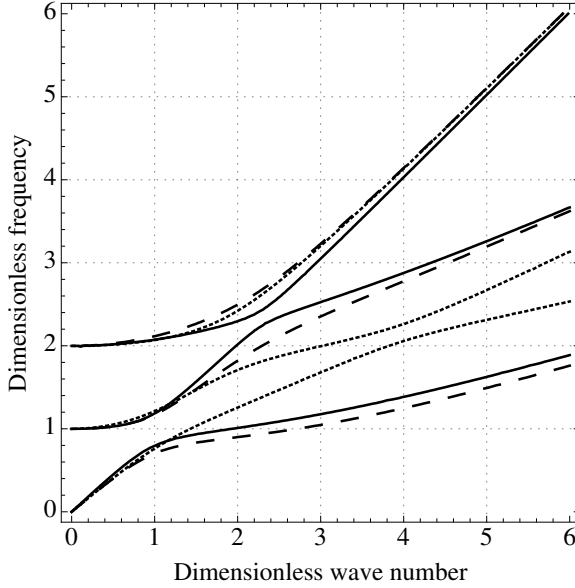


Figure 6. Comparison of dispersion curves of hierarchical microstructure model. Solid lines: Equation (43). Dashed lines: concurrent coupled microstructure model. Dotted lines: concurrent uncoupled microstructure model. Here $c_{A1} = c_{A2} = c_{A12} = 0.4c$, $c_1 = 0.5c$, $c_2 = 0.3c$.

given by

$$\gamma_{AB}^2 = c_A^2 / c_B^2 = D^2 I / \rho B^2 L_0^2 = \delta I^* D^2 / B^2, \quad (67)$$

where it is assumed that $I = \rho l^2 I^*$, $\delta = l^2 / L_0^2$. As follows from (67), it involves the scale parameter δ , which also gives weight to higher-order terms in the governing equations.

In the case of a hierarchical microstructure modelled by the system (36)–(38) or by (43), the dispersion relation reads as

$$(c^2 k^2 - \omega^2)(c_1 k^2 - \omega^2 + \omega_1^2)(c_2^2 k^2 - \omega^2 + \omega_2^2) - c_{A12}^2 \omega_2^2 k^2 (c^2 k^2 - \omega^2) - c_{A1}^2 \omega_1^2 k^2 (c_2^2 - \omega^2 + \omega_2^2) = 0. \quad (68)$$

Here, in addition to the notation of (43), we define $c_{A12}^2 = A_{12}^2 / I_1 B_2$, $\omega_1^2 = 1 / p_1^2$, and $\omega_2^2 = 1 / p_2^2$. The typical dispersion curves are shown in Figure 6.

This model may involve an interesting physical phenomenon: negative group velocity (NGV), analysed by Peets et al. [2013]. Indeed, such a case is shown in Figure 7. The physical explanation for this phenomenon may be the following. It is known that the optical branches are related to nonpropagating oscillations

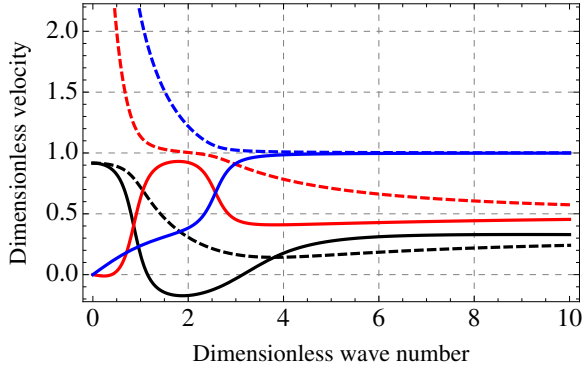


Figure 7. Group (solid line) and phase (dashed line) speed curves against the wave number, $c_A = 0.3c$, $c_1 = 0.2c$.

[Brillouin 1946]. In the case shown in Figure 6, two optical branches can be very close to each other at certain frequencies. This can be considered as a preresonant situation: these nonpropagating oscillations are coupled, resulting in the NGV. This is also the reason for the multivalued phase velocity (Figure 7). Note that in optics the NGV is usually space-dependent, [Dogariu et al. 2001] but here, as seen from Figure 7, the NGV is dependent on the wave number. Consequently, for an arbitrary excitation with a wide spectrum, only some spectral components are affected.

5.3. Wave profiles. Dispersion effects are certainly reflected in wave profiles. A typical profile is shown in Figure 8 [Berezovski et al. 2013], where the influence of optical and acoustic branches of dispersion curves is seen. It is noted that high frequency oscillations due to the optical dispersion branch appear. A detailed analysis of such effects is presented by Tamm and Peets [2013]. Clearly, these effects must be taken into account not only in solving the direct problems but especially in nondestructive testing with acoustic waves. Several numerical results are presented for an impact-type excitation in [Askes and Metrikine 2002; Fish et al. 2002; Peets and Tamm 2010], for a triangular pulse in [Wang and Sun 2002], for a harmonic pulse in [Peets and Tamm 2010], for a burst-type pulse in [Greene et al. 2012].

5.4. Influence of nonlinearity. The nonlinear models described in Section 4 lead to Boussinesq-type equations. The possible balance of dispersion and nonlinearity may lead to soliton-type solutions. There are three essential problems related to solitons: (i) existence of solitons, (ii) emergence of solitons, and (iii) interaction of solitons. Contrary to the celebrated KdV-solitons governed by an equation with first-order time derivative in a leading term, here the governing equations possess a second-order time derivative in leading terms. This means that, as in the classical wave equation, the waves propagate to the left and to the right (d'Alembert

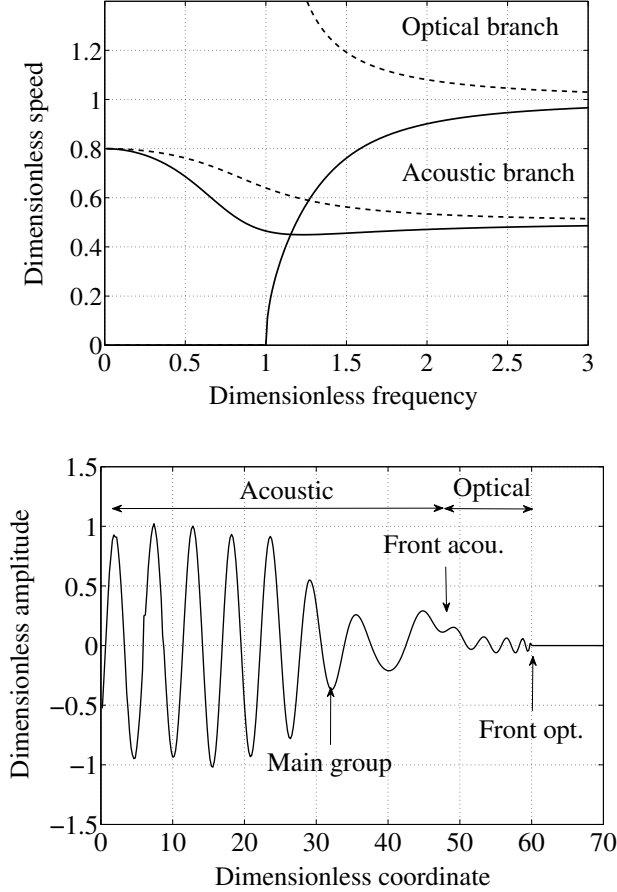


Figure 8. Top: phase (dotted lines) and group (solid lines) speed curves. Bottom: wave profile at 60 time steps. Here $c_A = 0.6c$, $c_1 = 0.5c$, dimensionless frequency for the boundary condition is 0.8.

solution), not in one direction, as results from the KdV equation. Most studies concerning solitons and the KdV equation focus on fluids. However, a historical review on solitons in elastic solids is presented in [Maugin 2011b]. Here we focus on models of nonlinear microstructured solids based on equations described in Section 4.

5.4.1. Existence of solitons. We take (48) as the basic equation. In its dimensionless form, it yields

$$V_{TT} - bV_{XX} - \frac{1}{2}\mu(V^2)_{XX} = \delta(\beta V_{TT} - \gamma V_{XX} + \delta^{1/2}\frac{1}{2}\kappa(V_X^2)_X)_{XX}, \quad (69)$$

where $V = U_X$, $U = u/U_0$, $X = x/l$, $T = ct/l$ and, as before $\delta = l^2/\lambda^2$. The

coefficients of (69) are related to the free energy function (44) by

$$b = 1 - \frac{D^2}{(\lambda + 2\mu)B}, \quad \mu = \frac{NU_0}{(\lambda + 2\mu)L_0}, \quad \beta = \frac{ID^2}{\rho l^2 B^2}, \quad (70)$$

$$\gamma = \frac{CD^2}{(\lambda + 2\mu)B^2 l^2}, \quad \kappa = \frac{D^3 MU_0}{(\lambda + 2\mu)B^3 l^3 L_0}.$$

The existence of a single solitary wave solution to (69) should satisfy the conditions [Janno and Engelbrecht 2005b]

$$\frac{c_s^2 - b}{\beta c_s^2 - \gamma} > 0, \quad \left(\frac{\beta c_s^2 - \gamma}{c_s^2 - b} \right)^3 > \frac{4\kappa}{\mu^2}, \quad (71)$$

$$\mu \neq 0, \quad \beta c_s^2 - \gamma \neq 0, \quad c_s^2 - b \neq 0, \quad (72)$$

where c_s is a characteristic speed of solitary waves. For other types of governing equations, the solitary waves are described in [Maugin 1999; Erofejev 2003; Porubov et al. 2009].

5.4.2. Emergence of solitons. In the classical example of the KdV equation, a harmonic initial condition leads to a train of solitons [Zabusky and Kruskal 1965]. Here the results should be two trains of solitons, propagating to the left and to the right

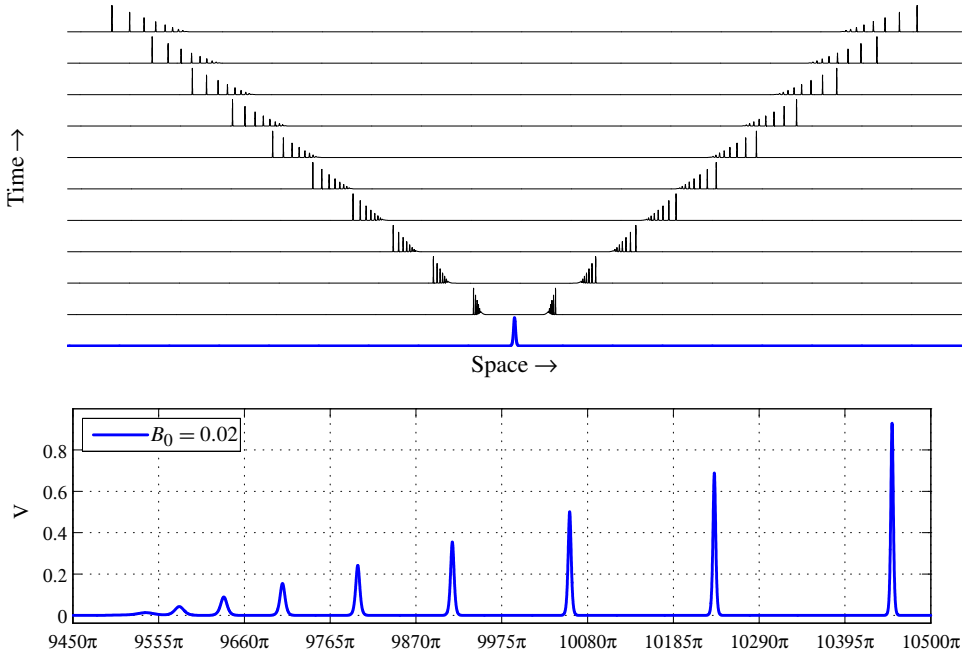


Figure 9. Formation of train of solitons for $B_0 = 0.02$, $K = 5500$. Profiles plotted every 1500 time steps.

right. Indeed, it has been shown by numerical simulations [Engelbrecht et al. 2006; 2011] that solving (69) with an initial condition in the form of a single bell-type pulse results in two trains of solitons. Figure 9 shows the emergence process in the course of time. If dispersion is controlled by other higher-order derivatives, then the emergence process is somewhat different. Several examples are presented in [Maugin 1999]. Emergence of solitons is described also in laminates where the stress-strain law of layers is nonlinear and dispersion is caused by layering [Engelbrecht et al. 2007].

5.4.3. Interaction of solitary waves. This is a crucial problem when determining whether solitary waves behave like solitons or not. A soliton should interact with another soliton, keeping its amplitude (velocity), and only a phase change is allowed. This process has been intensively studied by many authors [Soerensen et al. 1984; Maugin and Christov 1997; Bogdan and Kosevich 1997; Maugin 1999; Christov et al. 2007; Salupere et al. 2008; Porubov 2009]. An intriguing question is the shape of solitary waves. Bearing in mind the microstructured solids, two nonlinearities are presented in (68): nonlinearity of the macrostructure and nonlinearity of the microstructure. It has been shown [Janno and Engelbrecht 2005b] that the existence of two nonlinearities leads to the asymmetry of a solitary wave. Note that, with $\kappa = 0$ (no nonlinearity at the microstructure), (68) has the solitary wave solution [Porubov 2003; Janno and Engelbrecht 2005b]

$$\begin{aligned} V(X - c_s T) &= A_s \operatorname{sech}^2 \left[\frac{1}{2} \kappa_1 (X - c_s T) \right], \\ A_s &= 3(c_s^2 - b)/\mu, \quad \kappa_1^2 = (c_s^2 - b)/\delta(\beta c_s^2 - \gamma). \end{aligned} \quad (73)$$

This symmetric solution turns asymmetric if $\kappa \neq 0$ in (69). The evolution equation (one-wave equation) derived from (69) is a modified KdV-type equation, and for this an exact solution is found by Randrüüt and Braun [2010], which displays asymmetry due to the existence of the nonlinearity at the microstructure.

It is concluded by many authors that the interaction of solitary waves in such systems is usually accompanied by radiation [Christov et al. 2007; Salupere et al. 2008; Engelbrecht et al. 2011]. This means that the interaction can be considered elastic only in the course of several interactions, although the waves retain their individuality [Christov et al. 2007]. The governing equation may include more complicated nonlinearities, as in the case of chains of beads [Coste et al. 1997].

Remark 6. Turning again to waves in rods, the problems of emergence and interaction of solitary waves are studied in detail in [Porubov 2009].

6. Thermal effects

In Section 4, the governing equations were presented for microstructured thermoelastic solids. Definitely, the internal structure of thermoelastic solids displays not

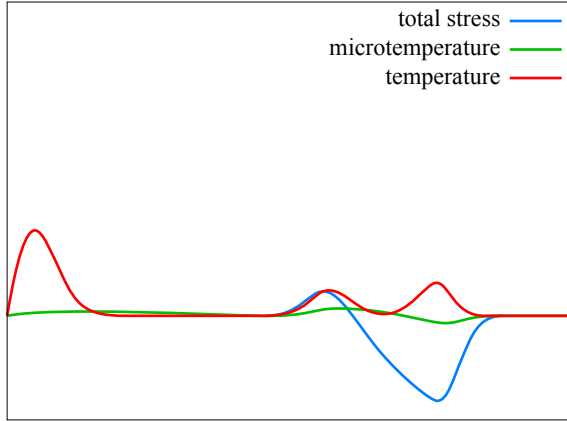


Figure 10. Distribution of temperature, stress, and microtemperature in a microstructured half-space at 350 time steps after thermal impact.

only differences in elastic properties but also in thermal characteristics. The internal temperature fluctuations which might be called microtemperature display a specific behaviour [Berezovski and Berezovski 2013; Berezovski and Engelbrecht 2013]. As an example, the propagation of a thermal pulse described by (52)–(54) is illustrated in Figure 10. Besides the usual diffusion of the macrotemperature θ in course of time close to boundary, wave-type behaviour of the total temperature is observed following the deformation wave. This is possible because of coupling effects between microtemperature (governed by a hyperbolic operator in (53)), stress, and macrotemperature.

7. Material identification

Physical effects due to the microstructure of solids serve as signatures about the structure. Changes in velocities and wave profiles and/or their spectra can be used to solve the inverse problems; that means determining material constants from the analysis of changes. As said before, waves are carriers of information. The problem, however, is complicated because the number of material constants is high. For example, Equation (33), which is a basic model in our discussion, involves, beside the properties of the macrostructure (density and the elastic constants), the properties of the microstructure (constants B, C, D, I) and of coupling (constants A, A'). In terms of the wave equation, these constants are grouped for coefficients. The situation is even more complicated in multiscale models or thermoelastic models (Section 4).

One possible approach to determine the material constants is to start from homogenisation methods [Santosa and Symes 1991; Forest 1998; 1999; Fish et al.

2002; Wang and Sun 2002]. Some constants are presented in [Erofeyev 2003]. More contemporary homogenisation methods are described in [Jänicke and Steeb 2012; Fish and Kuznetsov 2012]. On other hand, numerical methods can be combined with material characterisation [Gonella et al. 2011; Greene et al. 2012]. The latter approach is also supported by theoretical results [Neff 2005; Neff and Forest 2007].

Another approach is to solve an inverse problem: given the structure of a model and an initial excitation and results of measurements, one has to determine the coefficients of the model. This approach is widely used in nondestructive evaluation (NDE) of material properties. There are many methods of NDE [Hellier 2001]; here we limit ourselves only to the possibilities of ultrasound NDE, based on the usage of acoustic waves as carriers of information. A detailed description of solving the inverse problem for the Mindlin-type micromorphic model is given in [Janno and Engelbrecht 2011]. The basic model is either the linear equation (34) or its nonlinear modification (48), together with their basic systems of two equations, like the system (20)–(21). The conditions for the existence of the solution together with its uniqueness and stability guarantee a well-posed problem. Harmonic waves and wave packets are used in the case of linear problems, and solitons in the case of nonlinear problems. The main ideas are to use changes in phase velocities [Janno and Engelbrecht 2005c] and properties of solitary waves [Janno and Engelbrecht 2005a] for determining material constants. Harmonic waves and Gaussian wave packets are used in the linear case. In the nonlinear case, a novel method is proposed based on measuring the asymmetry of a solitary wave [Janno and Engelbrecht 2005a]. The crucial point is to establish a number of possible coefficients which can be determined from solving a corresponding well-posed inverse problem.

8. Discussion and final remarks

Technological demands for microstructured materials are high, and there is a growing need to predict the behaviour of such structures under high-intensity and high-frequency excitations. As shown above, there exists a general framework for building appropriate mathematical models in order to grasp microscopic-to-macroscopic relations in materials. One might say that the unifying goal of this framework is to understand better the bulk behaviour of matter which depends on microscopic constituents and their properties. In this context, there are several avenues of research.

The first avenue leads towards developing the theory of microstructured continua. It is reflected in many monographs [Eringen 1999; Capriz 1989; Maugin 1999; 2013] and overviews [Mariano 2002] together with a lot of research papers. Several subfields are important: modelling of elastic microstructures, modelling

of coupled fields (thermo-, electro-, magnetoelasticity), modelling of dislocations and phase transitions, etc. In this context, multiscale problems which depend on the character of excitations (the ratio L_0/l) become more and more important, resulting in hierarchical models.

The second avenue could be described as casting the theory of microstructured continua into concrete mathematical models, i.e., into systems of equations or single equations. In wave dynamics, this means deriving the modified systems of wave equations with leading terms of the second-order partial derivatives together with higher-order terms. These equations may be built in the form of certain hierarchies [Whitham 1974]. In this overview we moved along this avenue, presenting the mathematical models and analysing the corresponding physical effects.

The third avenue is related to numerical simulations. Due to complicated mathematical models and several scales, numerical schemes need to be modified in order to describe multiscales or coupling effects (see, for example, [Mariano and Stazi 2005; Vernerey et al. 2007; Berezovski et al. 2008]). Here we also use numerical simulations to demonstrate the changes in wave profiles.

The fourth avenue should lead to experimental verification. There are not very many results in this important direction. The early experiments of Potapov and Rodyushkin [2001] demonstrated the existence of solitary waves. The studies [Coste et al. 1997; Porter et al. 2009] described experiments with solitary waves in chains of beads, which give a possibility to build tunable one-dimensional phononic materials [Daraio et al. 2006]. Clearly, much is expected in moving along this avenue—not only phononic materials, but the general applications in the NDE should be further developed for more precise materials characterisation.

As said before, in this overview, attention was focussed on models of waves in their simplest one-dimensional setting. The concept of internal variables permits easy derivation of the mathematical models accounting for various physical effects. It is demonstrated that, beside the classical wave equation, the modified wave equations with higher-order terms form an interesting and challenging chapter in mathematical physics. These equations can be derived by satisfying thermodynamical constraints, and naturally involve both acoustic and optical branches in dispersion relations. This is extremely important in order to model the physical situation correctly (see, e.g., Figure 8).

The dispersion analysis reflects rich physical phenomena due to microstructure(s), and accounts for the multiscale problems, resulting in hierarchical equations. If nonlinear effects are included then the governing equations are of the Boussinesq type. The coupling of the macro- and microstructure leads to changes in velocities and wave profiles. The main conclusion from the analysis above is the following. The influence of the microstructure on wave propagation in solids

is modelled best if (i) microinertia is taken into account, and (ii) the corresponding dispersion relation includes both acoustic (in-phase) and optical (out-of-phase) branches. If, however, some asymptotic procedures are applied in order to simplify the full model, then the simplified model should in some sense grasp the influence of the optical branch.

The classical wave equation is a cornerstone in mechanics and mathematical physics. It describes the propagation of an excitation in homogeneous elastic media. What is discussed above is how to modify this beautiful mathematical model in order to come closer to reality. As a result, the mathematical models involve higher-order derivatives and nonlinear terms which stem from the properties of materials. Such models gain more and more attention in contemporary engineering problems of dynamical response of materials and constructions.

It must be noted that the existence of a microstructure in a bulk material means that the constituents interact with each other and influence the macrobehaviour. This is a typical problem of complexity, where the behaviour of constituents leads to changes in the global behaviour [Nicolis and Nicolis 2007]. There are also attempts to cast the analysis into this pattern in multiscale materials [Engelbrecht 2009; Liu et al. 2010; Engelbrecht and Pastrone 2011]. However, such an approach is not used for describing solids only, it is also noted in fluids (see [Engelbrecht et al. 2010]).

Finally, the ideas worked out theoretically during the last century [Mauguin 2013] have matured now to reach practical applications. The search certainly goes on, as said by Mariano [2012]:

...effective developments in applied sciences rely on a deep comprehension and command of the inner nature of the models involved and techniques utilised.

References

- [Achenbach et al. 1968] J. D. Achenbach, C.-T. Sun, and G. Herrmann, “On the vibrations of a laminated body”, *J. Appl. Mech. (ASME)* **35**:4 (1968), 689–696.
- [Andrianov et al. 2010] I. V. Andrianov, J. Awrejcewicz, and D. Weichert, “Improved continuous models for discrete media”, *Math. Probl. Eng.* **2010** (2010), Article ID 986242.
- [Andrianov et al. 2011] I. V. Andrianov, V. V. Danishevs’kyi, H. Topol, and D. Weichert, “Homogenization of a 1D nonlinear dynamical problem for periodic composites”, *Z. Angew. Math. Mech.* **91**:6 (2011), 523–534.
- [Andrianov et al. 2013] I. V. Andrianov, V. V. Danishevs’kyi, O. I. Ryzhkov, and D. Weichert, “Dynamic homogenization and wave propagation in a nonlinear 1D composite material”, *Wave Motion* **50**:2 (2013), 271–281.
- [Askar 1986] A. Askar, *Lattice dynamical foundations of continuum theories: elasticity, piezoelectricity, viscoelasticity, plasticity*, Theoretical and Applied Mechanics **2**, World Scientific, Philadelphia, 1986.

- [Askes and Aifantis 2006] H. Askes and E. C. Aifantis, “Gradient elasticity theories in statics and dynamics: a unification of approaches”, *Int. J. Fract.* **139**:2 (2006), 297–304.
- [Askes and Metrikine 2002] H. Askes and A. V. Metrikine, “One-dimensional dynamically consistent gradient elasticity models derived from a discrete microstructure, 2: Static and dynamic response”, *Eur. J. Mech. A Solids* **21**:4 (2002), 573–588.
- [Askes and Metrikine 2005] H. Askes and A. V. Metrikine, “Higher-order continua derived from discrete media: continualisation aspects and boundary conditions”, *Int. J. Solids Struct.* **42**:1 (2005), 187–202.
- [Askes et al. 2008] H. Askes, A. V. Metrikine, A. V. Pichugin, and T. Bennett, “Four simplified gradient elasticity models for the simulation of dispersive wave propagation”, *Philos. Mag.* **88**:28–29 (2008), 3415–3443.
- [Berezovski and Berezovski 2013] A. Berezovski and M. Berezovski, “Influence of microstructure on thermoelastic wave propagation”, *Acta Mech.* **224**:11 (2013), 2623–2633.
- [Berezovski and Engelbrecht 2013] A. Berezovski and J. Engelbrecht, “Thermoelastic waves in microstructured solids: dual internal variables approach”, *J. Coupled Syst. Multiscale Dyn.* **1**:1 (2013), 112–119.
- [Berezovski et al. 2008] A. Berezovski, J. Engelbrecht, and G. A. Maugin, *Numerical simulation of waves and fronts in inhomogeneous solids*, World Scientific Series on Nonlinear Science Series A **62**, World Scientific, Hackensack, NJ, 2008.
- [Berezovski et al. 2010] A. Berezovski, J. Engelbrecht, and T. Peets, “Multiscale modeling of microstructured solids”, *Mech. Res. Commun.* **37**:6 (2010), 531–534.
- [Berezovski et al. 2011a] A. Berezovski, J. Engelbrecht, and M. Berezovski, “Waves in microstructured solids: a unified viewpoint of modeling”, *Acta Mech.* **220**:1–4 (2011), 349–363.
- [Berezovski et al. 2011b] A. Berezovski, J. Engelbrecht, and G. A. Maugin, “Generalized thermo-mechanics with dual internal variables”, *Arch. Appl. Mech.* **81**:2 (2011), 229–240.
- [Berezovski et al. 2013] A. Berezovski, J. Engelbrecht, A. Salupere, K. Tamm, T. Peets, and M. Berezovski, “Dispersive waves in microstructured solids”, *Int. J. Solids Struct.* **50**:11–12 (2013), 1981–1990.
- [Berezovski et al. 2014] A. Berezovski, J. Engelbrecht, and P. Ván, “Weakly nonlocal thermoelasticity for microstructured solids: microdeformation and microtemperature”, *Arch. Appl. Mech.* **84**:9–11 (2014), 1249–1261.
- [Birman and Byrd 2007] V. Birman and L. W. Byrd, “Modeling and analysis of functionally graded materials and structures”, *Appl. Mech. Rev. (ASME)* **60**:5 (2007), 195–216.
- [Bogdan and Kosevich 1997] M. Bogdan and A. Kosevich, “Interaction of moving solitons in a dispersive medium and regimes of their radiationless motion”, *Proc. Estonian Acad. Sci. Phys. Math.* **46**:1–2 (1997), 14–23.
- [Born and von Kármán 1912] M. Born and T. von Kármán, “Über Schwingungen in Raumgittern”, *Physik. Z.* **13** (1912), 297–309.
- [Brillouin 1946] L. Brillouin, *Wave propagation in periodic structures: electric filters and crystal lattices*, McGraw-Hill, New York, 1946.
- [Capriz 1989] G. Capriz, *Continua with microstructure*, Springer Tracts in Natural Philosophy **35**, Springer, New York, 1989.
- [Casasso and Pastrone 2010] A. Casasso and F. Pastrone, “Wave propagation in solids with vectorial microstructures”, *Wave Motion* **47**:6 (2010), 358–369.

- [Challamel et al. 2009] N. Challamel, L. Rakotomanana, and L. Le Marrec, “A dispersive wave equation using nonlocal elasticity”, *C. R. Mécanique* **337**:8 (2009), 591–595.
- [Chen and Lee 2003] Y. Chen and J. D. Lee, “Connecting molecular dynamics to micromorphic theory, II: Balance laws”, *Physica A* **322** (2003), 377–392.
- [Chen et al. 2003] Y. Chen, J. D. Lee, and A. Eskandarian, “Examining the physical foundation of continuum theories from the viewpoint of phonon dispersion relation”, *Int. J. Eng. Sci.* **41**:1 (2003), 61–83.
- [Chen et al. 2004] Y. Chen, J. D. Lee, and A. Eskandarian, “Atomistic viewpoint of the applicability of microcontinuum theories”, *Int. J. Solids Struct.* **41**:8 (2004), 2085–2097.
- [Christov et al. 1996] C. I. Christov, G. A. Maugin, and M. G. Velarde, “Well-posed Boussinesq paradigm with purely spatial higher-order derivatives”, *Phys. Rev. E* **54**:4 (1996), 3621–3638.
- [Christov et al. 2007] C. I. Christov, G. A. Maugin, and A. V. Porubov, “On Boussinesq’s paradigm in nonlinear wave propagation”, *C. R. Mécanique* **335**:9–10 (2007), 521–535.
- [Cosserat and Cosserat 1909] E. Cosserat and F. Cosserat, *Théorie des corps déformables*, Hermann, Paris, 1909.
- [Coste et al. 1997] C. Coste, E. Falcon, and S. Fauve, “Solitary waves in a chain of beads under Hertz contact”, *Phys. Rev. E* **56**:5 (1997), 6104–6117.
- [Craster et al. 2010] R. V. Craster, J. Kaplunov, and A. V. Pichugin, “High-frequency homogenization for periodic media”, *Proc. R. Soc. Lond. A* **466**:2120 (2010), 2341–2362.
- [Curtin and Miller 2003] W. A. Curtin and R. E. Miller, “Atomistic/continuum coupling in computational materials science”, *Model. Simul. Mater. Sci. Eng.* **11**:3 (2003), R33–R68.
- [Daraio et al. 2006] C. Daraio, V. F. Nesterenko, E. B. Herbold, and S. Jin, “Tunability of solitary wave properties in one-dimensional strongly nonlinear phononic crystals”, *Phys. Rev. E* **73**:2 (2006), Article ID 026610.
- [dell’Isola et al. 2009] F. dell’Isola, G. Sciarra, and S. Vidoli, “Generalized Hooke’s law for isotropic second gradient materials”, *Proc. R. Soc. Lond. A* **465**:2107 (2009), 2177–2196.
- [dell’Isola et al. 2012] F. dell’Isola, A. Madeo, and L. Placidi, “Linear plane wave propagation and normal transmission and reflection at discontinuity surfaces in second gradient 3D continua”, *Z. Angew. Math. Mech.* **92**:1 (2012), 52–71.
- [Dogariu et al. 2001] A. Dogariu, A. Kuzmich, and L. J. Wang, “Transparent anomalous dispersion and superluminal light-pulse propagation at a negative group velocity”, *Phys. Rev. A* **63**:5 (2001), Article ID 053806.
- [Duhem 1911a] P. M. M. Duhem, *Traité d’énergétique ou de thermodynamique générale*, vol. 1, Gauthier-Villars, Paris, 1911.
- [Duhem 1911b] P. M. M. Duhem, *Traité d’énergétique ou de thermodynamique générale*, vol. 2, Gauthier-Villars, Paris, 1911.
- [Engelbrecht 1997] J. Engelbrecht, *Nonlinear wave dynamics: complexity and simplicity*, Kluwer Texts in the Mathematical Sciences **17**, Kluwer, Dordrecht, 1997.
- [Engelbrecht 2009] J. Engelbrecht, “Complexity in mechanics”, *Rend. Sem. Mat. Univ. Politec. Torino* **67**:3 (2009), 293–325.
- [Engelbrecht and Berezovski 2012] J. Engelbrecht and A. Berezovski, “Internal structures and internal variables in solids”, *J. Mech. Mater. Struct.* **7**:10 (2012), 983–996.
- [Engelbrecht and Braun 1998] J. Engelbrecht and M. Braun, “Nonlinear waves in nonlocal media”, *Appl. Mech. Rev. (ASME)* **51**:8 (1998), 475–488.

- [Engelbrecht and Pastrone 2003] J. Engelbrecht and F. Pastrone, “Waves in microstructured solids with nonlinearities in microscale”, *Proc. Estonian Acad. Sci. Phys. Math.* **52**:1 (2003), 12–20.
- [Engelbrecht and Pastrone 2011] J. Engelbrecht and F. Pastrone, “Non linear waves in complex microstructured solids”, *Mem. Accad. Sci. Torino Cl. Sci. Fis. Mat. Nat.* (5) **35** (2011), 23–36.
- [Engelbrecht and Salupere 2014] J. Engelbrecht and A. Salupere, “Scaling and hierarchies of wave motion in solids”, *Z. Angew. Math. Mech.* **94**:9 (2014), 775–783.
- [Engelbrecht et al. 2005] J. Engelbrecht, A. Berezovski, F. Pastrone, and M. Braun, “Waves in microstructured materials and dispersion”, *Philos. Mag.* **85**:33–35 (2005), 4127–4141.
- [Engelbrecht et al. 2006] J. Engelbrecht, F. Pastrone, M. Braun, and A. Berezovski, “Hierarchies of waves in nonclassical materials”, pp. 29–47 in *Universality of nonclassical nonlinearity*, edited by P. P. Delsanto, Springer, New York, 2006.
- [Engelbrecht et al. 2007] J. Engelbrecht, A. Berezovski, and A. Salupere, “Nonlinear deformation waves in solids and dispersion”, *Wave Motion* **44**:6 (2007), 493–500.
- [Engelbrecht et al. 2010] J. Engelbrecht, A. Berezovski, and T. Soomere, “Highlights in the research into complexity of nonlinear waves”, *Proc. Estonian Acad. Sci. Phys. Math.* **59**:2 (2010), 61–65.
- [Engelbrecht et al. 2011] J. Engelbrecht, A. Salupere, and K. Tamm, “Waves in microstructured solids and the Boussinesq paradigm”, *Wave Motion* **48**:8 (2011), 717–726.
- [Engelbrecht et al. 2013] J. Engelbrecht, T. Peets, K. Tamm, and A. Salupere, “Deformation waves in microstructured solids and dimensionless parameters”, *Proc. Estonian Acad. Sci. Phys. Math.* **62**:2 (2013), 109–115.
- [Eringen 1962] A. C. Eringen, *Nonlinear theory of continuous media*, McGraw-Hill, New York, 1962.
- [Eringen 1964] A. C. Eringen, “Simple microfluids”, *Int. J. Eng. Sci.* **2**:2 (1964), 205–217.
- [Eringen 1969] A. C. Eringen, “Micropolar fluids with stretch”, *Int. J. Eng. Sci.* **7**:1 (1969), 115–127.
- [Eringen 1972] A. C. Eringen, “Linear theory of nonlocal elasticity and dispersion of plane waves”, *Int. J. Eng. Sci.* **10**:5 (1972), 425–435.
- [Eringen 1999] A. C. Eringen, *Microcontinuum field theories, I: Foundations and solids*, Springer, New York, 1999.
- [Eringen and Suhubi 1964a] A. C. Eringen and E. S. Suhubi, “Nonlinear theory of simple microelastic solids, I”, *Int. J. Eng. Sci.* **2**:2 (1964), 189–203.
- [Eringen and Suhubi 1964b] A. C. Eringen and E. S. Suhubi, “Nonlinear theory of simple microelastic solids, II”, *Int. J. Eng. Sci.* **2**:4 (1964), 389–404.
- [Erofeyev 2003] V. I. Erofeyev, *Wave processes in solids with microstructure*, Stability, Vibration and Control of Systems, Series A **8**, World Scientific, Singapore, 2003.
- [Fish and Kuznetsov 2012] J. Fish and S. Kuznetsov, “From homogenization to generalized continua”, *Int. J. Comput. Methods Eng. Sci. Mech.* **13**:2 (2012), 77–87.
- [Fish et al. 2002] J. Fish, W. Chen, and G. Nagai, “Non-local dispersive model for wave propagation in heterogeneous media: one-dimensional case”, *Int. J. Numer. Methods Eng.* **54**:3 (2002), 331–346.
- [Fish et al. 2005] J. Fish, W. Chen, and Y. Tang, “Generalized mathematical homogenization of atomistic media at finite temperatures”, *Int. J. Multiscale Comput. Eng.* **3**:4 (2005), 393–413.
- [Forest 1998] S. Forest, “Mechanics of generalized continua: construction by homogenization”, *J. Phys. (France) IV* **8**:PR4 (1998), 39–48.
- [Forest 1999] S. Forest, “Homogenization methods and the mechanics of generalized continua”, pp. 35–48 in *Geometry, continua and microstructure* (Paris, 1997), edited by G. A. Maugin, Travaux en Cours **60**, Hermann, Paris, 1999.

- [Gates et al. 2005] T. S. Gates, G. M. Odegard, S. J. V. Frankland, and T. C. Clancy, “Computational materials: multi-scale modeling and simulation of nanostructured materials”, *Compos. Sci. Technol.* **65**:15–16 (2005), 2416–2434.
- [Germain 1973] P. Germain, “The method of virtual power in continuum mechanics, 2: Microstructure”, *SIAM J. Appl. Math.* **25**:3 (1973), 556–575.
- [Goddard 1986] J. D. Goddard, “Microstructural origins of continuum stress fields: a brief history and some unresolved issues”, pp. 179–208 in *Recent developments in structured continua* (Windsor, ON, 1985), edited by D. De Kee and P. N. Kaloni, Pitman Res. Notes Math. Ser. **143**, Longman, Harlow, 1986.
- [Gonella et al. 2011] S. Gonella, M. S. Greene, and W. K. Liu, “Characterization of heterogeneous solids via wave methods in computational microelasticity”, *J. Mech. Phys. Solids* **59**:5 (2011), 959–974.
- [Greene et al. 2012] M. S. Greene, S. Gonella, and W. K. Liu, “Microelastic wave field signatures and their implications for microstructure identification”, *Int. J. Solids Struct.* **49**:22 (2012), 3148–3157.
- [Hellier 2001] C. J. Hellier, *Handbook of nondestructive evaluation*, McGraw-Hill, New York, 2001.
- [Huang and Sun 2008] G. L. Huang and C.-T. Sun, “A higher-order continuum model for elastic media with multiphased microstructure”, *Mech. Adv. Mater. Struct.* **15**:8 (2008), 550–557.
- [Jakata and Every 2008] K. Jakata and A. G. Every, “Determination of the dispersive elastic constants of the cubic crystals Ge, Si, GaAs, and InSb”, *Phys. Rev. B* **77**:17 (2008), Article ID 174301.
- [Jänicke and Steeb 2012] R. Jänicke and H. Steeb, “Wave propagation in periodic microstructures by homogenisation of extended continua”, *Comput. Mater. Sci.* **52**:1 (2012), 209–211.
- [Janno and Engelbrecht 2005a] J. Janno and J. Engelbrecht, “An inverse solitary wave problem related to microstructured materials”, *Inverse Probl.* **21**:6 (2005), 2019–2034.
- [Janno and Engelbrecht 2005b] J. Janno and J. Engelbrecht, “Solitary waves in nonlinear microstructured materials”, *J. Phys. A* **38**:23 (2005), 5159–5172.
- [Janno and Engelbrecht 2005c] J. Janno and J. Engelbrecht, “Waves in microstructured solids: inverse problems”, *Wave Motion* **43**:1 (2005), 1–11.
- [Janno and Engelbrecht 2011] J. Janno and J. Engelbrecht, *Microstructured materials: inverse problems*, Springer, Heidelberg, 2011.
- [Kirchner and Steinmann 2004] N. Kirchner and P. Steinmann, “Modeling microstructured materials: a comparison of gradient and micromorphic continua”, pp. 35–42 in *Modelling of cohesive-frictional materials*, edited by H. J. Herrmann et al., Taylor and Francis, London, 2004.
- [Kröner 1968] E. Kröner, “Interrelations between various branches of continuum mechanics”, pp. 330–340 in *Mechanics of generalized continua* (Freudenstadt and Stuttgart, 1967), edited by E. Kröner, Springer, Berlin, 1968.
- [Kunin 1975] I. A. Kunin, Теория упругих сред с микроструктурой, Nauka, Moscow, 1975. Translated as *Elastic media with microstructure, I: One-dimensional models*, Springer Series in Solid-State Sciences **26**, Springer, Berlin, 1982.
- [Liu et al. 2010] W. K. Liu, D. Qian, S. Gonella, S. Li, W. Chen, and S. Chirputkar, “Multiscale methods for mechanical science of complex materials: bridging from quantum to stochastic multiresolution continuum”, *Int. J. Numer. Methods Eng.* **83**:8–9 (2010), 1039–1080.
- [Love 1944] A. E. H. Love, *A treatise on the mathematical theory of elasticity*, 4th ed., Dover, New York, 1944.

- [Madeo et al. 2013] A. Madeo, P. Neff, I.-D. Ghiba, L. Placidi, and G. Rosi, “Wave propagation in relaxed micromorphic continua: modeling metamaterials with frequency band-gaps”, *Contin. Mech. Therm.* (2013), 1–20. In press.
- [Mahamood et al. 2012] R. M. Mahamood, E. T. Akinlabi, M. Shukla, and S. Pityana, “Functionally graded material: an overview”, pp. 1593–1597 in *Proceedings of the World Congress on Engineering* (London, 2012), vol. III, edited by S. I. Ao et al., Lecture Notes in Engineering and Computer Science **2199**, Newswood, Hong Kong, 2012.
- [Maranganti and Sharma 2007] R. Maranganti and P. Sharma, “A novel atomistic approach to determine strain-gradient elasticity constants: tabulation and comparison for various metals, semiconductors, silica, polymers and the (Ir) relevance for nanotechnologies”, *J. Mech. Phys. Solids* **55**:9 (2007), 1823–1852.
- [Mariano 2002] P. M. Mariano, “Multifield theories in mechanics of solids”, pp. 1–93 *Advances in Applied Mechanics* **38**, Elsevier, New York, 2002.
- [Mariano 2012] P. M. Mariano, “Perspectives in continuum mechanics: a preface”, *Math. Methods Appl. Sci.* **35**:15 (2012), 1737–1740.
- [Mariano and Stazi 2005] P. M. Mariano and F. L. Stazi, “Computational aspects of the mechanics of complex materials”, *Arch. Comput. Methods Eng.* **12**:4 (2005), 391–478.
- [Maugin 1993] G. A. Maugin, *Material inhomogeneities in elasticity*, Applied Mathematics and Mathematical Computation **3**, Chapman and Hall, London, 1993.
- [Maugin 1995] G. A. Maugin, “On some generalizations of Boussinesq and KdV systems”, *Proc. Estonian Acad. Sci. Phys. Math.* **44**:1 (1995), 40–55.
- [Maugin 1999] G. A. Maugin, *Nonlinear waves in elastic crystals*, Oxford University Press, 1999.
- [Maugin 2006] G. A. Maugin, “On the thermomechanics of continuous media with diffusion and/or weak nonlocality”, *Arch. Appl. Mech.* **75**:10–12 (2006), 723–738.
- [Maugin 2011a] G. A. Maugin, *Configurational forces: thermomechanics, physics, mathematics, and numerics*, CRC, Boca Raton, FL, 2011.
- [Maugin 2011b] G. A. Maugin, “Solitons in elastic solids (1938–2010)”, *Mech. Res. Commun.* **38**:5 (2011), 341–349.
- [Maugin 2013] G. A. Maugin, *Continuum mechanics through the twentieth century: a concise historical perspective*, Solid Mechanics and its Applications **196**, Springer, Dordrecht, 2013.
- [Maugin and Christov 1997] G. A. Maugin and C. I. Christov, “Nonlinear duality between elastic waves and quasi-particles in microstructured solids”, *Proc. Estonian Acad. Sci. Phys. Math.* **46**:1–2 (1997), 78–84.
- [Maugin and Muschik 1994] G. A. Maugin and W. Muschik, “Thermodynamics with internal variables, I: General concepts”, *J. Non Equilib. Thermodyn.* **19**:3 (1994), 217–249.
- [Metrikine 2006] A. V. Metrikine, “On causality of the gradient elasticity models”, *J. Sound Vib.* **297**:3-5 (2006), 727–742.
- [Metrikine and Askes 2002] A. V. Metrikine and H. Askes, “One-dimensional dynamically consistent gradient elasticity models derived from a discrete microstructure, 1: Generic formulation”, *Eur. J. Mech. A Solids* **21**:4 (2002), 555–572.
- [Mindlin 1964] R. D. Mindlin, “Micro-structure in linear elasticity”, *Arch. Ration. Mech. Anal.* **16** (1964), 51–78.
- [Murdoch 2010] A. I. Murdoch, “On molecular modelling and continuum concepts”, *J. Elasticity* **100**:1-2 (2010), 33–61.

- [Neff 2005] P. Neff, “On material constants for micromorphic continua”, pp. 337–348 in *Trends in applications of mathematics to mechanics* (Seeheim, 2004), edited by Y. Wang and K. Hutter, Shaker, Aachen, 2005.
- [Neff 2006] P. Neff, “A finite-strain elastic-plastic Cosserat theory for polycrystals with grain rotations”, *Int. J. Eng. Sci.* **44**:8-9 (2006), 574–594.
- [Neff and Forest 2007] P. Neff and S. Forest, “A geometrically exact micromorphic model for elastic metallic foams accounting for affine microstructure. Modelling, existence of minimizers, identification of moduli and computational results”, *J. Elasticity* **87**:2-3 (2007), 239–276.
- [Neff and Jeong 2009] P. Neff and J. Jeong, “A new paradigm: the linear isotropic Cosserat model with conformally invariant curvature energy”, *Z. Angew. Math. Mech.* **89**:2 (2009), 107–122.
- [Neff et al. 2014] P. Neff, I.-D. Ghiba, A. Madeo, L. Placidi, and G. Rosi, “A unifying perspective: the relaxed linear micromorphic continuum”, *Contin. Mech. Therm.* **26**:5 (2014), 639–681.
- [Nicolis and Nicolis 2007] G. Nicolis and C. Nicolis, *Foundations of complex systems: nonlinear dynamics, statistical physics, information and prediction*, World Scientific, Hackensack, NJ, 2007.
- [Nowacki 1972] W. Nowacki, *Termosprężystość*, Polish Scientific Publishers, Warsaw, 1972. Translated as *Thermoelasticity*, 2nd ed., Pergamon, Oxford, 1986.
- [Papargyri-Beskou et al. 2009] S. Papargyri-Beskou, D. Polyzos, and D. E. Beskos, “Wave dispersion in gradient elastic solids and structures: a unified treatment”, *Int. J. Solids Struct.* **46**:21 (2009), 3751–3759.
- [Pastrone et al. 2004] F. Pastrone, P. Cermelli, and A. V. Porubov, “Nonlinear waves in 1-D solids with microstructure”, *Mater. Phys. Mech.* **7**:1 (2004), 9–16.
- [Peets and Tamm 2010] T. Peets and K. Tamm, “Dispersion analysis of wave motion in microstructured solids”, pp. 349–354 in *IUTAM Symposium on Recent Advances of Acoustic Waves in Solids* (Taipei, 2009), edited by T.-T. Wu and C.-C. Ma, IUTAM Bookseries **26**, Springer, Netherlands, 2010.
- [Peets et al. 2008] T. Peets, M. Randrüüt, and J. Engelbrecht, “On modelling dispersion in microstructured solids”, *Wave Motion* **45**:4 (2008), 471–480.
- [Peets et al. 2013] T. Peets, D. Kartofelev, K. Tamm, and J. Engelbrecht, “Waves in microstructured solids and negative group velocity”, *Europhys. Lett.* **103**:1 (2013), Article ID 16001.
- [Pichugin et al. 2008] A. V. Pichugin, H. Askès, and A. Tyas, “Asymptotic equivalence of homogenisation procedures and fine-tuning of continuum theories”, *J. Sound Vib.* **313**:3–5 (2008), 858–874.
- [Polyzos and Fotiadis 2012] D. Polyzos and D. I. Fotiadis, “Derivation of Mindlin’s first and second strain gradient elastic theory via simple lattice and continuum models”, *Int. J. Solids Struct.* **49**:3–4 (2012), 470–480.
- [Porter et al. 2009] M. A. Porter, C. Daraio, I. Szelengowicz, E. B. Herbold, and P. G. Kevrekidis, “Highly nonlinear solitary waves in heterogeneous periodic granular media”, *Physica D* **238**:6 (2009), 666–676.
- [Porubov 2000] A. V. Porubov, “Strain solitary waves in an elastic rod with microstructure”, *Rend. Sem. Mat. Univ. Politec. Torino* **58**:2 (2000), 189–198.
- [Porubov 2003] A. V. Porubov, *Amplification of nonlinear strain waves in solids*, Stability, Vibration and Control of Systems, Series A **9**, World Scientific, Singapore, 2003.
- [Porubov 2009] A. V. Porubov, Локализация нелинейных волн деформации: асимптотические и численные методы исследования, Fizmatlit, Moscow, 2009. Translated as *Localization of nonlinear waves: asymptotic and numerical methods of investigation*.

- [Porubov and Maugin 2005] A. V. Porubov and G. A. Maugin, “Longitudinal strain solitary waves in presence of cubic non-linearity”, *Int. J. Non-Linear Mech.* **40**:7 (2005), 1041–1048.
- [Porubov et al. 2009] A. V. Porubov, E. L. Aero, and G. A. Maugin, “Two approaches to study essentially nonlinear and dispersive properties of the internal structure of materials”, *Phys. Rev. E* **79**:4 (2009), Article ID 046608.
- [Potapov and Rodyushkin 2001] A. I. Potapov and V. M. Rodyushkin, “Экспериментальное исследование волн деформации в материалах с микроструктурой”, *Akust. Zh.* **47**:3 (2001), 407–412. Translated as “Experimental study of strain waves in materials with microstructure” in *Acoust. Phys.* **47**:3 (2001), 347–352.
- [Randrüüt and Braun 2010] M. Randrüüt and M. Braun, “On one-dimensional solitary waves in microstructured solids”, *Wave Motion* **47**:4 (2010), 217–230.
- [Salupere et al. 2008] A. Salupere, K. Tamm, and J. Engelbrecht, “Numerical simulation of interaction of solitary deformation waves in microstructured solids”, *Int. J. Non-Linear Mech.* **43**:3 (2008), 201–208.
- [Samsonov 2001] A. M. Samsonov, *Strain solitons in solids and how to construct them*, Chapman and Hall/CRC, Boca Raton, FL, 2001.
- [Santosa and Symes 1991] F. Santosa and W. W. Symes, “A dispersive effective medium for wave propagation in periodic composites”, *SIAM J. Appl. Math.* **51**:4 (1991), 984–1005.
- [Schrödinger 1914] E. Schrödinger, “Zur dynamik elastisch gekoppelter Punktsysteme”, *Ann. Phys.* **349**:14 (1914), 916–934.
- [Seeger 2010] A. Seeger, “Historical note: on the simulation of dispersive wave propagation by elasticity models”, *Philos. Mag.* **90**:9 (2010), 1101–1104.
- [Soerensen et al. 1984] M. P. Soerensen, P. L. Christiansen, and P. S. Lomdahl, “Solitary waves on nonlinear elastic rods, I”, *J. Acoust. Soc. Amer.* **76**:3 (1984), 871–879.
- [Sun et al. 1968] C.-T. Sun, J. D. Achenbach, and G. Herrmann, “Continuum theory for a laminated medium”, *J. Appl. Mech. (ASME)* **35**:3 (1968), 467–475.
- [Tamm and Peets 2013] K. Tamm and T. Peets, “On the influence of internal degrees of freedom on dispersion in microstructured solids”, *Mech. Res. Commun.* **47** (2013), 106–111.
- [Ván et al. 2008] P. Ván, A. Berezovski, and J. Engelbrecht, “Internal variables and dynamic degrees of freedom”, *J. Non Equilib. Thermodyn.* **33**:3 (2008), 235–254.
- [Vernerey et al. 2007] F. Vernerey, W. K. Liu, and B. Moran, “Multi-scale micromorphic theory for hierarchical materials”, *J. Mech. Phys. Solids* **55**:12 (2007), 2603–2651.
- [Wang and Sun 2002] Z.-P. Wang and C.-T. Sun, “Modeling micro-inertia in heterogeneous materials under dynamic loading”, *Wave Motion* **36**:4 (2002), 473–485.
- [Webb et al. 2008] E. B. Webb, III, J. A. Zimmerman, and S. C. Seel, “Reconsideration of continuum thermomechanical quantities in atomic scale simulations”, *Math. Mech. Solids* **13**:3-4 (2008), 221–266.
- [Whitham 1974] G. B. Whitham, *Linear and nonlinear waves*, Wiley, New York, 1974.
- [Yin et al. 2004] H. M. Yin, L. Z. Sun, and G. H. Paulino, “Micromechanics-based elastic model for functionally graded materials with particle interactions”, *Acta Mater.* **52**:12 (2004), 3535–3543.
- [Zabusky and Kruskal 1965] N. J. Zabusky and M. D. Kruskal, “Interaction of “solitons” in a collisionless plasma and the recurrence of initial states”, *Phys. Rev. Lett.* **15**:6 (1965), 240–243.
- [Zeng et al. 2006] X. Zeng, Y. Chen, and J. D. Lee, “Determining material constants in nonlocal micromorphic theory through phonon dispersion relations”, *Int. J. Eng. Sci.* **44**:18–19 (2006), 1334–1345.

[Zhou 2005] M. Zhou, “Thermomechanical continuum representation of atomistic deformation at arbitrary size scales”, *Proc. R. Soc. Lond. A* **461**:2063 (2005), 3437–3472.

[Ziegler 1977] F. Ziegler, “Wave propagation in periodic and disordered layered composite elastic materials”, *Int. J. Solids Struct.* **13**:4 (1977), 293–305.

[Zimmerman et al. 2002] J. A. Zimmerman, R. E. Jones, P. A. Klein, D. J. Bammann, E. B. Webb, III, and J. J. Hoyt, “Continuum definitions for stress in atomistic simulation”, Technical Report SAND2002-8608, Sandia National Laboratories, Livermore, CA and Albuquerque, NM, 2002.

Received 29 Oct 2013. Revised 16 May 2014. Accepted 21 Jul 2014.

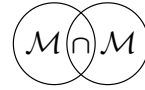
JÜRI ENGELBRECHT: je@ioc.ee

Centre for Nonlinear Studies (CENS), Institute of Cybernetics at Tallinn University of Technology, Akadeemia Tee 21, 12618 Tallinn, Estonia

ARKADI BEREZOVSKI: arkadi.berezovski@cs.ioc.ee

Centre for Nonlinear Studies (CENS), Institute of Cybernetics at Tallinn University of Technology, Akadeemia Tee 21, 12618 Tallinn, Estonia





ON THE APPROXIMATION THEOREM FOR STRUCTURED DEFORMATIONS FROM $BV(\Omega)$

MIROSLAV ŠILHAVÝ

This note deals with structured deformations introduced by Del Piero and Owen. As treated in the present paper, a structured deformation is a pair (\mathbf{g}, \mathbf{G}) where \mathbf{g} is a macroscopic deformation giving the position of points of the body and \mathbf{G} represents deformations without disarrangements. Here \mathbf{g} is a map of bounded variation on the reference region Ω , and \mathbf{G} is a Lebesgue-integrable tensor-valued map. For structured deformations of this level of generality, an approximating sequence \mathbf{g}_k of simple deformations is constructed from the space of maps of special bounded variation on Ω , which converges in the $L^1(\Omega)$ sense to (\mathbf{g}, \mathbf{G}) and for which the sequence of total variations of \mathbf{g}_k is bounded. The condition is optimal. Further, in the second part of this note, the limit relation of Del Piero and Owen is established on the above level of generality. This relation allows one to reconstruct the disarrangement tensor \mathbf{M} of the structured deformation (\mathbf{g}, \mathbf{G}) from the information on the approximating sequence.

1. Introduction and results

This paper deals with the geometry of deformation of nonclassical continua modeled as media capable of (first-order) structured deformations introduced by Del Piero and Owen [1993; 1995].¹ The main objective of the theory of structured deformations is to describe how a continuous body with microstructure will deform under the applied forces.

In the original setting [Del Piero and Owen 1993; 1995], a structured deformation is a triplet $(\mathcal{K}, \mathbf{g}, \mathbf{G})$ of objects whose nature will now be roughly described. The set \mathcal{K} , the crack site, is a subset of vanishing Lebesgue measure of the reference region Ω , the map $\mathbf{g} : \Omega \setminus \mathcal{K} \rightarrow \mathbb{R}^3$, the deformation map, is piecewise continuously differentiable and injective, and \mathbf{G} is a piecewise continuous map

Communicated by Gianpietro Del Piero.

MSC2010: primary 74R99; secondary 74A05.

PACS2010: 81.40.Lm.

Keywords: structured deformation, fracture, approximations, maps of bounded variation, maps of special bounded variation.

¹ The reader is referred to the proceedings [Del Piero and Owen 2004] and to the recent survey [Baía et al. 2011] for additional references and for further developments.

from $\Omega \sim \mathcal{K}$ to the set of invertible second-order tensors describing deformation without disarrangements. The following “accommodation inequality” is assumed:

$$0 < m \leq \det \mathbf{G} \leq \det D_a \mathbf{g}$$

in $\Omega \sim \mathcal{K}$, with m a suitable constant, where $D_a \mathbf{g}$ is the classical derivative of \mathbf{g} where it exists.² Within this context, a classical deformation is the triplet $(\mathcal{K}, \mathbf{g}, D\mathbf{g})$ with \mathbf{g} a continuously differentiable injective deformation function and with $\mathbf{G} := D\mathbf{g} = D_a \mathbf{g}$ the deformation gradient, where D denotes the derivative (gradient) operation on differentiable maps. A more general class of structured deformations is provided by simple deformations, which are triples $(\mathcal{K}, \mathbf{g}, D_a \mathbf{g})$ where \mathbf{g} is only piecewise-smooth injective with jump discontinuities describing partial or full separation of pieces of the body and $\mathbf{G} := D_a \mathbf{g}$. In view of these classes, where \mathbf{G} coincides with the deformation gradient, in the general case, the tensor of deficit

$$\mathbf{M} = D_a \mathbf{g} - \mathbf{G} \quad (1)$$

measures the departure of $(\mathcal{K}, \mathbf{g}, \mathbf{G})$ from the simple deformation $(\mathcal{K}, \mathbf{g}, D_a \mathbf{g})$.

A substantial step towards a concrete interpretation of the tensor \mathbf{G} is offered by the approximation theorem [Del Piero and Owen 1993, Theorem 5.8]. That theorem shows that each structured deformation $(\mathcal{K}, \mathbf{g}, \mathbf{G})$ is a limit of a suitable sequence of simple deformations $(\mathcal{K}_k, \mathbf{g}_k, D_a \mathbf{g}_k)$ in the sense that

$$\mathcal{K}_k \rightarrow \mathcal{K}, \quad \mathbf{g}_k \rightarrow \mathbf{g}, \quad \text{and} \quad D_a \mathbf{g}_k \rightarrow \mathbf{G} \quad (2)$$

with suitably defined convergences of the objects in (2). I note that the nontrivial feature of the proof of the approximation theorem lies in proving the injectivity of \mathbf{g}_k . Moreover, Del Piero and Owen [1993] prove the following the limit relation for the tensor \mathbf{M} :

$$\mathbf{M}(\mathbf{x}) = \lim_{\rho \rightarrow 0} \lim_{k \rightarrow \infty} (4\pi/3)^{-1} \rho^{-3} \int_{J(\mathbf{g}_k) \cap \mathbf{B}(\mathbf{x}, \rho)} [\mathbf{g}_k] \otimes \mathbf{n}_k d\mathcal{H}^2, \quad (3)$$

valid for any sequence (not just the one constructed in the proof of the approximation theorem) $(\mathcal{K}_k, \mathbf{g}_k, D_a \mathbf{g}_k)$ satisfying (2) and any $\mathbf{x} \in \Omega \sim \mathcal{K}$, where $\mathbf{B}(\mathbf{x}, \rho)$ is the open ball of center \mathbf{x} and radius ρ , $J(\mathbf{g}_k)$ is the set of all points of (jump) discontinuity of \mathbf{g}_k , $[\mathbf{g}_k]$ is the jump of \mathbf{g}_k at the points of $J(\mathbf{g}_k)$, \mathbf{n}_k is the normal to $J(\mathbf{g}_k)$, and \mathcal{H}^2 is the area measure.

To apply the relaxation techniques of the calculus of variations, Choksi and Fonseca [1997] later enlarged the space of structured deformations to contain all

² Later we shall identify $D_a \mathbf{g}$ with the absolutely continuous part of the derivative of a map \mathbf{g} of bounded variation.

pairs (\mathbf{g}, \mathbf{G}) where \mathbf{g} is in³ $SBV(\Omega, \mathbb{R}^m)$ and \mathbf{G} is in $L^1(\Omega, \mathbb{M}^{m \times n})$. Here m and n are positive integers, the dimensions of the spaces \mathbb{R}^m and \mathbb{R}^n of dependent and independent variables, respectively. Thus, in addition to weaker regularity, the authors relax the injectivity requirement and put the crack site \mathcal{K} equal to \emptyset . (The cracks are described by the omnipresent discontinuities of \mathbf{g} .)

Choksi and Fonseca [1997, Theorem 2.12] prove the following version of the approximation theorem, which is stated here in a slightly rephrased form as explained below:

Theorem 1.1. *Let $\Omega \subset \mathbb{R}^n$ be a bounded open set, and let $(\mathbf{g}, \mathbf{G}) \in L^1(\Omega, \mathbb{R}^m) \times L^1(\Omega, \mathbb{M}^{m \times n})$. Then there exists a sequence \mathbf{g}_k in $SBV(\Omega, \mathbb{R}^m)$ such that*

$$\mathbf{g}_k \rightarrow \mathbf{g} \text{ in } L^1(\Omega, \mathbb{R}^m) \quad \text{and} \quad D_a \mathbf{g}_k = \mathbf{G} \text{ over } \Omega. \tag{4}$$

Here $D_a \mathbf{g}_k$ is the absolutely continuous part of the generalized derivative of \mathbf{g}_k . The statement of [Choksi and Fonseca 1997, Theorem 2.12] is narrower since (a) the authors assume, in accord with the overall framework of their paper, that \mathbf{g} is in $SBV(\Omega, \mathbb{R}^m)$ and (b) since they replace the equality (4)₂ by the weak* convergence in the sense of measures (although they say that they will prove the equality). Their proof also shows that $\mathbf{g} \in L^1(\Omega, \mathbb{R}^m)$ suffices.

In connection with this generality, the question arises: what additional information beyond (4) can be imposed on the sequence \mathbf{g}_k if it is known that \mathbf{g} belongs to the smaller space $BV(\Omega, \mathbb{R}^m)$ or even to $SBV(\Omega, \mathbb{R}^m)$? An answer, one of the two goals of this note, given in the subsequent theorem, is proved for reference regions represented by admissible domains (which is a mild restriction on Ω , satisfied, e.g., by all open sets with lipschitzian boundary).⁴

Theorem 1.2 (approximation theorem). *If Ω is an admissible domain in \mathbb{R}^n and $(\mathbf{g}, \mathbf{G}) \in BV(\Omega, \mathbb{R}^m) \times L^1(\Omega, \mathbb{M}^{m \times n})$, then there exists a sequence $\mathbf{g}_k \in SBV(\Omega, \mathbb{R}^m)$ such that in addition to (4) the total variation $M(D\mathbf{g}_k)$ of \mathbf{g}_k satisfies*

$$\sup\{M(D\mathbf{g}_k) : k = 1, \dots\} < \infty; \tag{5}$$

hence, we have the following convergence (without passing to a subsequence):

$$D\mathbf{g}_k \rightharpoonup^* D\mathbf{g} \quad \text{in } \mathcal{M}(\Omega, \mathbb{M}^{m \times n}). \tag{6}$$

³ I use the standard notations for function spaces throughout this introduction: thus, $BV(\Omega, \mathbb{R}^n)$ and $SBV(\Omega, \mathbb{R}^n)$ are spaces of \mathbb{R}^n -valued maps on Ω of bounded variation and of special bounded variation, and $L^1(\Omega, \mathbb{R}^m)$ and $L^1(\Omega, \mathbb{M}^{m \times n})$ are spaces of (Lebesgue-)integrable \mathbb{R}^m - or $\mathbb{M}^{m \times n}$ -valued maps on Ω . $\mathcal{M}(\Omega, \mathbb{M}^{m \times n})$ is the space of $\mathbb{M}^{m \times n}$ -valued measures on Ω . The reader is referred to Sections 2 and 3 below for detailed definitions.

⁴ See Lemma 5.1 on page 93.

Thus, the extra information stemming from the inclusion $\mathbf{g} \in BV(\Omega, \mathbb{R}^m)$ is (5). It is easy to see that, conversely if $(\mathbf{g}, \mathbf{G}) \in L^1(\Omega, \mathbb{R}^m) \times L^1(\Omega, \mathbb{M}^{m \times n})$ is a pair satisfying (4) and (5) with $\mathbf{g}_k \in SBV(\Omega, \mathbb{R}^m)$, then necessarily $\mathbf{g} \in BV(\Omega, \mathbb{R}^m)$; in this sense, (5) is optimal. (Both directions are very intuitive.) The proof of the boundedness in the approximation theorem is based on the observation in Lemma 5.1 below, but otherwise the construction of the sequence essentially follows that of Choksi and Fonseca.⁵

The second goal of the present note is to give an analog to the limit relation (3) in the setting of maps of bounded variation.

Theorem 1.3 (the limit relation). *Let Ω be a bounded open subset of \mathbb{R}^n , let $(\mathbf{g}, \mathbf{G}) \in BV(\Omega, \mathbb{R}^m) \times L^1(\Omega, \mathbb{M}^{m \times n})$, and let $\mathbf{g}_k \in SBV(\Omega, \mathbb{R}^m)$ be a sequence satisfying*

$$\mathbf{g}_k \rightarrow \mathbf{g} \text{ in } L^1(\Omega, \mathbb{R}^m), \quad D_a \mathbf{g}_k \rightarrow \mathbf{G} \text{ in } L^1(\Omega, \mathbb{M}^{m \times n}), \quad (7)$$

and (6) (in particular, let \mathbf{g}_k be the sequence from Theorem 1.2). Then there exists a subsequence of \mathbf{g}_k (not relabeled) such that the tensor \mathbf{M} (see (1)) satisfies

$$\mathbf{M}(\mathbf{x}) = \text{ess lim}_{\rho \rightarrow 0} \lim_{k \rightarrow \infty} \kappa_n^{-1} \rho^{-n} \int_{J(\mathbf{g}_k) \cap \mathbf{B}(\mathbf{x}, \rho)} [\mathbf{g}_k] \otimes \mathbf{n}_k d\mathcal{H}^{n-1} \quad (8)$$

for almost every point \mathbf{x} of Ω .

Here $\text{ess lim}_{\rho \rightarrow 0}$ is the essential limit as $\rho \rightarrow 0$, i.e., the limit neglecting an exceptional set of ρ 's of vanishing Lebesgue measure.⁶ Further, κ_n is the volume of the unit ball in \mathbb{R}^n , $J(\mathbf{g}_k)$ is the set of all points of jump discontinuity of \mathbf{g}_k , $[\mathbf{g}_k]$ is the jump of \mathbf{g}_k at the points of $J(\mathbf{g}_k)$, \mathbf{n}_k is the normal to $J(\mathbf{g}_k)$, and \mathcal{H}^{n-1} is the $(n-1)$ -dimensional Hausdorff measure.⁷

The Appendix to the present paper also outlines a proof of a weaker version of the approximation theorem that does not use Alberti's theorem mentioned above. In that version, the equality (4)₂ is replaced by the convergence (7)₂.

2. Preliminaries, notation, and measures

Throughout, n is a positive integer, the dimension of the underlying space \mathbb{R}^n , and m is a positive integer, the dimension of the target space \mathbb{R}^m . We denote by $\mathbf{a} \cdot \mathbf{b}$ the scalar product in both these spaces and by $|\cdot|$ the euclidean norm. Further, $\mathbb{M}^{m \times n}$ is the set of all linear transformations from \mathbb{R}^n to \mathbb{R}^m . The value of $\mathbf{A} \in \mathbb{M}^{m \times n}$ on $\mathbf{x} \in \mathbb{R}^n$ is denoted by $\mathbf{A}\mathbf{x}$. We denote by $\mathbf{A} \cdot \mathbf{B} := \text{tr}(\mathbf{A}\mathbf{B}^T)$ the scalar product

⁵ In particular, Alberti's theorem [1991] (Theorem 3.7 below) is used in the same way as in [Choksi and Fonseca 1997].

⁶ See the definition in Section 2 below.

⁷ See Section 3 for precise definitions of these notions.

in $M^{m \times n}$, where $A^T \in M^{n \times m}$ is the transpose of A and tr denotes the trace. We further denote by $|A| = \sqrt{A \cdot A}$ the associated euclidean norm.

If f is a map with domain any set M and if $N \subset M$, then $f|N$ denotes the restriction of f to N .

The interior, closure, and boundary of a set $M \subset \mathbb{R}^n$ is denoted by $\text{int } M$, $\text{cl } M$, and $\text{bdry } M$. As in the introduction, $\mathbf{B}(\mathbf{x}, \rho)$ denotes the open ball in \mathbb{R}^n of center \mathbf{x} and radius ρ . The symbol κ_n denotes the volume of $\mathbf{B}(\mathbf{0}, 1)$.

Throughout, let Ω be an open subset of \mathbb{R}^n , later to be restricted by additional requirements. Let Z be a finite-dimensional inner-product space.

We denote by \mathcal{L}^n the Lebesgue measure in \mathbb{R}^n [Federer 1969, §2.6.5], and if k is an integer, $0 \leq k \leq n$, we denote by \mathcal{H}^k the k -dimensional Hausdorff measure in \mathbb{R}^n [ibid., §§2.10.2–2.10.60]; recall that $\mathcal{H}^n = \mathcal{L}^n$. If $A \subset \mathbb{R}^n$ is a Borel set, we denote by $\mathcal{H}^k \llcorner A$ the *restriction* of \mathcal{H}^k to A , which is the measure defined by

$$(\mathcal{H}^k \llcorner A)(B) = \mathcal{H}^k(A \cap B) \tag{9}$$

for each Borel set $B \subset \mathbb{R}^n$. If $A \subset \mathbb{R}^n$ is a Borel set and \mathbf{f} a Z -valued Borel map defined \mathcal{H}^k almost everywhere on A , integrable with respect to \mathcal{H}^k on A , then $\mathbf{f}\mathcal{H}^k \llcorner A$ denotes the Z -valued measure on \mathbb{R}^n defined by

$$(\mathbf{f}\mathcal{H}^k \llcorner A)(B) = \int_{A \cap B} \mathbf{f} \, d\mathcal{H}^k \tag{10}$$

for each Borel set $B \subset \mathbb{R}^n$. The definitions (9) and (10) also apply to $k = n$, i.e., to $\mathcal{L}^n \equiv \mathcal{H}^n$, resulting in $\mathcal{L}^n \llcorner A$ and $\mathbf{f}\mathcal{L}^n \llcorner A$.

We denote by $L^1(\Omega, Z)$ the set of all (classes of equivalence of) Lebesgue-integrable maps on Ω with values in Z ; we write $|\cdot|_{L^1(\Omega, Z)}$ for the norm on $L^1(\Omega, Z)$, defined by

$$|\mathbf{f}|_{L^1(\Omega, Z)} = \int_{\Omega} |\mathbf{f}| \, d\mathcal{L}^n$$

for each $\mathbf{f} \in L^1(\Omega, Z)$. We denote by $C_0^\infty(\Omega, Z)$ the set of all of indefinitely differentiable Z -valued maps \mathbf{f} on \mathbb{R}^n with compact support contained in Ω .

We denote by $\mathcal{M}(\Omega, Z)$ the set of all (finite) Z -valued measures on Ω . If $\mu \in \mathcal{M}(\Omega, Z)$, we denote by $|\mu|$ the *total variation (measure)* of μ , i.e., the smallest nonnegative measure on Ω such that $|\mu(B)| \leq |\mu|(B)$ for each Borel subset B of Ω . We denote by $M(\mu)$ the *mass* of μ , defined by $M(\mu) = |\mu|(\Omega)$. A standard result is that

$$M(\mu) = \sup \left\{ \int_{\Omega} \mathbf{f} \cdot d\mu : \mathbf{f} \in C_0^\infty(\Omega, Z), |\mathbf{f}| \leq 1 \text{ on } \Omega \right\}. \tag{11}$$

We say that a measure $\mu \in \mathcal{M}(\Omega, Z)$ is supported by a Borel set $A \subset \Omega$ if $\mu(B) = 0$ for every Borel set $B \subset \Omega$ such that $A \cap B = \emptyset$. The reader is referred to [Ambrosio et al. 2000, Chapter 1] for further details of measures with values in finite-dimensional inner-product spaces.

If f is a Z -valued map defined \mathcal{L}^1 almost everywhere in an interval $(0, \epsilon)$ where $\epsilon > 0$, we say that $a \in Z$ is an essential limit of f at 0 and write

$$a = \operatorname{ess\,lim}_{\rho \rightarrow 0} f(\rho) \quad (12)$$

if there exists an \mathcal{L}^1 null set $N \subset (0, \epsilon)$ such that

$$a = \lim_{\substack{\rho \rightarrow 0 \\ \rho \in (0, \epsilon) \setminus N}} f(\rho),$$

where the last limit is the ordinary limit relative to a subset of $(0, \epsilon)$. Note that, unlike the set N , the value a is uniquely determined, which justifies the notation (12).

3. Maps of bounded variation, sets of finite perimeter, and admissible domains

We state some basic definitions and properties of the space BV of maps of bounded variation, of the space SBV of special maps of bounded variation, of sets of finite perimeter, and of admissible domains that will be needed in the sequel. For more details, see [Ambrosio et al. 2000; Evans and Gariépy 1992; Ziemer 1989; Federer 1969].

Definition 3.1. We denote by $BV(\Omega, \mathbb{R}^m)$ the set of all $\mathbf{g} \in L^1(\Omega, \mathbb{R}^m)$ such that there exists a measure $D\mathbf{g} \in \mathcal{M}(\Omega, \mathbb{M}^{m \times n})$ satisfying

$$\int_{\Omega} \mathbf{g} \cdot \operatorname{div} \mathbf{T} \, d\mathcal{L}^n = - \int_{\Omega} \mathbf{T} \cdot dD\mathbf{g} \quad (13)$$

for each $\mathbf{T} \in C_0^\infty(\Omega, \mathbb{R}^{m \times n})$. Here $\operatorname{div} \mathbf{T}$ is an \mathbb{R}^m -valued map on Ω such that

$$\mathbf{a} \cdot \operatorname{div} \mathbf{T} = \operatorname{tr}(D(\mathbf{T}^T \mathbf{a}))$$

for each $\mathbf{a} \in \mathbb{R}^m$, where $D(\mathbf{T}^T \mathbf{a})$ denotes the classical derivative of the map $\mathbf{T}^T \mathbf{a}$. The elements of $BV(\Omega, \mathbb{R}^m)$ are called *maps of bounded variation*; the measure $D\mathbf{g}$ is uniquely determined by \mathbf{g} and is called the *weak (or generalized) derivative of \mathbf{g}* . We denote by $M(D\mathbf{g})$ the mass of the measure $D\mathbf{g}$ as defined in Section 2 and call $M(D\mathbf{g})$ the *total variation of \mathbf{g}* . Equations (11) and (13) provide

$$M(D\mathbf{g}) = \sup \left\{ \int_{\Omega} \mathbf{g} \cdot \operatorname{div} \mathbf{T} \, d\mathcal{L}^n : \mathbf{T} \in C_0^\infty(\Omega, \mathbb{R}^{m \times n}), |\mathbf{T}| \leq 1 \text{ on } \Omega \right\}. \quad \square$$

The choice of \mathbf{T} represented by a matrix function with only the (i, j) element different from 0, where $i \in \{1, \dots, m\}$ and $j \in \{1, \dots, n\}$, reduces (13) to the usual index definition of BV as in, e.g., [Ambrosio et al. 2000, Equation (3.2)].

The set $BV(\Omega, \mathbb{R}^m)$ is a Banach space under the norm

$$|\mathbf{g}|_{BV(\Omega, \mathbb{R}^m)} := |\mathbf{g}|_{L^1(\Omega, \mathbb{R}^m)} + M(D\mathbf{g}).$$

Definition 3.2. Let $\mathbf{g} \in L^1(\Omega, \mathbb{R}^m)$. We say that \mathbf{g} has an *approximate limit* at $\mathbf{x} \in \Omega$ if there exists $\mathbf{a} \in \mathbb{R}^m$ such that

$$\lim_{\rho \rightarrow 0} \kappa_n^{-1} \rho^{-n} \int_{\mathbf{B}(\mathbf{x}, \rho)} |\mathbf{g} - \mathbf{a}| d\mathcal{L}^n = 0.$$

The value \mathbf{a} is uniquely determined and is called the approximate limit of \mathbf{g} at \mathbf{x} . The complement $S(\mathbf{g}) \subset \Omega$ in Ω of the set of all $\mathbf{x} \in \Omega$ where the approximate limit of \mathbf{g} exists is called the *approximate discontinuity set* of \mathbf{g} . □

Definition 3.3. Let $\mathbf{g} \in L^1(\Omega, \mathbb{R}^m)$. We say that $\mathbf{x} \in \Omega$ is an *approximate jump point* of \mathbf{g} if there exist $\mathbf{a}, \mathbf{b} \in \mathbb{R}^m$, $\mathbf{a} \neq \mathbf{b}$, and $\mathbf{n} \in \mathbb{R}^n$ with $|\mathbf{n}| = 1$ such that

$$\begin{aligned} \lim_{\rho \rightarrow 0} \kappa_n^{-1} \rho^{-n} \int_{\mathbf{B}^+(\mathbf{x}, \rho, \mathbf{n})} |\mathbf{g} - \mathbf{a}| d\mathcal{L}^n &= 0, \\ \lim_{\rho \rightarrow 0} \kappa_n^{-1} \rho^{-n} \int_{\mathbf{B}^-(\mathbf{x}, \rho, \mathbf{n})} |\mathbf{g} - \mathbf{b}| d\mathcal{L}^n &= 0. \end{aligned} \tag{14}$$

Here

$$\mathbf{B}^\pm(\mathbf{x}, \rho, \mathbf{n}) = \{\mathbf{y} \in \mathbf{B}(\mathbf{x}, \rho), \pm(\mathbf{y} - \mathbf{x}) \cdot \mathbf{n} > 0\}.$$

The triplet $(\mathbf{a}, \mathbf{b}, \mathbf{n})$, if it exists, is uniquely determined to within the interchange of \mathbf{a} and \mathbf{b} and a simultaneous change of the sign of \mathbf{n} . In any case, the product

$$[\mathbf{g}] \otimes \mathbf{n}, \tag{15}$$

occurring frequently below, is uniquely determined, where

$$[\mathbf{g}] = \mathbf{a} - \mathbf{b}$$

is the jump of \mathbf{g} at \mathbf{x} . We denote by $J(\mathbf{g})$ the set of all approximate jump points of \mathbf{g} and call any $\pm\mathbf{n}$ the normal of $J(\mathbf{g})$ at \mathbf{x} . □

The following result describes the relationship between the sets $S(\mathbf{g})$ and $J(\mathbf{g})$:

Theorem 3.4. *If $\mathbf{g} \in BV(\Omega, \mathbb{R}^m)$, then:*

- (i) $J(\mathbf{g}) \subset S(\mathbf{g})$ and $\mathcal{H}^{n-1}(S(\mathbf{g}) \setminus J(\mathbf{g})) = 0$.
- (ii) $J(\mathbf{g})$ is countably $(\mathcal{H}^{n-1}, n-1)$ -rectifiable in the sense that \mathcal{H}^{n-1} almost all of $J(\mathbf{g})$ can be covered by countably many class-1 surfaces $C_k, k = 1, \dots$, of dimension $n-1$ in \mathbb{R}^n .

The derivative of a map of bounded variation has the following well known structure. The subsequent treatment uses especially the jump and the absolutely continuous parts of the derivative to be introduced now.

Theorem 3.5. *If $\mathbf{g} \in BV(\Omega, \mathbb{R}^m)$, then:*

(i) *The derivative $D\mathbf{g}$ has a unique decomposition*

$$D\mathbf{g} = D_a\mathbf{g} \mathcal{L}^n \llcorner \Omega + D_c\mathbf{g} + D_j\mathbf{g},$$

where $D_a\mathbf{g}$, the absolutely continuous part of $D\mathbf{g}$, is a map in $L^1(\Omega, \mathbb{M}^{m \times n})$; $D_c\mathbf{g}$, the Cantor part of $D\mathbf{g}$, is a measure on Ω singular with respect to \mathcal{L}^n and diffuse with respect to \mathcal{H}^{n-1} , i.e., $D_c\mathbf{g}$ is supported by a set of null Lebesgue measure in \mathbb{R}^n and $D_c\mathbf{g}(B) = \mathbf{0}$ for each Borel subset B of Ω of finite \mathcal{H}^{n-1} measure; and $D_j\mathbf{g}$, the jump part of $D\mathbf{g}$, is a measure absolutely continuous with respect to \mathcal{H}^{n-1} .

(ii) *The jump part $D_j\mathbf{g}$ is supported by $J(\mathbf{g})$, and in fact,*

$$D_j\mathbf{g} = [\mathbf{g}] \otimes \mathbf{n} \mathcal{H}^{n-1} \llcorner J(\mathbf{g}),$$

where, for every point \mathbf{x} of $J(\mathbf{g})$, the value $[\mathbf{g}] \otimes \mathbf{n}$ is the product (15).

(iii) *For \mathcal{L}^n almost every point \mathbf{x} of Ω , we have*

$$D_a\mathbf{g}(\mathbf{x}) = \lim_{\rho \rightarrow 0} \kappa_n^{-1} \rho^{-n} D(\mathbf{B}(\mathbf{x}, \rho)). \quad (16)$$

Definition 3.6. We denote by $SBV(\Omega, \mathbb{R}^m)$ the set of all $\mathbf{g} \in BV(\Omega, \mathbb{R}^m)$ with $D_c\mathbf{g} = \mathbf{0}$. The elements of $SBV(\Omega, \mathbb{R}^m)$ are called *special maps of bounded variation*. \square

$SBV(\Omega, \mathbb{R}^m)$ is a closed subspace of $BV(\Omega, \mathbb{R}^m)$ under the norm $|\cdot|_{BV(\Omega, \mathbb{R}^m)}$.

Theorem 3.7 [Alberti 1991]. *If Ω is bounded, then for any $\mathbf{G} \in L^1(\Omega, \mathbb{M}^{m \times n})$, there exists a $\mathbf{g} \in SBV(\Omega, \mathbb{R}^m)$ such that $D_a\mathbf{g} = \mathbf{G}$; moreover, there exists a constant $c \in \mathbb{R}$ depending only on Ω such that the map \mathbf{g} as above can be chosen to satisfy*

$$M(\mathbf{g}) \leq c |\mathbf{G}|_{L^1(\Omega, \mathbb{M}^{m \times n})}.$$

We conclude this section with basic information on sets of finite perimeter and on admissible domains. Sets of finite perimeter fall in the framework of BV as will be explained below. For a subset of the class of sets of finite perimeter called admissible domains (see below), we shall establish the approximation theorem. The distinguishing feature of admissible domains Ω is that maps from $BV(\Omega, \mathbb{R}^m)$ have well defined boundary values.

Definition 3.8. A set $E \subset \mathbb{R}^n$ is said to have a *finite perimeter* if $1_E \in BV(\mathbb{R}^n, \mathbb{R})$, where 1_E denotes the characteristic function of E . The *perimeter* of E is $M(D1_E)$.

The *measure-theoretic boundary* of E is the set $S(1_E)$ that differs from the *reduced boundary* $\text{bdry}_*(E) := J(1_E)$ by a set of \mathcal{H}^{n-1} measure 0. \square

Theorem 3.9. *If E is a set of finite perimeter, then for every $\mathbf{x} \in \text{bdry}_*(E)$, the triplet $(\mathbf{a}, \mathbf{b}, \mathbf{n})$ as in Definition 3.3 can be chosen to be $(0, 1, \mathbf{n}(\mathbf{x}))$; with this choice, $\mathbf{n}(\mathbf{x})$ is uniquely determined and is called the *measure-theoretic normal* to E at \mathbf{x} . Equations (14) then imply the following well known formulas:*

$$\begin{aligned} \lim_{\rho \rightarrow 0} \kappa_n^{-1} \rho^{-n} \mathcal{L}^n(E \cap \mathbf{B}^+(\mathbf{x}, \rho, \mathbf{n})) &= 0, \\ \lim_{\rho \rightarrow 0} \kappa_n^{-1} \rho^{-n} \mathcal{L}^n(\mathbf{B}^-(\mathbf{x}, \rho, \mathbf{n}) \sim E) &= 0, \end{aligned}$$

where $\mathbf{n} = \mathbf{n}(\mathbf{x})$. One has

$$D1_E = \mathbf{n} \mathcal{H}^{n-1} \llcorner \text{bdry}_* E.$$

Thus, even $1_E \in SBV(\mathbb{R}^n, \mathbb{R})$.

Definition 3.10 [Ziemer 1989, Definition 5.10.1]. A bounded open set $\Omega \subset \mathbb{R}^n$ is said to be an *admissible domain* if it has a finite perimeter and the following two conditions are satisfied:

- (i) $\mathcal{H}^{n-1}(\text{bdry } B \sim \text{bdry}_* B) = 0$.
- (ii) There exists a constant M , and for each $\mathbf{x} \in \text{bdry } \Omega$, there is a ball $\mathbf{B}(\mathbf{x}, r)$ with

$$\mathcal{H}^{n-1}(\text{bdry}_* E \cap \text{bdry}_* \Omega) \leq M \mathcal{H}^{n-1}(\Omega \cap \text{bdry}_* E)$$

whenever $E \subset \text{cl } \Omega \cap \mathbf{B}(\mathbf{x}, r)$ is a set of finite perimeter. \square

Each open bounded set with lipschitzian boundary is an admissible domain [Ziemer 1989, Remark 5.10.2]. The following two theorems describe the main virtues of admissible domains:

Theorem 3.11 (see [Ziemer 1989, Section 5.10]). *If Ω is an admissible domain and $\mathbf{g} \in BV(\Omega, \mathbb{R}^m)$, then there exist an \mathcal{H}^{n-1} -measurable map $\mathbf{g}_{\text{bdry } \Omega}$ on $\text{bdry } \Omega$ such that*

$$\int_{\Omega} \mathbf{g} \cdot \text{div } \mathbf{T} \, d\mathcal{L}^n + \int_{\Omega} \mathbf{T} \cdot dD\mathbf{g} = \int_{\text{bdry}(\Omega)} \mathbf{T} \mathbf{n} \cdot \mathbf{g}_{\text{bdry } \Omega} \, d\mathcal{H}^{n-1}$$

for every class-1 map \mathbf{T} on Ω with values in $\mathbb{M}^{m \times n}$ that has a continuous extension (again denoted by \mathbf{T}) to $\text{cl } \Omega$, where \mathbf{n} is the *measure-theoretic normal* to Ω . There exists a $c \in \mathbb{R}$ depending only on Ω such that

$$\int_{\text{bdry } \Omega} |\mathbf{g}_{\text{bdry } \Omega}| \, d\mathcal{H}^{n-1} \leq c |\mathbf{g}|_{BV(\Omega, \mathbb{R}^m)}.$$

The map $\mathbf{g}_{\text{bdry } \Omega}$ is determined to within a change on a set of \mathcal{H}^{n-1} -measure 0 and is called the trace of \mathbf{g} . One has

$$\lim_{r \rightarrow 0} \kappa_n^{-1} r^{-n} \int_{\mathbf{B}(\mathbf{y}, r) \cap \Omega} |\mathbf{g} - \mathbf{g}_{\text{bdry } \Omega}(\mathbf{y})| d\mathcal{L}^n = 0 \quad (17)$$

for \mathcal{H}^{n-1} almost every point \mathbf{y} of $\text{bdry } \Omega$.

Theorem 3.12 (cf. [Ziemer 1989, Lemma 5.10.4]). *If Ω is an admissible domain and $\mathbf{g} \in BV(\Omega, \mathbb{R}^m)$, then the extension \mathbf{g}_0 of \mathbf{g} to \mathbb{R}^n equal to 0 outside Ω satisfies $\mathbf{g}_0 \in BV(\mathbb{R}^n, \mathbb{R}^m)$,*

$$D\mathbf{g}_0 = D\mathbf{g} - \mathbf{g}_{\text{bdry } \Omega} \otimes \mathbf{n} \mathcal{H}^{n-1} \llcorner \text{bdry } \Omega,$$

and there exists a $c \in \mathbb{R}$ depending only on Ω such that

$$|\mathbf{g}_0|_{BV(\mathbb{R}^n, \mathbb{R}^m)} \leq c |\mathbf{g}|_{BV(\Omega, \mathbb{R}^m)}.$$

4. The BV setting of structured deformations

For the purpose of the approximation theorem and the limit relation (as stated in Section 1), we enlarge the set $SBV(\Omega, \mathbb{R}^m) \times L^1(\Omega, \mathbb{M}^{m \times n})$ of structured deformations of Choksi and Fonseca [1997] to form the set $BV(\Omega, \mathbb{R}^m) \times L^1(\Omega, \mathbb{M}^{m \times n})$. We furthermore interpret the elements $\mathbf{g} \in SBV(\Omega, \mathbb{R}^m)$ as the *macroscopic deformations* of the body Ω with *macroscopic crack site* $J(\mathbf{g})$. We note that the space of structured deformations $(\mathcal{K}, \mathbf{g}, \mathbf{G})$ of Del Piero and Owen [1993] as described in Section 1 with $\mathcal{K} = \emptyset$ is a subset of $SBV(\Omega, \mathbb{R}^m) \times L^1(\Omega, \mathbb{M}^{m \times n}) \subset BV(\Omega, \mathbb{R}^m) \times L^1(\Omega, \mathbb{M}^{m \times n})$. In a general, $(\mathbf{g}, \mathbf{G}) \in BV(\Omega, \mathbb{R}^m) \times L^1(\Omega, \mathbb{M}^{m \times n})$, the map \mathbf{g} is the possibly discontinuous *macroscopic displacement*, of the body Ω and \mathbf{G} is a *microscopic disarrangement* as explained in the introduction and in accord with the original papers by Del Piero and Owen [1993; 1995].

5. Proof of the approximation theorem

The proof of the Approximation Theorem is based on the decomposition of \mathbb{R}^n into the disjoint union of sufficiently small cubes of equal edge length and with faces parallel to the natural coordinate planes in \mathbb{R}^n . Various maps involved in the construction are then approximated by (generally) discontinuous maps constant on the cubes (as in the present section) or by discontinuous maps linear on the cubes (as in the Appendix below).

For each positive integer k , consider the decomposition of \mathbb{R}^n into the system of cubes

$$C(k, \mathbf{p}) := C/k + \mathbf{p}, \quad \mathbf{p} \in \mathbb{Z}^n/k, \quad (18)$$

where $C := [0, 1]^n$, $C/k := \{\mathbf{x}/k : \mathbf{x} \in C\}$, \mathbb{Z}^n is the set of n tuples of integers, and $\mathbb{Z}^n/k := \{z/k : z \in \mathbb{Z}^n\}$.

Let $\mathbf{e}_1, \dots, \mathbf{e}_n$ be the natural orthonormal basis in \mathbb{R}^n .

Lemma 5.1. *Let k be a positive integer, let $f \in C_0^\infty(\mathbb{R}^n, \mathbb{R}^m)$, and let $\mathbf{p}, \mathbf{q} \in \mathbb{Z}^n/k$ be such that $P := C(k, \mathbf{p})$ and $Q := C(k, \mathbf{q})$ are two adjacent cubes sharing the common face $F := \text{cl } P \cap \text{cl } Q \neq \emptyset$ of normal \mathbf{n} pointing from P to Q . Let $\mathbf{m} : P \cup Q \rightarrow \mathbb{R}^m$ be defined by*

$$\mathbf{m}(\mathbf{x}) = \begin{cases} \mathbf{a} & \text{if } \mathbf{x} \in P, \\ \mathbf{b} & \text{if } \mathbf{x} \in Q, \end{cases}$$

where

$$\mathbf{a} = k^n \int_P f \, d\mathcal{L}^n \quad \text{and} \quad \mathbf{b} = k^n \int_Q f \, d\mathcal{L}^n \quad (19)$$

are the averages of f over the two cubes. Then $\mathbf{m} \in \text{SBV}(\text{int}(P \cup Q), \mathbb{R}^m)$,

$$D\mathbf{m} = (\mathbf{b} - \mathbf{a}) \otimes \mathbf{n} \mathcal{H}^{n-1} \llcorner F, \quad D_a \mathbf{m} = \mathbf{0}, \quad (20)$$

and

$$M(D\mathbf{m}) \leq \int_{P \cup Q} |D_n f| \, d\mathcal{L}^n, \quad (21)$$

where $D_n f$ is the directional derivative of f in the direction \mathbf{n} .

Proof. We only prove (21) since the other assertions of the lemma are immediate. Let $\mathbf{x} \in P$ be arbitrary, and denote $\mathbf{y}(\mathbf{x}) := \mathbf{x} + \mathbf{n}/k$ so that $\mathbf{y}(\mathbf{x}) \in Q$. Then

$$f(\mathbf{y}(\mathbf{x})) - f(\mathbf{x}) = k^{-1} \int_0^1 D_n f(\mathbf{x} + t\mathbf{n}) \, dt,$$

and hence,

$$|f(\mathbf{y}(\mathbf{x})) - f(\mathbf{x})| \leq k^{-1} \int_0^1 |D_n f(\mathbf{x} + t\mathbf{n})| \, dt. \quad (22)$$

We have

$$\begin{aligned} U &:= \left| \int_Q f \, d\mathcal{L}^n - \int_P f \, d\mathcal{L}^n \right| = \left| \int_P f(\mathbf{y}(\mathbf{x})) \, d\mathcal{L}^n(\mathbf{x}) - \int_P f(\mathbf{x}) \, d\mathcal{L}^n(\mathbf{x}) \right| \\ &\leq \int_P |f(\mathbf{y}(\mathbf{x})) - f(\mathbf{x})| \, d\mathcal{L}^n(\mathbf{x}). \end{aligned}$$

Consequently, integrating (22) over P , we obtain

$$\begin{aligned}
U &\leq k^{-1} \int_0^1 \int_P |\mathbf{D}_n \mathbf{f}(\mathbf{x} + t\mathbf{n})| d\mathcal{L}^n(\mathbf{x}) dt = k^{-1} \int_0^1 \int_{P+t\mathbf{n}} |\mathbf{D}_n \mathbf{f}| d\mathcal{L}^n dt \\
&\leq k^{-1} \int_0^1 \int_{P \cup Q} |\mathbf{D}_n \mathbf{f}| d\mathcal{L}^n dt \\
&= k^{-1} \int_{P \cup Q} |\mathbf{D}_n \mathbf{f}| d\mathcal{L}^n;
\end{aligned}$$

the last *inequality* above follows from $P + t\mathbf{n} \subset P \cup Q$ for each $t \in [0, 1]$. Multiplying the just proved inequality

$$\left| \int_Q \mathbf{f} d\mathcal{L}^n - \int_P \mathbf{f} d\mathcal{L}^n \right| \leq k^{-1} V, \quad V := \int_{P \cup Q} |\mathbf{D}_n \mathbf{f}| d\mathcal{L}^n,$$

by k^n , we obtain

$$|\mathbf{b} - \mathbf{a}| \leq k^{n-1} V,$$

and a combination with (20)₁ provides that the total variation (measure) $|\mathbf{D}\mathbf{m}|$ satisfies

$$|\mathbf{D}\mathbf{m}| = |\mathbf{b} - \mathbf{a}| \mathcal{H}^{n-1} \llcorner F \leq k^{n-1} V \mathcal{H}^{n-1} \llcorner F.$$

Integrating over \mathbb{R}^n , we obtain

$$M(\mathbf{D}\mathbf{m}) = |\mathbf{D}\mathbf{m}|(\mathbb{R}^n) \leq k^{n-1} V \mathcal{H}^{n-1}(F) = V,$$

which is (21). □

Proposition 5.2. *Let $\mathbf{f} \in C_0^\infty(\mathbb{R}^n, \mathbb{R}^m)$. There exists a sequence $\mathbf{m}_k \in SBV(\mathbb{R}^n, \mathbb{R}^m)$ such that*

$$\mathbf{m}_k \rightarrow \mathbf{f} \quad \text{in } L^1(\mathbb{R}^n, \mathbb{R}^m), \quad (23)$$

$$\mathbf{D}_a \mathbf{m}_k = \mathbf{0} \quad \text{on } \mathbb{R}^n \text{ for all } k = 1, \dots, \quad (24)$$

and

$$M(\mathbf{D}\mathbf{m}_k) \leq 2n \int_{\mathbb{R}^n} |\mathbf{D}\mathbf{f}| d\mathcal{L}^n. \quad (25)$$

Proof. For each positive integer k , consider the decomposition of \mathbb{R}^n into the system of cells as in (18). Let $\mathbf{m}_k : \mathbb{R}^n \rightarrow \mathbb{R}^m$ be defined by

$$\mathbf{m}_k(\mathbf{x}) = \mathbf{f}(k, \mathbf{p}) \quad (26)$$

for each $\mathbf{x} \in \mathbb{R}^n$, where $\mathbf{p} \in \mathbb{Z}^n/k$ is uniquely determined by the requirement that $\mathbf{x} \in C(k, \mathbf{p})$ and where

$$\mathbf{f}(k, \mathbf{p}) = k^n \int_{C(k, \mathbf{p})} \mathbf{f} d\mathcal{L}^n.$$

Then \mathbf{m}_k is piecewise constant, with all points of jump discontinuity contained in the union

$$\bigcup_{i=1}^n \bigcup_{l \in \mathbb{Z}/k} P_{k,i,l},$$

where

$$P_{k,i,l} = \{\mathbf{x} \in \mathbb{R}^n : \mathbf{x} \cdot \mathbf{e}_i = l\}$$

for any $l \in \mathbb{Z}/k$. Here for each $i = 1, \dots, n$, the system

$$\mathcal{S}_{k,i} = \{P_{k,i,l} : l \in \mathbb{Z}/k\}$$

forms an equidistant system of parallel planes perpendicular to \mathbf{e}_i .

We now fix $k = 1, \dots$ and $i = 1, \dots, n$ and denote by $S_{k,i} \subset \mathbb{R}^n$ the union of the system $\mathcal{S}_{k,i}$ of planes perpendicular to \mathbf{e}_i . Next we apply Lemma 5.1 to each pair of adjacent cubes $C(k, \mathbf{p})$ and $C(k, \mathbf{q})$ with $\mathbf{p}, \mathbf{q} \in \mathbb{Z}^n/k$ sharing a common face perpendicular to \mathbf{e}_i . Summing the inequality (21) over all such pairs, we obtain

$$M(\mathbf{Dm}_k \llcorner S_{k,i}) \leq 2 \int_{\mathbb{R}^n} |D_{\mathbf{e}_i} \mathbf{f}| d\mathcal{L}^n,$$

where $D_{\mathbf{e}_i} \mathbf{f}$ is the directional derivative of \mathbf{f} in the direction \mathbf{e}_i . Summing over all i , we obtain (25). Relation (23) follows immediately from the well known properties of the piecewise-constant approximations on system of cubes of decreasing edge length. Finally (24) follows from the piecewise-constant character of \mathbf{m}_k . \square

Proof of the approximation theorem. By Alberti's theorem (Theorem 3.7), there exists $\mathbf{h} \in SBV(\Omega, \mathbb{R}^m)$ such that

$$D_a \mathbf{h} = \mathbf{G} \quad \text{on } \Omega. \tag{27}$$

Put $\mathbf{l} := \mathbf{g} - \mathbf{h}$, which is an element of $BV(\Omega, \mathbb{R}^m)$. Since Ω is an admissible domain, the extension \mathbf{l}_0 of \mathbf{l} to \mathbb{R}^n equal to $\mathbf{0}$ outside Ω satisfies $\mathbf{l}_0 \in BV(\mathbb{R}^n, \mathbb{R}^m)$ by Theorem 3.12. Let \mathbf{f}_k be a sequence of mollifications of \mathbf{l}_0 on \mathbb{R}^n with the mollification parameter tending to 0 so that $\mathbf{f}_k \in C_0^\infty(\mathbb{R}^n, \mathbb{R}^m)$,

$$\begin{aligned} \int_{\mathbb{R}^n} |D \mathbf{f}_k| d\mathcal{L}^n &\leq M(D\mathbf{l}_0), \\ \mathbf{f}_k &\rightarrow \mathbf{l}_0 \quad \text{in } L^1(\mathbb{R}^n, \mathbb{R}^m), \end{aligned} \tag{28}$$

and hence in particular

$$\mathbf{f}_k|_\Omega \rightarrow \mathbf{l} \quad \text{in } L^1(\Omega, \mathbb{R}^m). \tag{29}$$

Applying Proposition 5.2 with f replaced by f_k , we find that for each k there exists an $\mathbf{m}_k \in SBV(\mathbb{R}^n, \mathbb{R}^m)$ such that

$$|\mathbf{m}_k - \mathbf{f}_k|_{L^1(\mathbb{R}^n, \mathbb{R}^m)} < 1/k, \quad (30)$$

$$D_a \mathbf{m}_k = \mathbf{0} \quad \text{on } \mathbb{R}^n, \quad (31)$$

and

$$M(D\mathbf{m}_k) \leq 2n \int_{\mathbb{R}^n} |Df_k| d\mathcal{L}^n. \quad (32)$$

We put

$$\mathbf{g}_k = \mathbf{m}_k|_{\Omega} + \mathbf{h}$$

for $k = 1, \dots$ so that $\mathbf{g}_k \in SBV(\Omega, \mathbb{R}^m)$. Equations (29) and (30) imply

$$\mathbf{m}_k|_{\Omega} \rightarrow \mathbf{l} \quad \text{in } L^1(\Omega, \mathbb{R}^m) \text{ as } k \rightarrow \infty,$$

and hence, we have (4)₁. Further, (31) and (27) imply (4)₂. Finally, (32), (28), and $\mathbf{h} \in SBV(\Omega, \mathbb{R}^m)$ imply (5). Assertion (6) then follows by an easy argument that is left to the reader. \square

6. Proof of the limit relation

Lemma 6.1. *Let Ω be bounded, let \mathbf{g} be a map (not a class of equivalence) in $BV(\Omega, \mathbb{R}^m)$, let $\mathbf{x} \in \Omega$, and let $\epsilon > 0$ be such that $\mathbf{B}(\mathbf{x}, \epsilon) \subset \Omega$. Then for \mathcal{L}^1 almost every $\rho \in (0, \epsilon)$, $\mathbf{g}|_{\text{bdry } \mathbf{B}(\mathbf{x}, \rho)}$ is the trace of $\mathbf{g}|_{\mathbf{B}(\mathbf{x}, \rho)} \in BV(\mathbf{B}(\mathbf{x}, \rho), \mathbb{R}^m)$.*

Proof. By the Lebesgue differentiation theorem, there exists a Borel set $E \subset \Omega$ with $\mathcal{L}^n(E) = 0$ such that for every $\mathbf{y} \in \Omega \sim E$ we have

$$\lim_{r \rightarrow 0} \kappa_n^{-1} r^{-n} \int_{\mathbf{B}(\mathbf{y}, r) \cap \Omega} |\mathbf{g} - \mathbf{g}(\mathbf{y})| d\mathcal{L}^n = 0. \quad (33)$$

Since by Fubini's theorem

$$0 = \mathcal{L}^n(E) = \int_0^\infty \mathcal{H}^{n-1}(E \cap \text{bdry } \mathbf{B}(\mathbf{x}, \rho)) d\mathcal{L}^1(\rho),$$

we see that for \mathcal{L}^1 almost every $\rho > 0$ we have

$$\mathcal{H}^{n-1}(E \cap \text{bdry } \mathbf{B}(\mathbf{x}, \rho)) = 0.$$

For every such a $\rho \in (0, \epsilon)$, we have (33) for \mathcal{H}^{n-1} almost every $\mathbf{y} \in \text{bdry } \mathbf{B}(\mathbf{x}, \rho)$ and hence in particular also

$$\lim_{r \rightarrow 0} \kappa_n^{-1} r^{-n} \int_{\mathbf{B}(\mathbf{y}, r) \cap \mathbf{B}(\mathbf{x}, \rho)} |\mathbf{g} - \mathbf{g}(\mathbf{y})| d\mathcal{L}^n = 0$$

since $\mathbf{B}(\mathbf{x}, \rho) \subset \Omega$. A comparison with (17) of Theorem 3.11 written for Ω replaced by $\mathbf{B}(\mathbf{x}, \rho)$ shows that $\mathbf{g}(\mathbf{y})$ coincides with the trace of $\mathbf{g}|_{\mathbf{B}(\mathbf{x}, \rho)}$ for \mathcal{H}^{n-1} almost every $\mathbf{y} \in \text{bdry } \mathbf{B}(\mathbf{x}, \rho)$. \square

Proof of the limit relation. Let us extend \mathbf{g} and \mathbf{g}_k by $\mathbf{0}$ outside Ω . We first note that by (7)₁ we may pass to a subsequence of \mathbf{g}_k (not relabeled) such that $\|\mathbf{g} - \mathbf{g}_k\|_{L^1(\Omega, \mathbb{R}^m)} < 2^{-k}$ so that the function

$$\varphi(\mathbf{x}) = \sum_{k=1}^{\infty} |\mathbf{g}(\mathbf{x}) - \mathbf{g}_k(\mathbf{x})|$$

satisfies

$$\int_{\Omega} \varphi d\mathcal{L}^n \leq 1. \quad (34)$$

Let $\mathbf{x} \in \Omega$ be fixed, and let $\epsilon > 0$ be any number satisfying $\mathbf{B}(\mathbf{x}, \epsilon) \subset \Omega$. Since

$$\int_0^{\infty} \int_{\text{bdry } \mathbf{B}(\mathbf{x}, \rho)} \varphi d\mathcal{H}^{n-1} d\rho = \int_{\Omega} \varphi d\mathcal{L}^n \leq 1$$

by (34), there exists a subset N_1 of $(0, \epsilon)$ with $\mathcal{L}^1(N_1) = 0$ such that

$$\int_{\text{bdry } \mathbf{B}(\mathbf{x}, \rho)} \varphi d\mathcal{H}^{n-1} \equiv \sum_{k=1}^{\infty} \int_{\text{bdry } \mathbf{B}(\mathbf{x}, \rho)} |\mathbf{g} - \mathbf{g}_k| d\mathcal{H}^{n-1} < \infty \quad (35)$$

for every $\rho \in (0, \epsilon) \sim N_1$. Hence, for every $\rho \in (0, \epsilon) \sim N_1$, we have

$$\int_{\text{bdry } \mathbf{B}(\mathbf{x}, \rho)} |\mathbf{g} - \mathbf{g}_k| d\mathcal{H}^{n-1} \rightarrow 0$$

and hence

$$\mathbf{g}_k \rightarrow \mathbf{g} \quad (36)$$

in the Lebesgue space $L^1(\text{bdry } \mathbf{B}(\mathbf{x}, \rho), \mathcal{H}^{n-1})$ on $\text{bdry } \mathbf{B}(\mathbf{x}, \rho)$ relative to the measure \mathcal{H}^{n-1} . By Lemma 6.1, for every $k = 1, \dots$, there exists a subset M_k of $(0, \epsilon)$ with $\mathcal{L}^1(M_k) = 0$ such that for every $\rho \in (0, \epsilon) \sim M_k$ the restriction of the map $\mathbf{g}_k|_{\text{bdry } \mathbf{B}(\mathbf{x}, \rho)}$ is the trace of $\mathbf{g}_k|_{\mathbf{B}(\mathbf{x}, \rho)} \in BV(\mathbf{B}(\mathbf{x}, \rho), \mathbb{R}^m)$. Let

$$N = N_1 \cup \bigcup_{k=1}^{\infty} M_k,$$

so that $\mathcal{L}^1(N) = 0$. For every $\rho \in (0, \epsilon) \sim N$, we have

$$\int_{\text{bdry } \mathbf{B}(\mathbf{x}, \rho)} \varphi \mathbf{g}_k \otimes \mathbf{n} d\mathcal{H}^{n-1} = \int_{\mathbf{B}(\mathbf{x}, \rho)} \mathbf{g}_k \otimes D\varphi d\mathcal{L}^n + \int_{\mathbf{B}(\mathbf{x}, \rho)} \varphi D\mathbf{g}_k \quad (37)$$

for all $k = 1, \dots$ and for any $\varphi \in C_0^\infty(\mathbf{R}^n)$ where \mathbf{n} is the normal to $\mathbf{B}(\mathbf{x}, \rho)$. The limit using (36), (7)₁, and (6) then gives

$$\int_{\text{bdry } \mathbf{B}(\mathbf{x}, \rho)} \varphi \mathbf{g} \otimes \mathbf{n} d\mathcal{H}^{n-1} = \int_{\mathbf{B}(\mathbf{x}, \rho)} \mathbf{g} \otimes D\varphi d\mathcal{L}^n + \int_{\mathbf{B}(\mathbf{x}, \rho)} \varphi dD\mathbf{g}, \quad (38)$$

and hence, $\mathbf{g}|_{\text{bdry } \mathbf{B}(\mathbf{x}, \rho)}$ is the trace of $\mathbf{g}|_{\mathbf{B}(\mathbf{x}, \rho)} \in BV(\mathbf{B}(\mathbf{x}, \rho), \mathbf{R}^m)$ for every $\rho \in (0, \epsilon) \sim N$. In particular, for $\varphi \equiv 1$ on \mathbf{R}^n , we obtain from (37) and (38)

$$D\mathbf{g}_k(\mathbf{B}(\mathbf{x}, \rho)) \rightarrow \int_{\text{bdry } \mathbf{B}(\mathbf{x}, \rho)} \mathbf{g} \otimes \mathbf{n} d\mathcal{H}^{n-1} = D\mathbf{g}(\mathbf{B}(\mathbf{x}, \rho)),$$

i.e.,

$$D\mathbf{g}_k(\mathbf{B}(\mathbf{x}, \rho)) \rightarrow D\mathbf{g}(\mathbf{B}(\mathbf{x}, \rho))$$

as $k \rightarrow \infty$ for each $\rho \in (0, \epsilon) \sim N$.⁸ Combining with (7)₂, we then obtain

$$(D\mathbf{g}_k - D_a \mathbf{g}_k \mathcal{L}^n \llcorner \Omega)(\mathbf{B}(\mathbf{x}, \rho)) \rightarrow (D\mathbf{g} - \mathbf{G} \mathcal{L}^n \llcorner \Omega)(\mathbf{B}(\mathbf{x}, \rho)) \quad (39)$$

as $k \rightarrow \infty$; noting that

$$D\mathbf{g}_k - D_a \mathbf{g}_k \mathcal{L}^n \llcorner \Omega = [\mathbf{g}_k] \otimes \mathbf{n}_k \mathcal{H}^{n-1} \llcorner J(\mathbf{g}_k),$$

where $[\mathbf{g}_k]$ is the jump of \mathbf{g}_k on $J(\mathbf{g}_k)$ and \mathbf{n}_k is the normal to $J(\mathbf{g}_k)$, we see that (39) reads

$$\lim_{k \rightarrow \infty} \int_{J(\mathbf{g}_k) \cap \mathbf{B}(\mathbf{x}, \rho)} [\mathbf{g}_k] \otimes \mathbf{n}_k d\mathcal{H}^{n-1} = D\mathbf{g}(\mathbf{B}(\mathbf{x}, \rho)) - \int_{\mathbf{B}(\mathbf{x}, \rho)} \mathbf{G} d\mathcal{L}^n \quad (40)$$

for every $\rho \in (0, \epsilon) \sim N$. This holds for every $\mathbf{x} \in \Omega$ where $N = N(\mathbf{x})$. Dividing (40) by $\kappa_n \rho^n$ and using that (16) and

$$\mathbf{G}(\mathbf{x}) = \lim_{\rho \rightarrow 0} \kappa_n^{-1} \rho^{-n} \int_{\mathbf{B}(\mathbf{x}, \rho)} \mathbf{G} d\mathcal{L}^n$$

hold simultaneously for \mathcal{L}^n almost every $\mathbf{x} \in \Omega$, we see that for every such an \mathbf{x} we have

$$\lim_{\substack{\rho \rightarrow 0 \\ \rho \in (0, \epsilon) \sim N}} \lim_{k \rightarrow \infty} \int_{J(\mathbf{g}_k) \cap \mathbf{B}(\mathbf{x}, \rho)} [\mathbf{g}_k] \otimes \mathbf{n}_k d\mathcal{H}^{n-1} = D_a \mathbf{g} - \mathbf{G}(\mathbf{x}),$$

i.e., (8) holds. □

⁸ This is otherwise *not* a direct consequence of (6).

**Appendix: Elementary proof of a weaker form
of the approximation theorem**

We here outline a proof of the following form of the approximation theorem without using Alberti's theorem:

Theorem A.1. *If Ω is an admissible domain and*

$$(\mathbf{g}, \mathbf{G}) \in BV(\Omega, \mathbb{R}^m) \times L^1(\Omega, \mathbb{M}^{m \times n}),$$

then there exist two sequences $\mathbf{m}_k, \mathbf{h}_k \in SBV(\Omega, \mathbb{R}^m)$ such that

$$\mathbf{m}_k \rightarrow \mathbf{g} \text{ in } L^1(\Omega, \mathbb{R}^m) \quad \text{and} \quad D_a \mathbf{m}_k = \mathbf{0} \text{ over } \Omega, \tag{1}$$

$$\mathbf{h}_k \rightarrow \mathbf{0} \text{ in } L^1(\Omega, \mathbb{R}^m) \quad \text{and} \quad D_a \mathbf{h}_k \rightarrow \mathbf{G} \text{ in } L^1(\Omega, \mathbb{M}^{m \times n}), \tag{2}$$

and

$$\sup\{M(D\mathbf{m}_k) : k = 1, \dots\} < \infty \quad \text{and} \quad \sup\{M(D\mathbf{h}_k) : k = 1, \dots\} < \infty; \tag{3}$$

consequently, the sequence $\mathbf{g}_k = \mathbf{m}_k + \mathbf{h}_k \in SBV(\Omega, \mathbb{R}^m)$ satisfies

$$\mathbf{g}_k \rightarrow \mathbf{g} \text{ in } L^1(\Omega, \mathbb{R}^m) \quad \text{and} \quad D_a \mathbf{g}_k \rightarrow \mathbf{G} \text{ in } L^1(\Omega, \mathbb{M}^{m \times n}) \tag{4}$$

and

$$\sup\{M(D\mathbf{g}_k) : k = 1, \dots\} < \infty \quad \text{and} \quad D\mathbf{g}_k \rightharpoonup^* D\mathbf{g} \text{ in } \mathcal{M}(\Omega, \mathbb{M}^{m \times n}).$$

Proof outline. We denote by \mathbf{g}_0 the extension of \mathbf{g} to \mathbb{R}^n equal to 0 outside Ω . Since Ω is an admissible domain, we have $\mathbf{g}_0 \in BV(\mathbb{R}^n, \mathbb{R}^m)$ by Theorem 3.12. Let \mathbf{f}_k be a sequence of mollifications of \mathbf{g}_0 on \mathbb{R}^n with the mollification parameter tending to 0. Applying Proposition 5.2 in the same way as in the proof of the approximation theorem (Section 1), we find a sequence $\mathbf{m}_k \in SBV(\mathbb{R}^n, \mathbb{R}^m)$ such that $\|\mathbf{f}_k - \mathbf{m}_k\|_{L^1(\mathbb{R}^n, \mathbb{R}^m)} < 1/k$. The sequence $\mathbf{m}_k|_\Omega$ (again denoted \mathbf{m}_k) then satisfies (1) and (3)₁.

Next, let \mathbf{G}_0 be the extension of \mathbf{G} to \mathbb{R}^n equal to $\mathbf{0}$ outside Ω , and put

$$\mathbf{h}_k(\mathbf{x}) = \mathbf{G}(k, \mathbf{p})(\mathbf{x} - \mathbf{x}(k, \mathbf{p}))$$

for any $\mathbf{x} \in \mathbb{R}^n$ where $\mathbf{p} \in \mathbb{Z}^n/k$ is uniquely determined by the requirement $\mathbf{x} \in C(k, \mathbf{p})$, $\mathbf{x}(k, \mathbf{p})$ is the barycenter of $C(k, \mathbf{p})$, and

$$\mathbf{G}(k, \mathbf{p}) = k^n \int_{C(k, \mathbf{p})} \mathbf{G} d\mathcal{L}^n.$$

Then \mathbf{h}_k is easily seen to satisfy (2) and (3)₂. □

Acknowledgment

The author thanks David Owen for his encouragement to complete this work, which was initiated in 2008. The research was supported by RVO 67985840 and by the grant 201/09/0473 of GA ČR. The supports are gratefully acknowledged.

References

- [Alberti 1991] G. Alberti, “A Lusin type theorem for gradients”, *J. Funct. Anal.* **100**:1 (1991), 110–118.
- [Ambrosio et al. 2000] L. Ambrosio, N. Fusco, and D. Pallara, *Functions of bounded variation and free discontinuity problems*, Oxford University Press, New York, 2000.
- [Baía et al. 2011] M. Baía, J. Matias, and P. M. Santos, “A survey on structured deformations”, *São Paulo J. Math. Sci.* **5**:2 (2011), 185–201.
- [Choksi and Fonseca 1997] R. Choksi and I. Fonseca, “Bulk and interfacial energy densities for structured deformations of continua”, *Arch. Rational Mech. Anal.* **138**:1 (1997), 37–103.
- [Del Piero and Owen 1993] G. Del Piero and D. R. Owen, “Structured deformations of continua”, *Arch. Rational Mech. Anal.* **124**:2 (1993), 99–155.
- [Del Piero and Owen 1995] G. Del Piero and D. R. Owen, “Integral-gradient formulae for structured deformations”, *Arch. Rational Mech. Anal.* **131**:2 (1995), 121–138.
- [Del Piero and Owen 2004] G. Del Piero and D. R. Owen (editors), *Multiscale modeling in continuum mechanics and structured deformations*, CISM Courses and Lectures **447**, Springer, Vienna, 2004.
- [Evans and Gariepy 1992] L. C. Evans and R. F. Gariepy, *Measure theory and fine properties of functions*, CRC, Boca Raton, FL, 1992.
- [Federer 1969] H. Federer, *Geometric measure theory*, Die Grundlehren der Mathematischen Wissenschaften **153**, Springer, New York, 1969.
- [Ziemer 1989] W. P. Ziemer, *Weakly differentiable functions: Sobolev spaces and functions of bounded variation*, Graduate Texts in Mathematics **120**, Springer, New York, 1989.

Received 12 Mar 2014. Revised 11 Jun 2014. Accepted 15 Jul 2014.

MIROSLAV ŠILHAVÝ: silhavy@math.cas.cz

Institute of Mathematics, Academy of Sciences of the Czech Republic, Žitná 25, 115 67 Prague 1, Czech Republic



Guidelines for Authors

Authors may submit manuscripts in PDF format on-line at the submission page.

Originality. Submission of a manuscript acknowledges that the manuscript is original and is not, in whole or in part, published or under consideration for publication elsewhere. It is understood also that the manuscript will not be submitted elsewhere while under consideration for publication in this journal.

Language. Articles in MEMOCS are usually in English, but articles written in other languages are welcome.

Required items. A brief abstract of about 150 words or less must be included. It should be self-contained and not make any reference to the bibliography. If the article is not in English, two versions of the abstract must be included, one in the language of the article and one in English. Also required are keywords and a Mathematics Subject Classification or a Physics and Astronomy Classification Scheme code for the article, and, for each author, postal address, affiliation (if appropriate), and email address if available. A home-page URL is optional.

Format. Authors are encouraged to use L^AT_EX and the standard amsart class, but submissions in other varieties of T_EX, and exceptionally in other formats, are acceptable. Initial uploads should normally be in PDF format; after the refereeing process we will ask you to submit all source material.

References. Bibliographical references should be complete, including article titles and page ranges. All references in the bibliography should be cited in the text. The use of B_IB_T_EX is preferred but not required. Tags will be converted to the house format, however, for submission you may use the format of your choice. Links will be provided to all literature with known web locations and authors are encouraged to provide their own links in addition to those supplied in the editorial process.

Figures. Figures must be of publication quality. After acceptance, you will need to submit the original source files in vector graphics format for all diagrams in your manuscript: vector EPS or vector PDF files are the most useful.

Most drawing and graphing packages — Mathematica, Adobe Illustrator, Corel Draw, MATLAB, etc. — allow the user to save files in one of these formats. Make sure that what you are saving is vector graphics and not a bitmap. If you need help, please write to graphics@msp.org with as many details as you can about how your graphics were generated.

Bundle your figure files into a single archive (using zip, tar, rar or other format of your choice) and upload on the link you been provided at acceptance time. Each figure should be captioned and numbered so that it can float. Small figures occupying no more than three lines of vertical space can be kept in the text (“the curve looks like this:”). It is acceptable to submit a manuscript with all figures at the end, if their placement is specified in the text by means of comments such as “Place Figure 1 here”. The same considerations apply to tables.

White Space. Forced line breaks or page breaks should not be inserted in the document. There is no point in your trying to optimize line and page breaks in the original manuscript. The manuscript will be reformatted to use the journal’s preferred fonts and layout.

Proofs. Page proofs will be made available to authors (or to the designated corresponding author) at a Web site in PDF format. Failure to acknowledge the receipt of proofs or to return corrections within the requested deadline may cause publication to be postponed.

- Effects of damping on the stability of the compressed Nicolai beam 1
Angelo Luongo, Manuel Ferretti and Alexander P. Seyranian
- Responses of first-order dynamical systems to Matérn, Cauchy, and Dagum excitations 27
Lihua Shen, Martin Ostoja-Starzewski and Emilio Porcu
- Reflections on mathematical models of deformation waves in elastic microstructured solids 43
Jüri Engelbrecht and Arkadi Berezovski
- On the approximation theorem for structured deformations from $BV(\Omega)$ 83
Miroslav Šilhavý

MEMOCS is a journal of the International Research Center for the Mathematics and Mechanics of Complex Systems at the Università dell'Aquila, Italy.

